

Archvied in Dspace@nitr

<http://dspace.nitrkl.ac.in/dspace>

PERFORMANCE EVALUATION OF PHASE- OPTIMIZED SPREADING CODES IN NON-LINEAR DS-CDMA RECEIVER

Ipsita Bhanja



**Department of Electronics & Communication Engineering.
National Institute of Technology,
Rourkela-769 008
July 2006**

PERFORMANCE EVALUATION OF PHASE- OPTIMIZED SPREADING CODES IN NON-LINEAR DS-CDMA RECEIVER

A thesis submitted in partial fulfillment of the requirements for the degree of

**Master of Technology (Research)
in
Electronics & Communication Engineering
2004-2006**

By

Ipsita Bhanja
Roll No: 60407005

Under the Supervision of

Dr. Sarat Kumar Patra
Professor



Department of Electronics & Communication Engineering
National Institute of Technology, Rourkela
July 2006

Abstract

Spread spectrum (SS) is a modulation technique in which the signal occupies a bandwidth much larger than the minimum necessary to send the information. A synchronized reception with the code at the receiver is used for despreading the information before data recovery. Bandsread is accomplished by means of a code which is independent of the data. Bandspreading code is pseudo-random, thus the spread signal resembles noise.

The coded modulation characteristic of SS system uniquely qualifies it for navigation applications. Any signal used in ranging is subject to time/distance relations. A SS signal has advantage that its phase is easily resolvable. Direct-sequence (DS) form of modulation is mostly preferred over Frequency Hopping system (FH) as FH systems do not normally possess high resolution properties. Higher the chip rate, the better the measurement capability. The basic resolution is one code chip.

Initially, some existing code families e.g. Gold, Kasami (large and small) and Maximal length sequence have been studied. Some of their important properties have been briefly described in part one of the present work. The most important consideration of this part is that, the performance of codes of different lengths is compared at the output of a direct sequence spread-spectrum multiple-access (DS-CDMA) system and conclusions are drawn which can be treated as guidelines for choosing spreading codes for different applications. The spreading codes are optimized by auto-optimal/least sidelobe energy (AO/LSE), least sidelobe energy/auto-optimal (LSE/AO), maximum sidelobe energy/auto-optimal (MSE/AO), cross-optimal/minimum mean-square cross-correlation (CO/MSQCC), and minimum mean-square cross-correlation/cross-optimal (MSQCC/CO) criteria. Signal-to-noise ratio (SNR) at the receiver output is used as performance measure in all the work.

In the second part, a non-linear receiver is considered when the spreading codes are gold sequence and randomly generated sequence with seven chips length. The non-linear receiver is based on radial basis function network (RBFN) architecture. DS-CDMA system presents a non-linearly separable scenario and hence a non-linear receiver structure performs better when compared with established linear receivers like matched and Weiner (MMSE) filter. Both AWGN and multipath channel conditions are considered and preprocessing based (PPB) architecture is used for the new receiver. The RBFN considers both Euclidean and Mahalanobis distance criteria for calculating the basis function. Taking computational complexity into account, the number of centers of the receiver is reduced.

Declaration of Originality

This thesis was composed entirely by me. The work reported herein was conducted exclusively by me in the Department of Electronics and Communication Engineering at National Institute of Technology, Rourkela.

Ipsita Bhanja
Roll No: 60407005

Certificate

This is to certify that the work in this thesis entitled “Performance Evaluation of Phase-Optimized Spreading Codes in Nonlinear DS-CDMA Receiver” by Ms. Ipsita Bhanja has been carried out under my supervision in partial fulfillment of the requirements for the degree of Masters of Technology (Research) in Electronics and Instrumentation Engineering during session 2004-2006 in the Department of Electronics and Communication Engineering, National Institute of Technology, Rourkela, and this work has not been submitted elsewhere for a degree.

Dr. S. K. Patra
Professor,
Dept. of Electronics & Communication Engg.
NIT, Rourkela.

Acknowledgements

I would like to thank the following people for their invaluable assistance during the course of this work:

- Prof. Sarat Kumar Patra, my supervisor for his continuous guidance and support.
- Prof. G. S. Rath for allowing me to waste his precious time and disturbing him with problems both personal and academic.
- Prof. K. K. Mahapatra for being very kind and considerate.
- All my teachers in the department of Electronics & Communication Engg. for being very patient and supportive.
- Dr. S. Ghosh of Electrical Engg. for making my stay in Rourkela a comfortable and unforgettable one.
- All the staffs of the department of Electronics & Communication Engg. for their kind help and support.
- All those “anonymous” for filling my void days with their bright smiles.

Lastly, I would like to thank all my friends and family for supporting me incessantly to keep “the fire burning”!

Ipsita Bhanja
Roll No: 60407005

Contents

Abstract	i
Declaration of originality	iii
Certificate	iv
Acknowledgements	v
Contents	vi
List of figures	ix
List of tables	xii
Abbreviations	xiii
Nomenclature	xv
1 Introduction	1
1.1 Introduction	1
1.2 History of Mobile Communication	1
1.3 Mobile Systems around the World	3
1.4 Wireless Communications Services	4
1.4.1 Types of Wireless Services	4
1.4.2 Cellular Mobile Radio Systems	4
1.4.2.1 Evolution of Cellular Mobile Radio Systems	5
1.5 Modulation Techniques for Mobile Radio	6
1.5.1 Spread Spectrum Modulation Techniques	6
1.5.1.1 Principle of Spread spectrum	7
1.5.1.2 Why spread spectrum	7
1.5.1.3 Types of Spread spectrum	9
1.5.1.4 Application of Spread spectrum	10
1.5.2 Direct Sequence Spread Spectrum (DS-SS)	10
1.6 Multiple Access Techniques for Wireless Communications	12
1.6.1 Duplexing	12
1.6.2 Multiple Access	13
1.7 Layout of Thesis	15
1.8 Conclusion	16
2 CDMA Overview	17
2.1 Introduction	17
2.2 CDMA Principle	17
2.3 IS-95 Standards – Fundamentals	20
2.4 Reverse Traffic Channel	22
2.4.1 Convolutional Encoder	24
2.4.2 Interleaving	25
2.4.3 64 ary Orthogonal Modulator	26
2.4.4 Long code Spreading	26

2.4.5	Quadrature Modulation	27
2.4.6	Baseband Filtering	29
2.5	Forward Traffic Channel	30
2.6	Modification to IS-95	31
2.7	Conclusion	32
3	Overview of Coding Techniques	33
3.1	Introduction	33
3.2	Advantages of Spreading	34
3.3	Properties of Spreading Code	35
3.3.1	Linear Codes	36
3.4	Maximal Sequence	37
3.4.1	Properties	39
3.4.2	Implementation	42
3.4.2.1	Convention for Feedback Specification	43
3.5	Gold Sequence	45
3.6	Kasami Sequence	47
3.7	Orthogonal Codes	47
3.7.1	Walsh Codes	48
3.7.2	Variable-Length Orthogonal Codes	48
3.8	Multiple Spreading	49
3.9	Forward Error Correction	50
3.9.1	Convolutional Codes	50
3.9.1.1	Example of Convolutional Encoder	52
3.9.1.2	Theoretical Analysis of Convolutional codes	53
3.10	Conclusion	55
4	Phase Optimization	56
4.1	Introduction	56
4.2	Correlation Parameters and Performance Measures	56
4.2.1	Definition of AO / LSE, LSE / AO and MSE / AO Phase Optimization Criteria.	58
4.2.2	Definition of CO/MSQCC and MSQCC/CO phase optimization Criteria.	60
4.2.3	Significance of PN Sequence Initial Phases	62
4.3	Optimization Results	62
4.3.1	Discussion	69
4.4	Conclusion	71
5	Nonlinear Receiver	72
5.1	Introduction	72
5.2	Multiuser receiver	73
5.3	Linear receiver	75

5.3.1	Matched Filter Receiver	76
5.3.2	Weiner Filter	77
5.4	Nonlinear receiver	81
5.5	RBF for DS-CDMA	81
5.6	CLB RBF	83
5.6.1	CLB Based RBF Receiver	86
5.7	Preprocessed based RBF receiver	90
5.8	Reduced PPB RBF receiver	94
5.8.1	Center construction	95
5.9	Simulation result	96
5.9.1	AWGN channel	96
5.9.2	Multipath channel	98
5.10	Discussion	102
5.11	Conclusion	104
6	Conclusion	105
6.1	Introduction	105
6.2	Summary	105
6.3	Achievement of the thesis	106
6.4	Limitations of the work	107
6.5	Scope for further research	107
Appendix A	System Description	108
Appendix B	Ranging application of spread spectrum	112
References		116
Biodata		125

List of figures

1.1	The growth of mobile telephony as compared with other popular inventions	2
1.2	Cellular communication system	5
1.3	Various upgrade paths for 2G technologies.	6
1.4	General model of spread spectrum system	7
1.5	Interference rejection in spread spectrum.	8
1.6	A spectrum analyzer photo of a FH spread spectrum signal	9
1.7	A spectrum analyzer photo of a DS spread spectrum signal	9
1.8	DS-SS system	11
1.9	Time domain representation of the signals at the transmitter of a DS system.	12
1.10	Frequency domain representation of the received signal in a DS system.	12
1.11	(a) FDD provides two simplex channels at the same time;	13
	(b) TDD provides two simplex time slots at the same frequency.	13
1.12	Frequency division multiple access (FDMA).	13
1.13	Time division multiple access (TDMA).	14
1.14	Code division multiple access (CDMA).	14
1.15	Structure of the thesis.	15
2.1	Two user DS-CDMA system	19
2.2	CDMA in a DSSS environment	20
2.3	IS-95 Forward channel schematic	21
2.4	IS-95 Reverse channel schematic	22
2.5	Reverse Channel Transmitter for IS-95	23
2.6	Convolutional Encoder for IS-95 Reverse Channel	25
2.7	Long PN code generator for IS-95	27
2.8	IS-95 reverse channel signal constellation	29
2.9	Convolution of pulse-shaping filter with matched filter	30
2.10	Forward CDMA channel modulation process.	31
3.1	Spreading of Data signal: $p(t)$ by Code Signal: $c(t)$	33
3.2	(a) linear code generator for p -ary shift register (each stage has p possible states);	
	(b) nonlinear code generator using p -ary shift register (there are $p^n - 1$ possible states for each feedback condition);	
	(c) nonlinear code generator based on linear generator.	37
3.3	Shift Register Generator for 1023-chip Nonmaximal Codes.	42
3.4	Fibonacci implementation of LFSR.	42
3.5	Galois implementation of LFSR	43
3.6	Gold code sequence generator configuration	45
3.7	Generation of 31 bit Gold code.	46
3.8	Multiple Spreading	49
3.9	Forward error correction using block and convolutional encoders.	50
3.10	General block diagram of convolutional encoder	51

3.11	Rate $\frac{1}{2}$, constraint length 3 $(7,5)_8$ convolutional encoder.	52
3.12	The state diagram for the $(7,5)_8$ convolutional encoder.	53
4.1	Set of M-sequences of length 31	63
4.2	Set of Gold sequences of length 31	63
4.3	Set of M-sequences of length 63.	64
4.4	Set of Gold sequences of length 63.	64
4.5	Set of Kasami sequences (small family) of length 63.	65
4.6	Set of Kasami sequences (large family) of length 63.	65
4.7	Set of M-sequences of length 127.	66
4.8	Set of Gold sequences of length 127.	66
4.9	Set of M-sequences of length 255.	67
4.10	Set of Kasami-sequences (small family) of length 255.	67
4.11	Set of Kasami -sequences (large family) of length 255.	68
4.12	Set of M –sequences of length 511.	68
4.13	Set of Gold sequences of length 511.	69
5.1	DS-CDMA correlator receiver with 8 tap delay.	72
5.2	Conventional bank of single user receivers with MFs or RAKEs.	74
5.3	Verdu's proposed multiuser detector scheme with MFs for the AWGN channel.	74
5.4	Chip rate based receiver.	75
5.5	Symbol rate based receiver.	76
5.6	Matched filter	77
5.7	A bank of matched filters, the preprocessing stage, as for the optimum multiuser receiver.	79
5.8	BER against the number of users in AWGN at $E_b/N_o = 7$ dB and with randomly generated spreading codes with 7 chips.	80
5.9	BER against the number of users in a stationary multipath, at $E_b/N_o = 7$ dB and with randomly generated spreading codes with 7 chips.	80
5.10	The decision surface (shape) of the Bayesian receiver structure for a two user CDMA scenario in AWGN and $E_b/N_o = 7$ dB. The axis r_1 and r_2 are the outputs of the preprocessor. Each hub represents the noise distribution around one of the four possible noise free signal states.	82
5.11	Circular clusters of two user CDMA system. (Noise is uncorrelated)	85
5.12	The structure of the CLB RBF network.	86
5.13	Center construction (<i>From a chip level perspective</i>)	88
5.14	Elliptical clusters of two user CDMA system. (Noise is correlated)	93
5.15	Two decision boundaries for two different PPB RBF structures for a two user CDMA system with 7 chip Gold codes and $E_b/N_o = 7$ dB. Shown are the decision boundaries obtained with Euclidean distance measure (ERBF) and Mahalanobis distance measure (MRBF).	94
5.16	The effect of ISI on the chips (vector perspective)	95

5.17	BER against the number of users for a CDMA scenario in AWGN with randomly generated 7 chip spreading codes and $E_b / N_0 = 7\text{dB}$ in an AWGN channel.	97
5.18	BER against the number of users for a CDMA scenario in AWGN with 7 chip Gold spreading codes and $E_b / N_0 = 7\text{dB}$ in an AWGN channel.	98
5.19	BER against the number of users for a CDMA scenario with randomly generated 7 chip spreading codes and $E_b / N_0 = 7\text{dB}$ in a multipath channel.	99
5.20	BER against the number of users for a CDMA scenario with 7 chip Gold codes and $E_b / N_0 = 7\text{dB}$ in a multipath channel.	100
5.21	BER against the number of users for a CDMA scenario with randomly generated 16 chip spreading codes and $E_b / N_0 = 7\text{dB}$ in a multipath channel.	101
5.22	BER against the SNR for a CDMA scenario with randomly generated 16 chip spreading codes and a multipath channel.	102
A.1	Spread spectrum model.	108
A.2	The uplink scenario (<i>mobiles to base station</i>) for U mobiles.	109
A.3	The downlink scenario (<i>base station to mobile</i>).	109
B.1	Direct sequence ranging system (<i>Transmitter</i>)	113.
B.2	Direct sequence ranging system (<i>Receiver</i>)	113.
B.3	Code-sequence comparisons at transmitter & receiver.	114

List of tables

1.1	Major mobile radio standards in North America	3
1.2	Multiple access techniques used in different wireless communication systems.	15
2.1	Reverse traffic channel modulation parameters	23
2.2	IS-95 forward traffic channel modulation parameters.	31
3.1	Feedback connections for linear m-sequences	39
3.2	Correlation function(Reference sequence: 1110010)	40
3.3	Transition table showing output code words for each input data bit at each state for the $(7,5)_8$ convolutional encoder	53
B.1	Code sequence periods for various m-sequence lengths, 1-Mcps rate	115
B.2	Chip rates for various basic range resolutions	115

Abbreviations

AIP	average interference parameter
ACF	auto correlation function
ANN	artificial neural network
AWGN	additive white Gaussian noise
BER	bit error ratio
BS	base station
BSC	base station controller
bps	bits per second
CCF	cross correlation function
CLB	chip level based (receiver)
CDMA	code division multiple access
CRBF	chip level based radial basis function receiver
DS	direct sequence
DECO	decorrelating detector
EGC	equal gain combining
ERBF	radial basis function with Euclidean distance measure
FDMA	frequency division multiple access
FH	frequency hopping
HNN	Hopfield neural network
IMT 2000	International Mobile Telecommunications 2000
ICI	inter chip interference
ISI	inter symbol interference
IS-95	interim standard-95
ITU	International Telecommunication Union
kbps	kilo bit per second
LSE	least square error
Mchip/s	mega chips per second
MAI	multiple access interference
MF	matched filter
ML	maximum likelihood
MLP	multilayer perceptron
MLSE	maximum likelihood sequence estimator
MLSD	maximum likelihood symbol detector
MMSE	minimum mean square error
MRBF	radial basis function with Mahalanobis distance measure
MRC	maximum ratio combining
MSC	mobile switching centre
MSD	multistage detector
MSE	mean square error
MUD	multiuser detector
NN	neural network
pdf	probability density function
PG	processing gain

PN	pseudo-noise or pseudo-random
PPB	preprocessing based (receiver)
RBF	radial basis function
RBFN	radial basis function network
RLS	least recursive square
SS	spread spectrum
SRBF	radial basis function with super centres
TDMA	time division multiple access
TH	time hopping
UMTS	Universal Mobile Telecommunication Standard
WCDMA	wideband CDMA
ZF	zero forcing

Nomenclature

ω_c	carrier frequency
ω_i	i th class
μ	mean
μ_m	m th mean, or m th permutation
ϕ_u	carrier phase shift for user u
$\phi(.)$	nonlinear function
Φ	matrix having $\phi(.)$ as rows
$\psi(t)$	chip waveform
σ	standard deviation
σ_m	m th neuron's spread
σ^2	variance or noise power
τ_u	time delay of the u th user
$\ .\ $	Euclidean norm
$ \mathbf{A} $	determinate of matrix \mathbf{A}
\mathbf{A}	a ($i \times j$) matrix with i rows j columns
$a_{i,j}$	element of i th row and j th column
\mathbf{a}_i	i th row in \mathbf{A}
\mathbf{a}	a vector
a_i	i th vector element
$\mathbf{A}^T, \mathbf{a}^T$	the transpose
B	(narrowband) bandwidth
\mathbf{B}	($M \times U$) combination matrix containing all $M = 2^U$ binary combinations
\mathbf{C}	matrix containing all spreading codes
$c_{u,n}$	element of u th row n th column in \mathbf{C}
\mathbf{c}_u	u th users's spreading code
\mathbf{c}_m	m th RBF centre
$D_d(k)$	k th data bit of the desired user d
$D_u(k)$	k th data bit of the user u
$d(.)$	desired response
$E[.]$	expected value
E_b	energy per bit
$e(.)$	error
$\exp(.)$	natural exponential function
f	frequency
$f_i(.)$	i th function
G_i	i th group
$g(t)$	white Gaussian noise
$\mathbf{g}(k)$	k th symbol's noise term
\mathbf{H}	channel matrix
H_i	i th hypothesis

H_{ch}	channel impulse response
\mathbf{I}	identity matrix
J_{min}	minimum mean square error
K	average factor
L	number of channel taps
LR	likelihood ratio
N	processing gain
N_J	jamming power
N_j	number of patterns in the j th class
P_u	u th user's signal power
P_e	probability of error
\mathbf{P}	generating matrix with all possible signals combinations
\mathbf{p}	prototype pattern (point)
p_i	i th group
$p(x y)$	conditional probability density function of x given y
$Q(\cdot)$	Gaussian error function
\mathfrak{R}^d	d - dimensional space
\mathbf{R}_{yy}	autocorrelation matrix
\mathbf{r}_{xy}	crosscorrelation vector
$\mathbf{r}(k)$	k th preprocessed signal at symbol rate
$r_u(\cdot)$	received preprocessed signal of user u
\mathbf{S}	covariance matrix, or crosscorrelation matrix
\mathbf{s}_d	desired signal
\mathbf{s}_m	m th signal
SNR	signal to noise ratio
s_d	d th element of signal \mathbf{s}
$s_u(t)$	spreading waveform of user u
$\text{sgn}(\cdot)$	sign operator
T	bit interval
T_c	chip duration
t	time
U	number of transmitting users
W	spread bandwidth
\mathbf{w}	filter weights
\mathbf{X}	set containing all possible noise free signal states
$\mathbf{x}(k)$	k th received noise free signal at chip rate
\mathbf{x}_m	m th pattern
$x(t)$	received (noise free) signal
$x_u(t)$	received signal of the u th user
$y(t)$	received noise corrupted signal
$y(kN+n)$	n th chip of the k th symbol with spreading length N
$\mathbf{y}(k)$	k th received symbol at symbol rate

Chapter 1

Introduction

1.1 Introduction

The ability to communicate with people on the move has evolved remarkably since Gugliemlo Marconi first demonstrated radio's ability to provide continuous contact with ships sailing in the English Channel. This was in 1897, and since then the new wireless communications methods and services have been enthusiastically adopted by people throughout the world. Particularly during the past ten years, the mobile radio communication industry has grown by order of magnitude, fueled by digital and RF circuit fabrication improvements, new very large-scale circuit integration, and other miniaturization technologies which make portable radio equipment smaller, cheaper , and more reliable. Digital switching networks have facilitated the large scale deployment of affordable, easy-to-use radio communication networks. These trends will continue at an even greater pace during the next decade.

The next few sections briefly describe the history and types of wireless communication system. Section 1.5 introduces spread spectrum modulation technique with particular emphasis on direct sequence form of spread spectrum. Section 1.6 describes with the aid of suitable figures, the three important multiple access techniques namely FDMA, TDMA and CDMA.

1.2 History of Mobile Communication

Techno-politics are a fundamental driver in the evolution of new technology and services, since radio spectrum usage is controlled by governments, not by service providers, equipment manufacturers, entrepreneurs, or researchers [1]. Progressive involvement in

technology development is vital for a government if it hopes to keep its own country competitive in the rapidly changing field of wireless personal communications. Figure 1.1 illustrates how mobile telephony has penetrated our daily lives compared with other popular inventions [2].

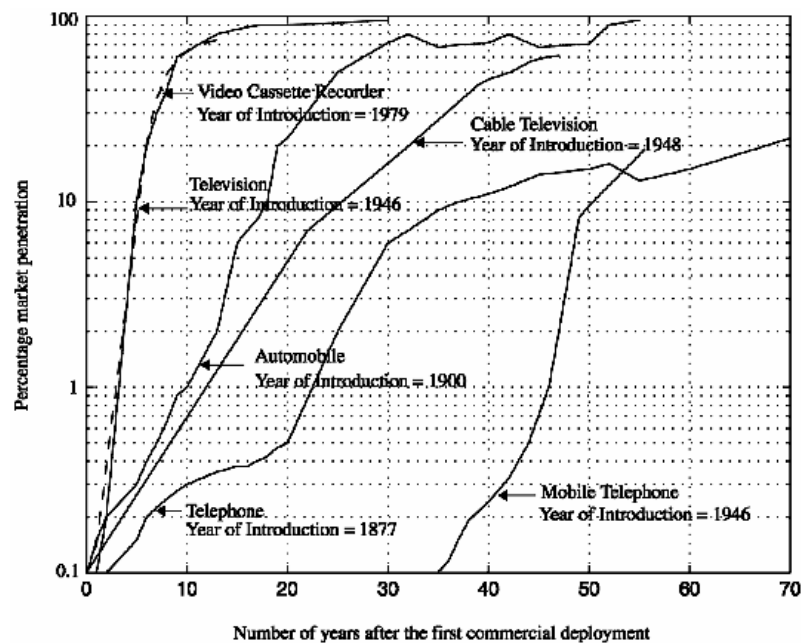


Figure 1.1: The growth of mobile telephony as compared with other popular inventions

A cellular system based on code division multiple access (CDMA) has been developed by Qualcomm Inc. and standardized by the Telecommunications Industry Association (TIA) as an Interim Standard (IS-95) [3]. This system supports a variable number of users in 1.25 MHz wide channels using direct sequence spread spectrum. While the analog AMPS system requires that the signal be at least 18 dB above the co-channel interference to provide acceptable call quality, CDMA systems can operate at much higher interference resistance properties. The ability of CDMA to operate with a much smaller signal-to-noise ratio (SNR) than conventional narrowband FM techniques allows CDMA systems to use the same set of frequencies in every cell, which provides a large improvement in capacity [4]. Unlike other digital cellular systems, the Qualcomm system uses a variable rate vocoder with voice activity detection which considerably reduces the required data rate and also the battery drain by the mobile transmitter.

1.3 Mobile Systems around the World

Many mobile standards have been developed for wireless systems throughout the world, and more standards are likely to emerge [5]. Table 1.1 lists the most common paging, cordless, cellular, and personal communications standards in North America, Europe, and Japan.

Table 1.1 Major Mobile Radio Standards in North America

Standard	Type	Year of Introduction	Multiple Access	Frequency Band	Modulation	Channel Bandwidth
AMPS	Cellular	1983	FDMA	824-894 MHz	FM	30 kHz
NAMPS	Cellular	1992	FDMA	824-894 MHz	FM	10 kHz
USDC	Cellular	1991	TDMA	824-894 MHz	$\pi/4$ -DQPSK	30 kHz
CDPD	Cellular	1993	FH/ Packet	824-894 MHz	GMSK	30 kHz
IS-95	Cellular/ PCS	1993	CDMA	824-894 MHz 1.8-2.0 GHz	QPSK/ BPSK	1.25 MHz
GSC	Paging	1970s	Simplex	Several	FSK	12.5 kHz
POCSAG	Paging	1970s	Simplex	Several	FSK	12.5 kHz
FLEX	Paging	1993	Simplex	Several	4-FSK	15 kHz
DCS-1900 (GSM)	PCS	1994	TDMA	1.85-1.99 GHz	GMSK	200 kHz
PACS	Cordless/ PCS	1994	TDMA/ FDMA	1.85-1.99 GHz	$\pi/4$ -DQPSK	300 kHz
MIRS	SMR/PCS	1994	TDMA	Several	16-QAM	25 kHz
iDen	SMR/PCS	1995	TDMA	Several	16-QAM	25 kHz

Table 1.1: Major mobile radio standards in North America

1.4 Wireless Communications Services

1.4.1 Types of Wireless Services

Consumers today have access to many different kinds of wireless products and services, having widely varying range of coverage. Short-range products include cordless telephones and wireless local area networks (WLANs). Long-range products include satellite-based wireless units. At various intermediate ranges are products such as cellular telephones, wide-area wireless data and radio paging services, specialized satellite-based message services in the freight industry, and internet access from hand-held units. Clearly, wireless communications today encompasses many technologies, systems and services, aimed at many different applications. Wireless technologies and systems can be divided into six distinct groups [6]:

1. Cellular mobile telephone systems
2. Cordless telephones
3. Wide-area wireless data systems
4. High-speed WLANs
5. Paging/messaging systems
6. Satellite-based mobile systems

Of these, the most widely used are cellular mobile telephone systems.

1.4.2 Cellular Mobile Radio Systems

Cellular mobile radio systems aim to provide high-mobility, wide-ranging, two-way wireless voice communications. These systems accomplish their task by integrating wireless access with large-scale networks, capable of managing mobile users. Cellular radio technology generally uses transmitter power at a level around 100 times that used by a cordless telephone (approximately 2 W for cellular) [7].

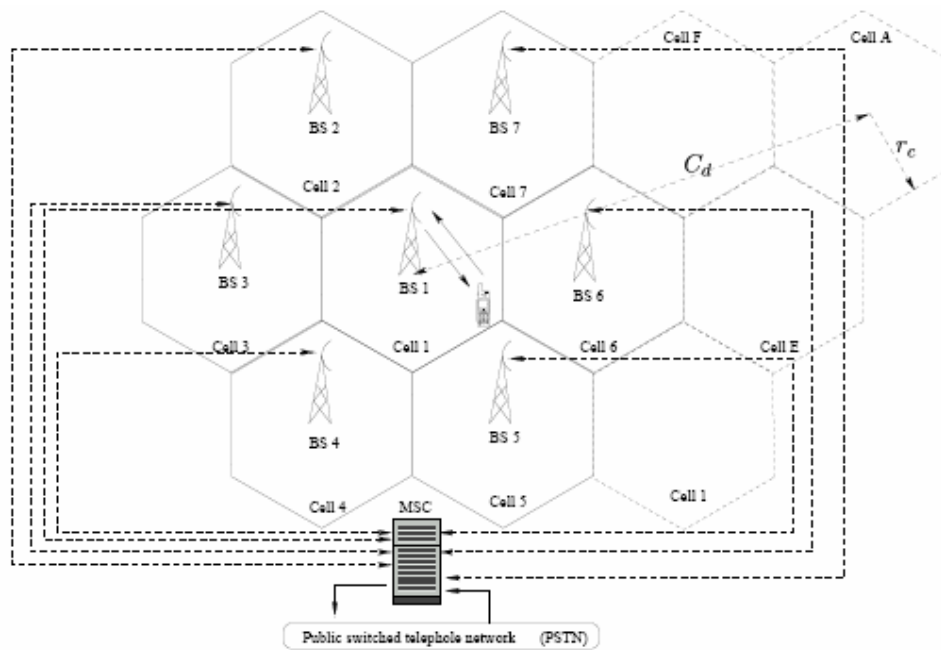


Figure 1.2: Cellular communication system

1.4.2.1 Evolution of Cellular Mobile Radio Systems

The most popular second generation standards include three TDMA standards and one CDMA standard [6] [11].

- I- *Global System Mobile (GSM)*
- II- *Interim Standard 136 (IS-136)*
- III- *Pacific Digital Cellular (PDC)*
- IV- *Interim Standard 95 Code Division Multiple Access (IS-95)*

IS-136 is also known as North America Digital Cellular (NADC). PDC is a Japanese TDMA standard is similar to IS-136 and the popular 2G CDMA standard, IS-95 is also known as *cdmaone*. Figure 1.3 shows various upgrade paths for 2G technologies [8][9].

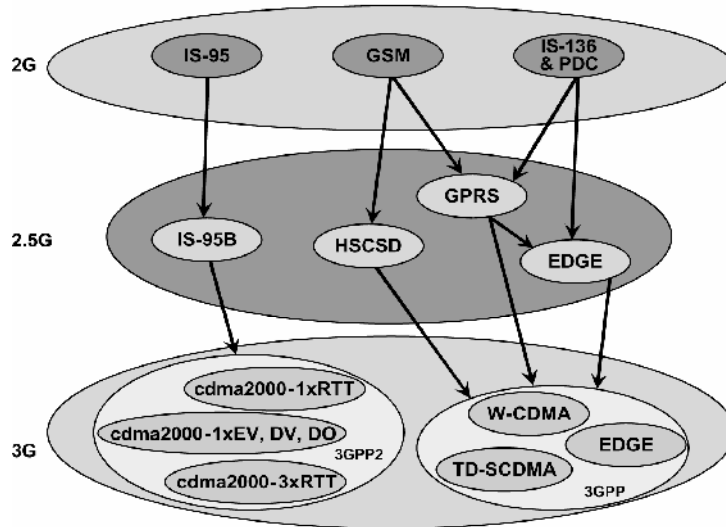


Figure 1.3: Various upgrade paths for 2G technologies.

1.5 Modulation Techniques for Mobile Radio

The aim of incorporating modulation and demodulation techniques is to achieve greater bandwidth or power efficiency in a stationary white Gaussian noise channel [6]. Since bandwidth is a limited resource, one of the primary design objectives of all the modulation schemes is to minimize the required transmission bandwidth.

In the following section, a popular modulation technique named spreads spectrum is discussed briefly.

1.5.1 Spread Spectrum Modulation Techniques

Spread spectrum techniques employ a transmission bandwidth that is several orders of magnitude greater than the minimum required signal bandwidth [10]. While the system is very bandwidth inefficient for a single user, the advantage of spread spectrum is that many users can simultaneously use the same bandwidth without significantly interfering

with one another. In a multiple-user, multiple access interference (MAI) environment, spread spectrum systems become very bandwidth efficient.

1.5.1.1 Principle of Spread spectrum

Spread spectrum (SS) is a technique whereby an already modulated signal is modulated a second time in such a way as to produce a waveform which interferes in a barely noticeable way with any other signal operating in the same frequency band. Thus, we say that interfering signals are *transparent* to spread spectrum signals and spread spectrum signals are transparent to interfering signals [12]. To provide the “transparency” described above, the spread spectrum technique is to modulate an already modulated waveform, either using amplitude modulation or wideband frequency modulation, so as to produce a very wideband signal.

Band spreading is accomplished by means of a code which is independent of the data [13]. This band spreading code is pseudo-random in nature and thus the spread signal resembles noise. A synchronized reception with the code at the receiver is used for de spreading the information before data recovery. Figure 1.4 provides a general model of spread spectrum system [15][16].

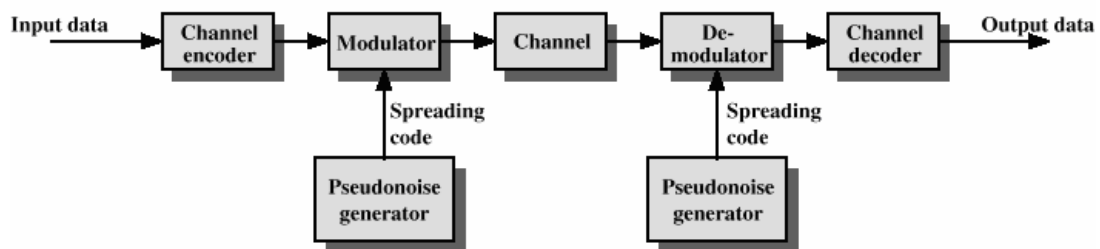


Figure 1.4: General model of spread spectrum system

1.5.1.2 Why Spread spectrum

Spread spectrum (SS) system techniques have produced results in communications, navigation and test systems that are not possible with standard signal formats. In many applications, the advent of high-speed transistors and integrated circuits was the key to practical-sized-and-powered equipment based on SS modulation. Spread spectrum is a widely adopted means of modulation due to the following characteristics [17][18].

Anti-jam / anti-interference capability: SS makes use of unpredictable bandspreading code. This signal de-spreading can then reject strong undesired signals that are even stronger than the desired ones. Figure 1.5 shows the process of interference rejection [19]. An important parameter in this regard is *Processing gain* which is usually defined as

$$G_p = \frac{\text{Transmitted signal bandwidth}}{\text{Original data bandwidth}}$$

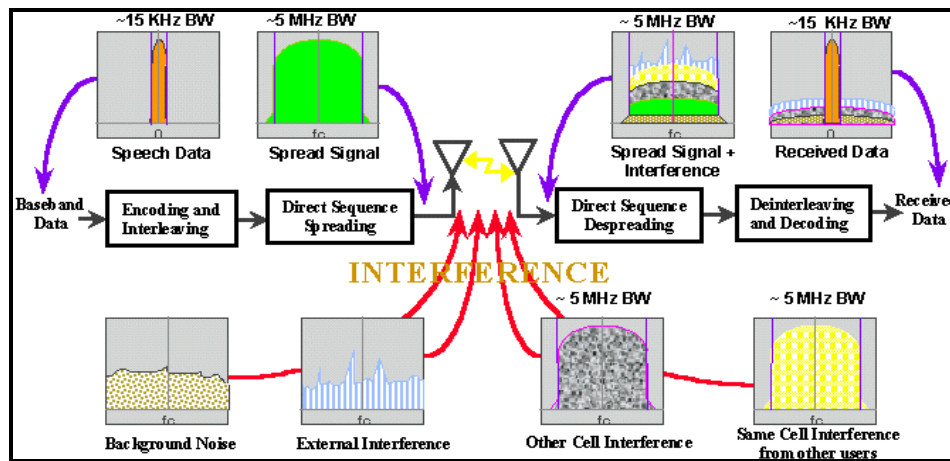


Figure 1.5: Interference rejection in spread spectrum.

Low probability of intercept (LPI): The signal is spread uniformly in the frequency domain and thus masks the transmitted signal in the background noise and making the detection of it by a surveillance receiver difficult [19].

Anti-multipath capability: Number of resolvable paths is essentially given by the bandwidth of the SS signal times the delay spread of the channel. So, there is a possibility for diversity gain by a RAKE receiver.

Multiple access: Multiple spread spectrum links can share the same band with minimal co-channel interference. Thus, benefits are obtained especially at the system level [20][21].

Accurate universal timing: Spread spectrum can be used to recover very precise timing of the received signal [22][23].

1.5.1.3 Types of Spread spectrum

In this section four important types of spread spectrum are described.

Frequency hopping (FH): The signal is rapidly switched between different frequencies within the hopping bandwidth pseudo-randomly, and the receiver knows before hand where to find the signal at any given time. Figure 1.6 is a spectrum analyzer picture of FH-SS signal [24].

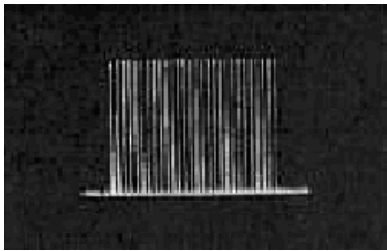


Figure 1.6: A spectrum analyzer photo of a FH spread spectrum signal

Time hopping (TH): The signal is transmitted in short bursts pseudo-randomly, and the receiver knows beforehand when to expect the burst.

Direct sequence (DS): The digital data is directly coded at a much higher frequency. The code is generated pseudo-randomly, the receiver knows how to generate the same code, and correlates the received signal with that code to extract the data. Figure 1.7 is a spectrum analyzer picture of DS-SS signal [13][25][26].

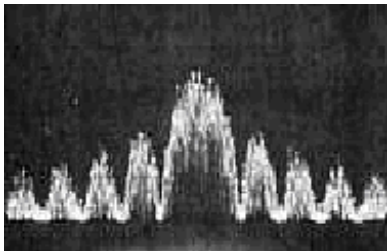


Figure 1.7: A spectrum analyzer photo of a DS spread spectrum signal

Hybrid system: This system uses combination of above mentioned techniques. The often used combinations of spread spectrum signals are:

- a- Simultaneous frequency hopping and direct sequence modulations,
- b- Simultaneous time and frequency hopping,

c- Simultaneous time hopping and direct sequence modulations [13].

1.5.1.4 Application of Spread spectrum

Due to the low probability of intercept (LPI), anti jam/interference (AJ) characteristics, the most popular applications of spread spectrum are in fields where security in transmission is an important consideration. The coded modulation characteristic of SS uniquely qualifies it for navigation – from the standpoints of both range measurements and direct finding [28]. Direct sequence spread spectrum is the most preferred form of modulation for ranging. Also, in positioning applications, spread spectrum system is used due to its excellent ability to keep track of time of transmission and reception [29].

The ability of spread spectrum system to support multiple access enables many users to operate at the same time without much interference [30]. Each receiver receives the signal intended for it because the code used at transmitting end is only known to the corresponding receiver.

In the next section, some multiple access techniques are briefly described.

1.5.2 Direct Sequence Spread Spectrum (DS-SS)

A direct sequence (DS) spread spectrum technique is performed by multiplying a radio frequency (RF) carrier and a pseudo-noise (PN) digital signal. Figure 1.7 shows a basic DS/SS system for both the transmitter and the receiver. First the PN code is modulated onto the data signal, using one of several modulation techniques (*e.g* BPSK, QPSK, etc). Then the PN modulated data signal and the RF carrier are multiplied. This process causes that the RF signal to be replaced with a very wide bandwidth signal with the spectral equivalent of a noise signal. In the reception of the signal, the receiver must not only know the code sequence to despread the signal but also it requires to be synchronised with the code generator in the transmitter.

The multiplication in the time domain of the data signal by the PN code sequence results in a signal with a frequency spectrum similar to the spectrum of the PN code signal (due

to the fact that $T_c < T$, where T_c and T represent the duration of one chip in the PN code and one symbol in the data signal respectively). Therefore, the effects of increasing the data rate from R (symbol level) to R_c (chip level) are a reduction in the amplitude spectrum (from T to T_c) and an expansion of the signal in the frequency domain. Since the wide bandwidth of the PN codes allows us to reduce the amplitude spectrum to noise levels (without loss information), the generated signals appears as background noise in the frequency domain. From another perspective, the bandwidth of the data signal is basically spread by a factor $N = T/T_c$, which corresponds to the processing gain in the DS/SS system [13][14]. In this type of systems the length of the code is the same as the processing gain. Several families of PN codes exist and some of them will be addressed in later sections. To illustrate the spread spectrum concepts, Figure 1.9 and Figure 1.10 show a sketch of the time-domain and frequency-domain representation of the signals in the DS/SS system of Figure 1.8.

From the viewpoint of a CDMA system, the most important properties of a spread spectrum technique are: multiple access capabilities, multipath interference rejection, narrowband interference rejection, and secure and privacy capabilities [14].

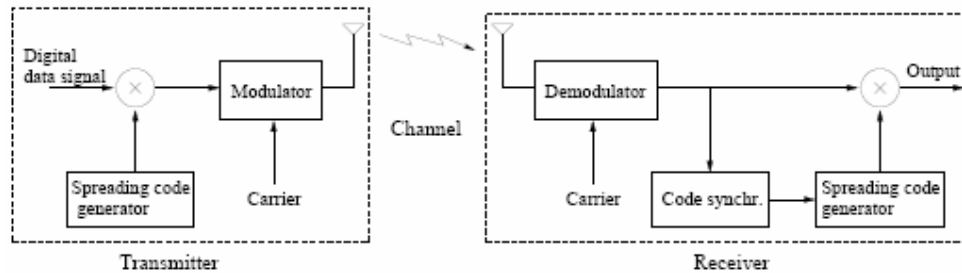


Figure 1.8: DS-SS system

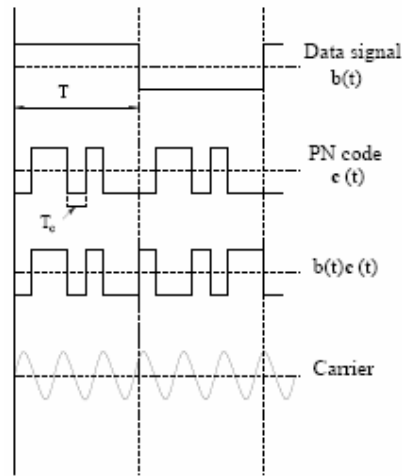


Figure 1.9: Time domain representation of the signals at the transmitter of a DS system.

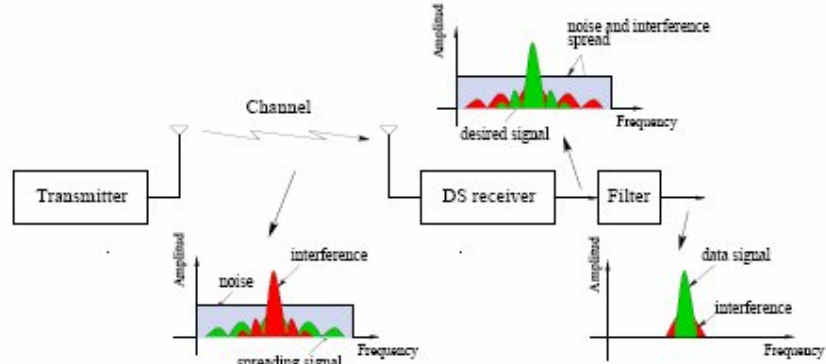


Figure 1.10: Frequency domain representation of the received signal in a DS system.

1.6 Multiple Access Techniques for Wireless Communications

Multiple access schemes are used to allow many mobile users to share simultaneously a finite amount of radio spectrum [4]. The sharing of spectrum is required to achieve high capacity by simultaneously allocating the available bandwidth (or the available amount of channels) to multiple users.

1.6.1 Duplexing

In wireless communications systems, it is often desirable to allow the subscriber to send simultaneously while receiving information to the base station while receiving information from the base station. This effect is called *duplexing* and a device called *duplexer* is used inside each subscriber unit and base station. Duplexing may be done

using frequency or time domain techniques. Figure 1.11 illustrates FDD (Frequency Division Duplexing) and TDD (Time Division Duplexing).

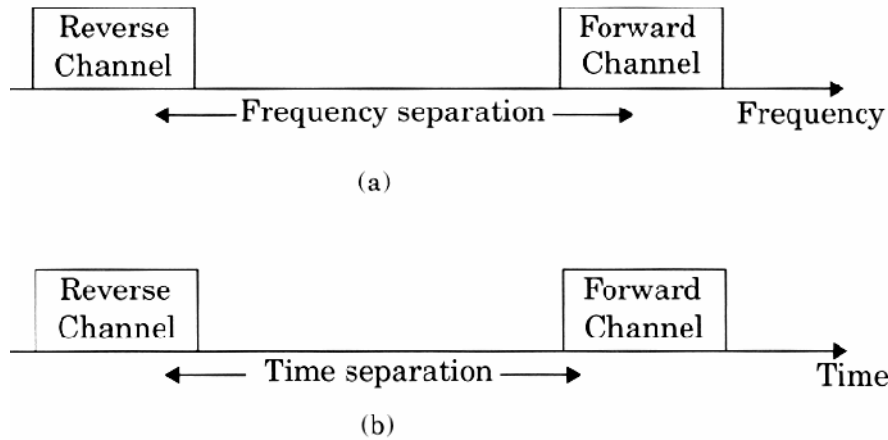


Figure 1.11: (a) FDD provides two simplex channels at the same time; (b) TDD provides two simplex time slots at the same frequency.

1.6.2 Multiple Access

Three types of multiple access techniques are used in wireless communications.

FDMA (*Frequency Division Multiple Access*): Each user is allocated a unique frequency band or channel [32]. These channels are assigned on demand to users who request service. During the period of the call, no other user can share the same channel. If an FDMA channel is not in use, then it sits idle and cannot be used by other users to increase or share capacity. It is essentially a wasted resource. Figure 1.12 illustrates a FDMA system.

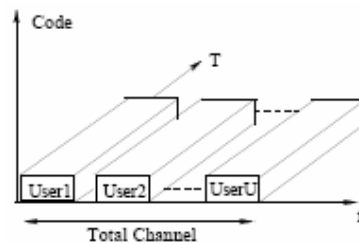


Figure 1.12: Frequency division multiple access (FDMA).

TDMA (*Time Division Multiple Access*): TDMA system divide the radio spectrum into time slots, and in each slot only one user is allowed to transmit and receive [32]. It can be

seen from Figure 1.13 that each user occupies a cyclically repeating time slot, so a channel may be thought of as a particular time slot that reoccurs every frame, where N time slots comprise a frame.

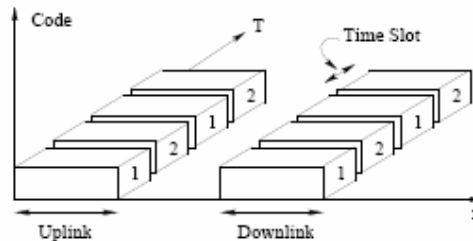


Figure 1.13: Time division multiple access (TDMA).

CDMA (Code Division Multiple Access): In CDMA systems, the narrowband message signal is multiplied by a very large bandwidth signal called the *spreading signal* [14]. The spreading signal is a pseudo-noise code sequence that has a chip rate which is orders of magnitudes greater than the data rate of the message. All users in a CDMA system, as seen from figure 1.14, use the same carrier frequency and may transmit simultaneously. Each user has its own pseudorandom codeword which is approximately orthogonal to all other codewords. The receiver performs a time correlation operation to detect only the specific desired codeword. All other codewords appear as noise due to decorrelation. For detection of the message signal, the receiver needs to know the codeword used by the transmitter. Each user operates independently with no knowledge of the other users.

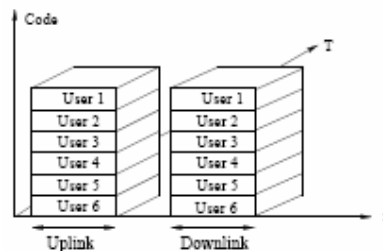


Figure 1.14: Code division multiple access (CDMA).

Table 1.2 [6] shows the different multiple access techniques being used in various wireless communications systems around the world.

Cellular System	Multiple Access Technique
Advanced Mobile Phone System(AMPS)	FDMA/FDD
Global System for Mobile(GSM)	TDMA/FDD
US Digital Cellular(USDC)	TDMA/FDD
Pacific Digital Cellular(PDC)	TDMA/FDD
CT2(Cordless Telephone)	FDMA/TDD
Digital European Cordless Telephone(DECT)	FDMA/TDD
US Narrowband Spread Spectrum(IS-95)	CDMA/FDD
W-CDMA(3GPP)	CDMA/FDD CDMA/TDD
cdma2000(3GPP2)	CDMA/FDD CDMA/TDD

Table 1.2: Multiple access techniques used in different wireless communication systems.

1.7 Layout of Thesis

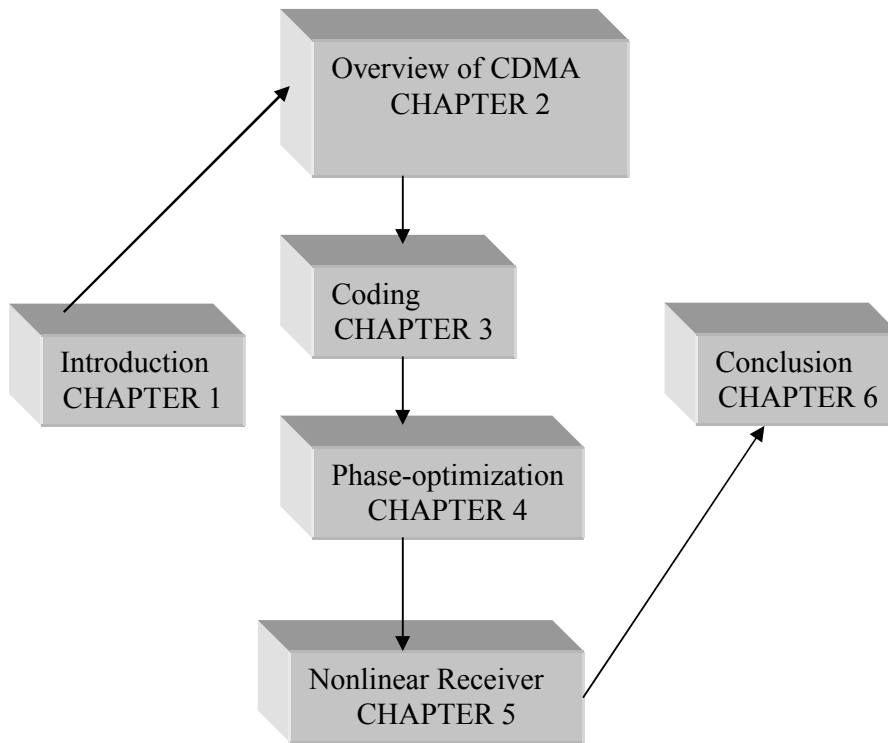


Figure 1.15: Structure of the thesis.

Figure 1.15 depicts schematically, the whole structure of the thesis. Chapter 1 is an introductory channel and briefly describes the wireless technology. Chapter 2 gives an overview of DS-CDMA. Chapter 3 considers various types of spreading sequences and

summarizes their property. Chapter 4 optimizes these codes so that their performance is standardized. Chapter 1, 2, 3 and 4 together constitute the part I of this thesis. Part II of this thesis which consists of chapter 5, considers a nonlinear receiver. The proposed receiver is based on RBF structure and exploits the PPB architecture.

1.8 Conclusion

After a brief introduction to wireless technology and its evolution, this chapter focuses primarily on spread spectrum technique. Some of the properties of SS along with its widespread application are also described in this chapter. Emphasis is given on DS-SS, the direct sequence form of spread spectrum as DS-CDMA is considered in this thesis. Various multiple access techniques with the aid of figures are also described.

Chapter 2

CDMA Overview

2.1 Introduction

Spread spectrum multiple access (SSMA) uses signals which have a transmission bandwidth that is several orders of magnitude greater than the minimum required RF bandwidth. A pseudo-noise (PN) sequence converts a narrowband signal to a wideband noise-like signal before transmission. SSMA also provides immunity to multipath interference and robust multiple access capability. SSMA is not very bandwidth efficient when used by a single user. However, since many users can share the same spread spectrum bandwidth without interfering with one another, spread spectrum systems become bandwidth efficient in a multiple user environment. It is exactly this situation that is of interest to wireless system designers. There are two main types of spread spectrum multiple access techniques; *frequency hopped multiple access (FH)* and *direct sequence multiple access (DS)*. Direct sequence multiple access is also called *code division multiple access (CDMA)*.

Next section describes the CDMA principle. Later sections are devoted for describing the IS-95 standard. These sections describe both forward and reverse channel schematically and major functional blocks are treated with the aid of diagrams in subsections.

2.2 CDMA Principle

In direct-sequence CDMA (DS-CDMA), users can share the same channel because they are assigned unique spreading codes to minimize mutual interference [6][14]. To illustrate the application of spread spectrum technique in this multiple access scheme, consider two users in a system as shown in Figure 2.1 [31][34]. The spreading codes of the two users, $s_1(t)$ and $s_2(t)$, are distinct from each other. Assuming a noise free channel,

the output signals of both transmitters arrive at both receivers as a single signal, which is given as $b_1(t) s_1(t) + b_2(t) s_2(t)$. Each receiver correlates the received signal with their respective spreading code. From the normalized autocorrelation, $s_1^2(t) = s_2^2(t) = 1$, the resulting outputs are $b_1(t) + b_2(t) s_1(t) s_2(t)$ and $b_2(t) + b_1(t) s_1(t) s_2(t)$. If orthogonal spreading codes are used, the ideal cross correlation is $s_1(t) s_2(t) = 0$, and the idealized outputs are simply $b_1(t)$ and $b_2(t)$ respectively. However, this is usually not the case. The residual, non-zero term translates to CCI for other users in the CDMA system and this interference is called multiple access interference (MAI). Fortunately, the residual cross-correlation term, which appears like background noise to a simple receiver, is small and the desired information can still be recovered successfully, as seen in the spectrum of the output. As the number of users increases, the power of the MAI also increases and the system performance degrades. The work here focuses only on the intra-cell interference (interference from users within the same cell), and inter-cell interference (leakage from adjoining cells) is modeled as a contribution to the background Gaussian noise. Hence, there is a limitation to the number of users in the CDMA system sharing the same spectrum. This limitation is affected by the processing gain, the correlation of the spreading codes, the relative power of transmission, noise and many other factors. Therefore, the capacity of a CDMA system is softly limited, i.e., the maximum number of users is not clear-cut, unlike the other two schemes (FDMA and TDMA), where the number of users cannot go beyond the number of frequency bands or time slots [32].

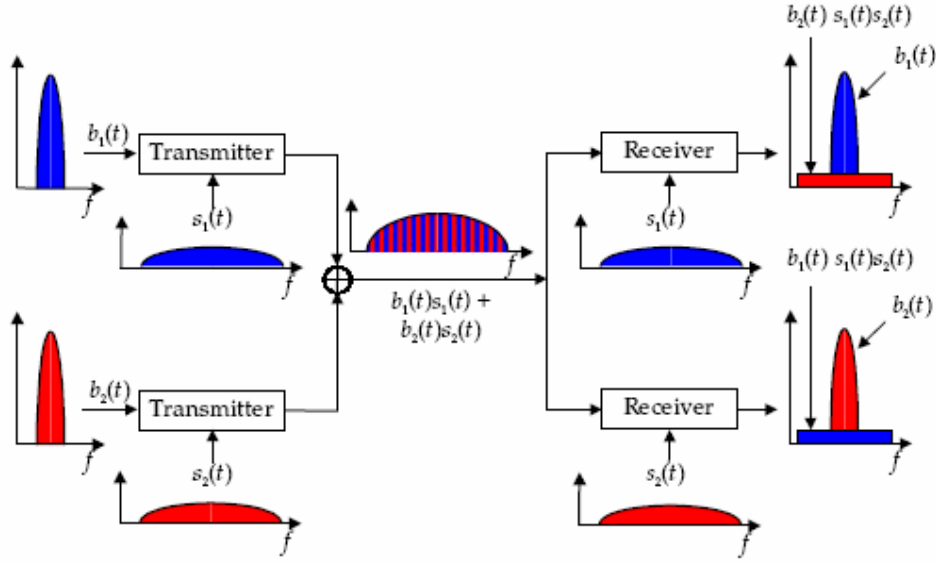


Figure 2.1: Two user DS-CDMA system

CDMA from the viewpoint of a DSS system using BPSK is considered next. Figure 2.2 depicts a configuration, in which there are n users, each transmitting using a different, orthogonal, PN sequence. For each user, the datastream to be transmitted, $d_i(t)$, is BPSK modulated to produce a signal with a bandwidth of W_s and then multiplied by the spreading code of that user, $c_i(t)$. All of the signals, plus noise, are received at the receiver's antenna. Suppose that the receiver is attempting to recover the data of user 1. The incoming signal is multiplied by the spreading code of user 1 and then demodulated [35]. The effect of this is to narrow the bandwidth of that portion of the incoming signal corresponding to user 1 to the original bandwidth of the unspread signal, which is proportional to the data rate. Because the remainder of the incoming signal is orthogonal to the spreading code of user 1, that remainder still has the bandwidth W_s . Thus the unwanted signal is concentrated in a narrow bandwidth. The bandpass filter at the demodulator can therefore recover the desired signal [36].

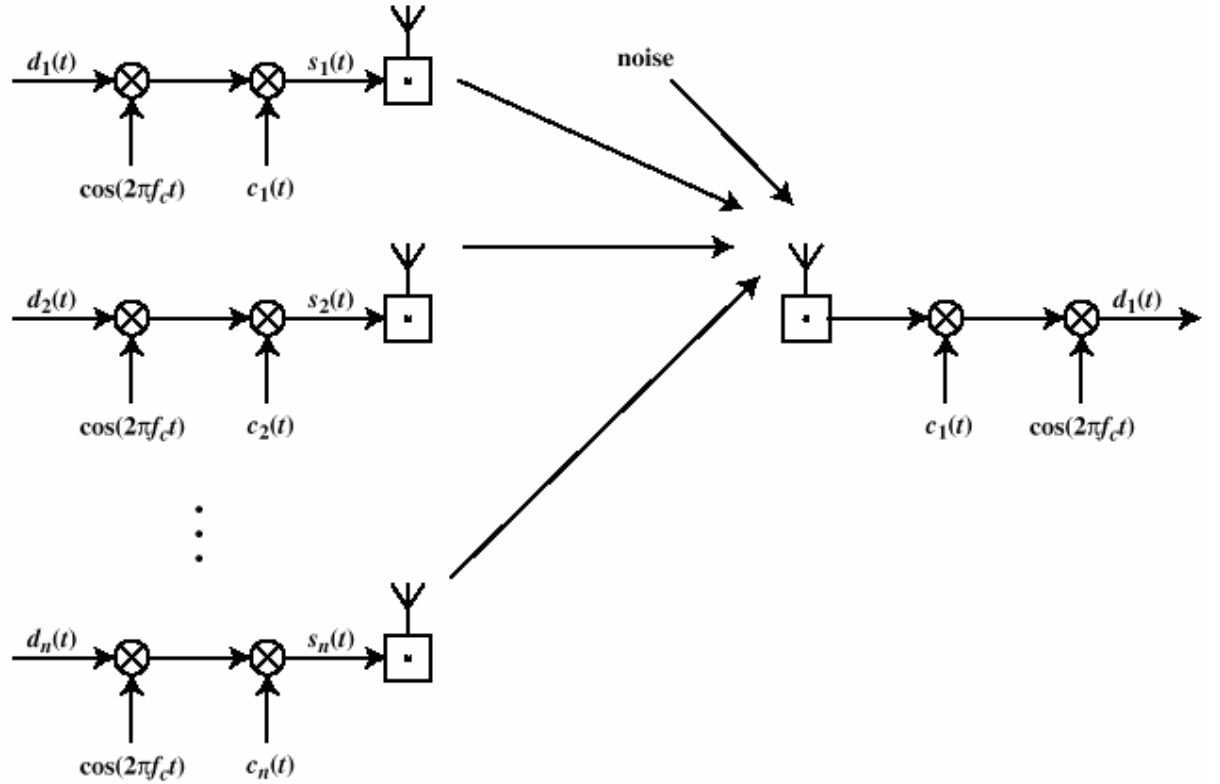


Figure 2.2: CDMA in a DSSS environment

2.3 IS-95 Standards - Fundamentals

Unlike other cellular standards, the user data rate (but not the channel chip rate) changes in real time, depending on the voice activity and requirements in the network. Also IS-95 uses a different modulation and spreading technique for the forward and reverse link. On the forward link, the base station simultaneously transmits the user data for all mobiles in the cell by using a different spreading sequence for each mobile. A pilot code is also transmitted simultaneously and at a higher power level, thereby allowing all mobiles to use coherent carrier detection while estimating the channel conditions. On the reverse link, all mobiles respond in an asynchronous fashion and have ideally a constant signal level due to power control applied by the base station.

The system used for simulation in this thesis is based on the IS-95 CDMA standard proposed by QUALCOMM [37]. This standard describes both forward and reverse channels which are composed of traffic, paging, pilot, access, and synchronization

channels [4][38]. The forward channel is defined as the link from the base station to the handset and the reverse channel is the link from the handset to the mobile. The forward channel is composed of one pilot channel, up to seven paging channels, up to one synchronization channel, and up to 63 traffic channels. The pilot channel transmits a zero information signal and is used for coherent demodulation at the handset. The synchronization channel is optional and provides relative offset information for the pilot channel. Paging channels are used for call setup and other networking features. The traffic channels represent the physical layer of the system where voice (and possibly data) information is exchanged. One possible configuration is to operate the system with the pilot channel and 63 traffic channels. The reverse channel is composed of access channels and traffic channels. Access channels are used to respond to pages and to initiate contact with the base station. There must be at least one access channel for every paging channel supported. All the channels use DS-CDMA, but only the traffic channels are of critical concern. The simulation models only reverse traffic channels since the receiver structures presented are only practical at the base station. The following descriptions are taken from the IS-95 standard [38]. Other works have covered the IS-95 standard such as [39] which describes the forward and reverse traffic channels in greater detail. Figure 2.3 and figure 2.4 show the channel schematic (both forward and reverse) of IS-95 standard.

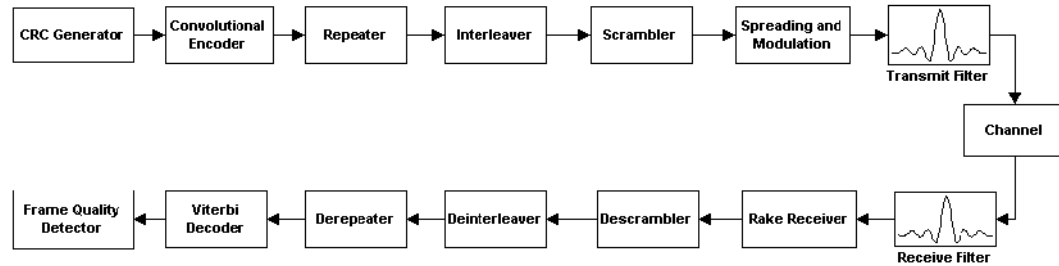


Figure 2.3: IS-95 Forward channel schematic

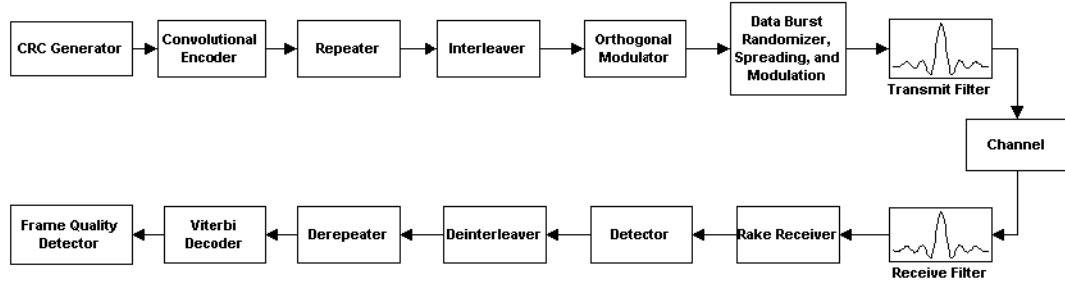


Figure 2.4: IS-95 Reverse channel schematic

2.4 Reverse Traffic Channel

The IS-95 standard allows for multiple speech data rates in the reverse traffic channel. These include 9600, 4800, 2400, and 1200 bps (subsequent versions of the standard now also allow for a 13.6 kbps voice coder). These varying data rates take into account the voice activity of a particular user. For this simulation, we will limit the data rate to 9600 bps for all users. This generates a worst-case scenario for a CDMA system as the transmitted power will be constant in a full-rate transmission as opposed to a reduced-rate. The interference, consequently, will never be reduced by voice activity detection.

Data on the reverse traffic channel is grouped into 20 ms frames. At 9600 bps, the number of data bits output from the vocoder is 172 which correspond to an 8.6 kbps vocoder rate. A 12 bit CRC check is appended to this in order to provide a frame quality indicator. Another 8 bits of padded zeroes are also added. These zeroes flush out and reset the convolutional encoder shift register. This 192 bit frame is then encoded by a 1/3 rate convolutional encoder and interleaved. The interleaved bits are then grouped into code symbols which are orthogonally modulated. These modulation symbols are then spread at a rate of 1.2288 million chips per second (Mcps). Table 2.1 from [38] demonstrates the resulting transmission rates. Figure 2.5 depicts the critical elements of the reverse channel modulation process [6].

<i>Parameter</i>	<i>Data Rate (bps)</i>			
User data rate	9600	4800	2400	1200
Code rate	1/3	1/3	1/3	1/3
Tx Duty Cycle (%)	100.0	50.0	25.0	12.5

Coded Data Rate (sps)	28,800	28,800	28,800	28,800
Bits per Walsh Symbol	6	6	6	6
Walsh Symbol Rate	4800	4800	4800	4800
Walsh Chip Rate (kcps)	307.2	307.2	307.2	307.2
Walsh Symbol Duration (μ s)	208.33	208.33	208.33	208.33
PN Chips/Code Symbol	42.67	42.67	42.67	42.67
PN Chips/Walsh Symbol	256	256	256	256
PN Chips/Walsh Chip	4	4	4	4
PN Chip Rate (Mcps)	1.2288	1.2288	1.2288	1.2288

Table 2.1: Reverse traffic channel modulation parameters

Some parameters were not included in this simulation of IS-95 in order to reduce complexity. One of these parameters is the power control mechanism. IS-95 uses both open-loop and closed-loop power control. Open-loop power control is used by the handset. The received power at the handset is used as a reference point so that when the received signal power is low, the handset assumes it is farther away from the base station and boosts its transmit power. The sum of the received and transmitted power in dB must yield a constant. The base station uses closed-loop power control to force the handset to deviate from its current transmitting power level. Every 1.25 ms a power control bit is sent, by puncturing the transmitted bits that adjusts the handset's power by 1 dB [40]. The power control function was not directly implemented in this simulation. Instead, either ideal power control was assumed or a fixed power differential was assigned to groups of users.

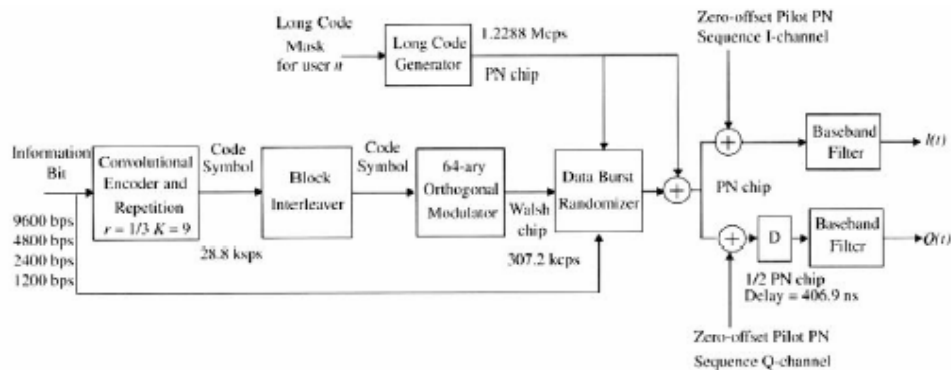


Figure 2.5: Reverse Channel Transmitter for IS-95

The data burst randomizer used immediately after orthogonal modulation was also not included as this component is a function of the data rate and serves no purpose at 9600 bps.

2.4.1 Convolutional Encoder

Convolutional encoders play an important role in the development of modulation schemes for wireless systems. Convolutional codes add a structured redundancy to the information source that mitigates the effect of random noise corrupting the data stream. Convolutional codes perform better in the marginal regions of bit error rates ($10^{-2} - 10^{-4}$) than block codes such as Reed-Solomon [41]. Since voice communications systems perform satisfactorily in this range and are often designed for those bit error rates convolutional codes are a common element in wireless systems. Convolutional codes gain their name from the fact that the information source is mathematically convolved with the impulse response of the code [42]. This impulse response is defined by generator functions for a particular code. There is a generator function for every output of a convolutional encoder. These convolutional encoders are physically constructed by using shift registers with taps determined by the generator functions. The rate of the encoder is defined as the ratio of inputs to outputs. The number of taps on the shift register determines how many of the output bits are influenced by the input bits. The number of influenced output bits is called the constraint length. To avoid confusion, in practice the constraint length of an encoder is usually taken to be the number of memory elements in the shift register plus one. Advantage of shift registers is that they can be readily implemented in any programming language making them easy to simulate. IS-95 defines a rate 1/3 encoder with constraint length $K = 9$, thus there are eight memory elements in the shift register. The generator functions in octal are $g_0 = 557$, $g_1 = 663$, and $g_2 = 711$. Figure 2.6 shows the necessary taps for the IS-95 reverse channel convolutional encoder.

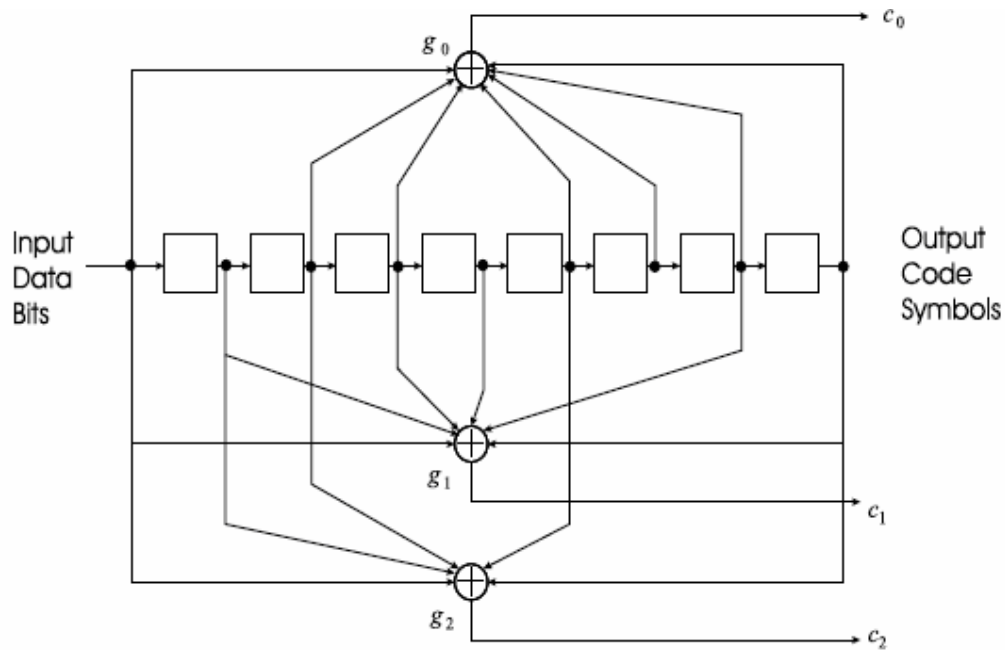


Figure 2.6: Convolutional Encoder for IS-95 Reverse Channel

2.4.2 Interleaving

While convolutional codes perform well in correcting random errors typical in a Gaussian noise environment, they are very susceptible to deep fades. The burst of errors that may occur in a fade common to a multipath environment can be prevented by randomizing the placement of the errors. One possible implementation of interleaving is the block interleaver. Bits are input to an $m \times n$ matrix by columns and read out by rows. The number of rows in the interleaver must be at least as large as the average fading duration expected in the channel to effectively randomize the code symbols. For finite block lengths the maximum separation between symbols cannot be larger than the block size of the interleaver. For a slowly changing channel, such as low-speed vehicles, it may not be possible to completely decorrelate any two symbols. For this reason many interleavers are chosen so that symbols related to an input bit are evenly spaced throughout the interleaver block [43]. In order to achieve such a spread, the number of columns in the interleaver must be greater than the constraint length of the convolutional encoder. IS-95 uses a 32×18 matrix which spans the 20 ms frame. For reduced data rates, the interleaver introduces redundancy into the information by repeating symbols.

2.4.3 64 ary Orthogonal Modulator

The modulation type for the reverse channel is 64-ary orthogonal modulation. Every six code symbols select one of 64 possible orthogonal modulation symbols. The modulation symbols are generated using Walsh functions. The 64 modulation symbols are numbered 0 through 63 and are selected according to the following formula [38].

$$\text{Modulation symbol number} = c_0 + 2c_1 + 4c_2 + 8c_3 + 16c_4 + 32c_5 \quad (2.1)$$

where the c_n represents the n th code symbol. The 64 by 64 matrix of modulation symbols is readily generated by recursion with

$$W_{2n} = \begin{bmatrix} W_n & W_n \\ W_n & \overline{W_n} \end{bmatrix} \quad (2.2)$$

where the seeding function is $W_1 = 0$, and continues with

$$W_2 = \begin{bmatrix} 00 \\ 01 \end{bmatrix} \quad (2.3)$$

The value n is a power of 2. The Walsh chip rate is 307.2 kilo chips per second (kcps).

2.4.4 Long code Spreading

After modulation the Walsh chips are spread by direct sequence using the long PN sequence. Each user is uniquely assigned a long PN sequence of period $2^{42}-1$ chips. Since the sequence is clocked at 1.2288 Mcps, this period corresponds to about 41 days. The long code is defined by the polynomial:

$$p(x) = x^{42} + x^{35} + x^{33} + x^{31} + x^{27} + x^{26} + x^{25} + x^{22} + x^{21} + x^{19} + x^{18} + x^{17} + x^{16} + x^{10} + x^7 + x^6 + x^5 + x^3 + x^2 + x^1 + 1 \quad (2.4)$$

Every PN chip is generated by the modulo-2 product of the long code shift register and the long code mask. Figure 2.7 is a diagram of the long PN sequence generator. The initial state of the generator is such that the output is a '1' followed by 41 zeroes. The long code mask has three states: an initialization state, a public mask used for setup that is unique to the handset's electronic serial number (ESN), and a private mask unique to

the mobile station identification number (MIN). The initialization state of the mask has the most significant bit (MSB) set to '1' and the remaining 41 bits set to zeroes. The public mask has the ten most significant bits set to '1100011000' with the remaining 32 bits composed of a permutation of the ESN. This permutation has this format:

$$\text{ESN} = (E_{31}, E_{30}, E_{29}, E_{28}, E_{27}, \dots, E_3, E_2, E_1, E_0)$$

$$\text{Permuted ESN} = (E_0, E_{31}, E_{22}, E_{13}, E_4, E_{26}, E_{17}, E_8, E_{30}, E_{21}, E_{12}, E_3, E_{25}, E_{26}, E_7, E_{29}, E_{20}, E_{11}, E_2, E_{24}, E_{15}, E_6, E_{28}, E_{19}, E_{10}, E_1, E_{31}, E_{23}, E_{14}, E_5, E_{27}, E_{18}, E_9)$$

The private mask is generated through a confidential process and was not used in the simulation. After the initial state is generated, the public mask is used for all frame transmissions. The ESN used was a random bit sequence.

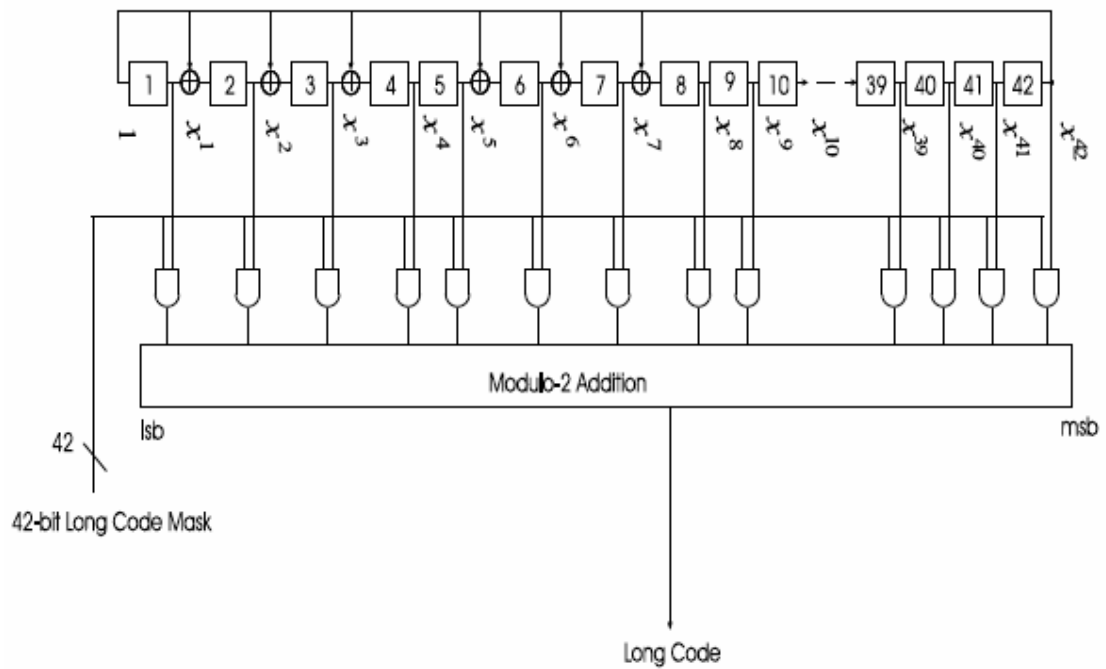


Figure 2.7: Long PN code generator for IS-95

2.4.5 Quadrature Modulation

After the long code spreading, the chips are sent to both in-phase (I) and quadrature (Q) arms where they are further spread by separate I and Q PN sequences. The resulting Q symbol stream is delayed by one half a PN chip (406.901 ns). This is offset quadrature

phase shift keying (OQPSK) PN spreading combined with binary phase shift keying data modulation. Figure 2.8 shows the signal constellation for OQPSK. OQPSK is used in the reverse channel to control the spectral characteristics of the RF signal. The lack of 180 degree phase transitions in the signal constellation means that the envelope of a bandlimited (or pulse shaped) signal will not go to zero. Power efficient nonlinear amplification will not cause large sidelobe regeneration improving spectral efficiency [1]. QPSK type modulation may also be detected noncoherently eliminating the need for a pilot tone, consequently improving the power efficiency.

The clock rate of these I and Q chips is matched to the data rate so no bandwidth spreading occurs. The purpose of these sequences is to allow for rapid acquisition of the signal at the receiver and to prevent any I and Q mixing products. Both sequences have a 15 element shift register with a period of $2^{15} - 1$. This is increased to 2^{15} by shifting in a zero after 14 zeroes have occurred to give the all zeroes state. The initial state of both these sequences has the MSB set to the value 1 and all remaining registers set to 0. The I PN sequence polynomial is [6][38]

$$P_I(x) = x^{15} + x^{10} + x^8 + x^7 + x^6 + x^2 + 1; \quad (2.5)$$

The Q PN sequence polynomial is

$$P_Q(x) = x^{15} + x^{13} + x^{11} + x^{10} + x^9 + x^5 + x^4 + x^3 + x^1 + 1 \quad (2.6)$$

These I and Q PN sequences are not guaranteed to be orthogonal over the entire transmission; although, it is hoped that the crosscorrelation is very low. This has consequences when dealing with a noncoherent link such as the reverse channel in IS-95. It will be shown later that mixing of the I and Q channels may degrade the system performance.

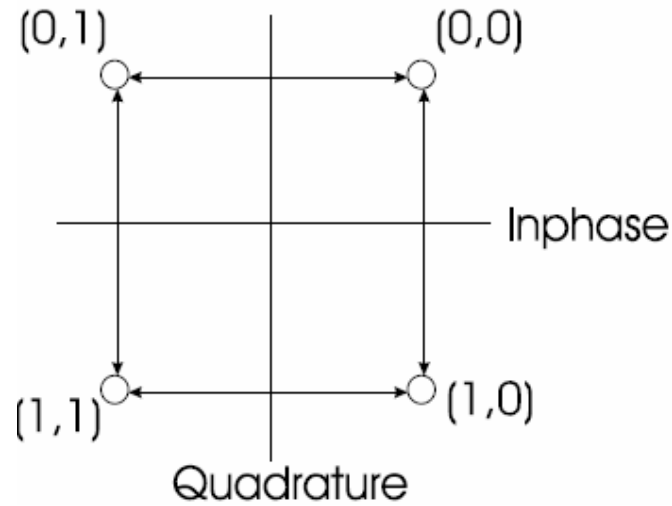


Figure 2.8: IS-95 reverse channel signal constellation

2.4.6 Baseband Filtering

Pulse-shaping is required for both the I and Q channels. The purpose of this pulse shaping is to bandlimit the signal to meet FCC regulations. This pulse-shaping filter is identical for both I and Q channels. These coefficients are separated in time by one fourth a PN chip (203.5 ns).

Most filtering used in mobile communications obeys Nyquist's pulse-shaping criterion for zero intersymbol interference (ISI). His theorem states that the received pulse shape, $p_r(t)$, must have the property

$$p_r(nT) = \begin{cases} 1, n = 0 \\ 0, n \neq 0 \end{cases}$$

Where T is the symbol period and n is any integer. For matched filtering, one would convolve the transmitted pulse-shape with a time-reversed version in order to minimize the noise [44]. All sampling instants after convolution must occur at $t = nT$ for there to be zero ISI. For IS-95, the receiver filter is identical to the pulse-shaping filter due to symmetry. The convolution of the two filters is shown in Figure 2.9 with the sampling instances marked by the symbol 'X'. It is notable that where the sampling instances occur, the waveform is not equal to zero. The modified pulse-shape has better spectral characteristics than conventional raised cosine filter. The resulting ISI is acceptable when attempting to meet stringent bandwidth constraints.

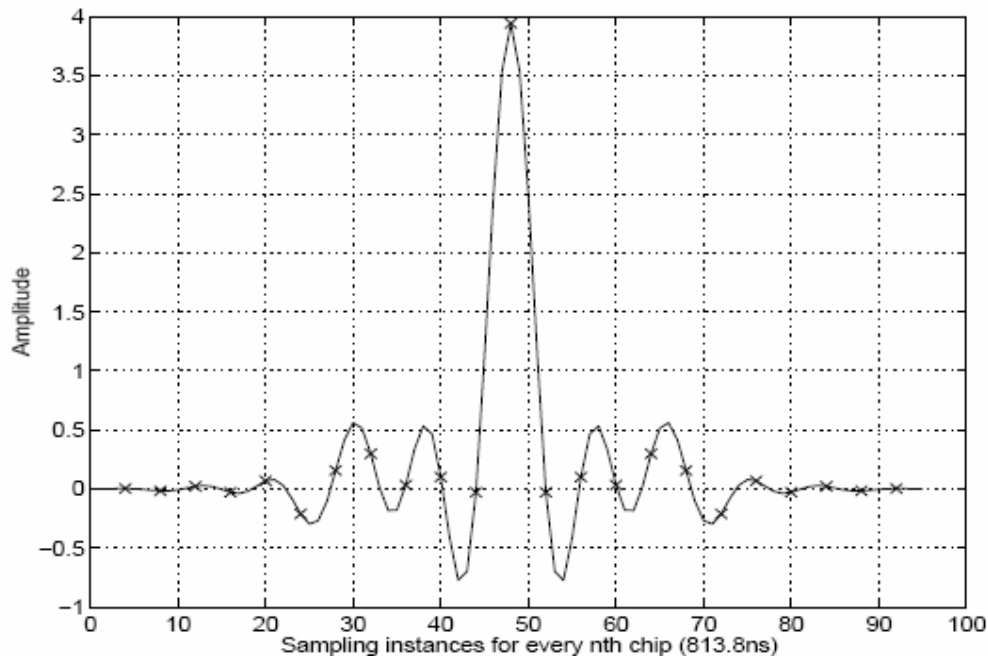


Figure 2.9: Convolution of pulse-shaping filter with matched filter; appropriate sampling instances for each chip are marked with 'X'.

2.5 Forward Traffic Channel

The forward CDMA channel consists of a pilot channel, synchronization channel, up to seven paging channels, and up to sixty-three forward traffic channels [39]. The pilot channel allows a mobile station to acquire timing for the forward CDMA channel, provides a phase reference for coherent demodulation, and provides each mobile with a means for signal strength comparisons between base stations for determining when to hand off. The synchronization channel broadcasts synchronization messages to the mobile stations and operates at 1200 bps. The paging channel is used to send control information and paging messages from the base station to the mobiles and operates at 9600, 4800, and 2400 bps. The forward traffic channel (FTC) supports variable user data rates at 9600, 4800, 2400, or 1200 bps.

The forward traffic channel modulation process is described in figure 2.10 [45]. Data on the forward traffic channel is grouped into 20ms frames. The user data is first convolutionally coded and then formatted and interleaved to adjust for the actual user data rate, which may vary. Then the signal is spread with a Walsh code and a long PN

sequence at a rate of 1.2288 Mcps. Table 2.2 [6] lists the coding and repetition parameter for the forward traffic channel. The speech data rate applied to the transmitter is variable over the range of 1200bps to 9600bps.

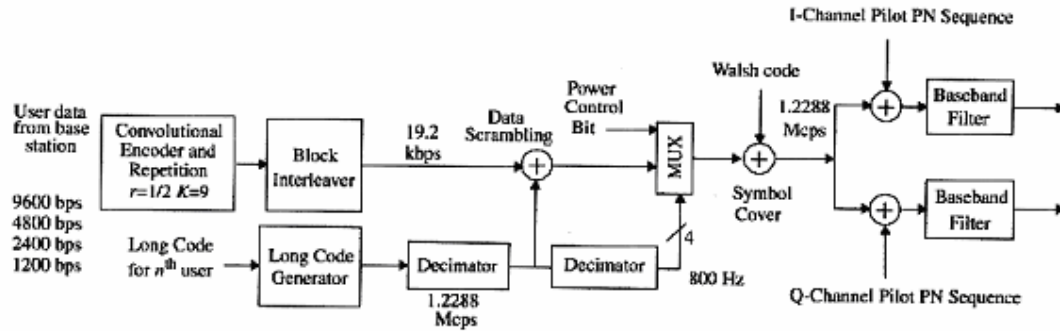


Figure 2.10: Forward CDMA channel modulation process.

Parameter	Data Rate(bps)			
User data rate	9600	4800	2400	1200
Coding Rate	1/2	1/2	1/2	1/2
User Data Repetition Period	1	2	4	8
Baseband Coded Data Rate	19,200	19,200	19,200	19,200
PN Chips/Coded Data Bit	64	64	64	64
PN Chip Rate(Mcps)	1.2288	1.2288	1.2288	1.2288
PN Chips/Bit	128	256	512	1024

Table 2.2: IS-95 forward traffic channel modulation parameters.

2.6 Modification to IS-95

In an attempt to improve the speech quality of IS-95, the physical layer has been modified to accommodate a higher data rate [37]. On the forward link, the convolutional encoder has been modified from a rate 1/2 to a rate 3/4 by puncturing the code stream, i.e. removing symbols that would only increase redundancy. The reverse channel has been modified by reducing the 1/3 rate code to a 1/2 rate code. Consequently, the data rates possible are now increased by 50%. The new speech codec developed by QUALCOMM has been modified to take advantage of the increased data rates by increasing the quantization of the speech and improving voice activity detection. The increased data rate makes the CDMA standard more attractive to data users. In this thesis, however, we focus primarily on the 9600 bps data rate.

2.7 Conclusion

Since CDMA is direct sequence form of spread spectrum signal, after chapter 1 in which spread spectrum modulation technique is described, this chapter focuses primarily on CDMA technology. The IS-95 standardized parameters are summarized in tabular form. Both forward (downlink) and reverse (uplink) modulation processes are considered.

Chapter 3

Overview of Coding Techniques

3.1 Introduction

The definition of spread spectrum [10][26] mentions that the band spread is accomplished by a means of a code which is independent of the data and a synchronized reception with the code at the receiver is used for despreading and subsequent data recovery.

The “code” in this definition is a pseudorandom code that is mixed with the data to “spread” the signal. Thus for the spread signal to appear noiselike, the code needs to be random but reproducible [36]. This is an apparent contradiction in terms since a truly random signal is unpredictable. Nevertheless, pseudorandom number generation is statistically random, repeatable and well-understood. In order to recover the spread signal, both the transmitter and the receiver must know the coding sequence and be able to synchronize to one another [36][46]. Thus the spreading code is a pseudorandom sequence and is called the pseudo noise (PN) code. Figure 3.1 illustrates the spreading done on the data signal $p(t)$ by the spreading signal $c(t)$ resulting in the message signal to be transmitted, $m(t)$.

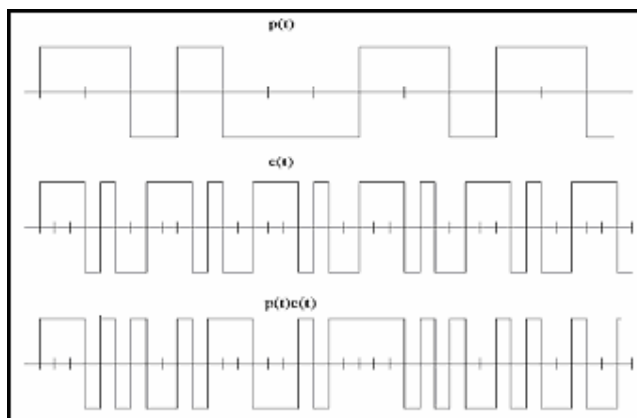


Figure 3.1: Spreading of Data signal: $p(t)$ by Code Signal: $c(t)$

Here code sequence $c(t)$ is a sequence of binary digits and is shared by both transmitter and receiver.

Next section outlines the advantages of spreading. Later sections describe important properties of spreading codes like Gold, Kasami and M-sequence. Section 3.8 describes the concept of multiple spreading and section 3.9 is devoted to error correcting codes. The chapter ends with summarization of all coding techniques.

3.2 Advantages of Spreading

Spreading causes increase in data rate which is equal to that of spreading sequence. Spreading also increases bandwidth but at the cost of the redundancy of the system. It should be noted that coding is necessary to provide properties to spread spectrum which are advantageous for communication and ranging application [13]. The properties which are claimed by a spread spectrum system due to coding are:

- Selective addressing capability.
- Code division multiplexing is possible for multiple access.
- Low-density power spectra for signal hiding.
- Message screening from eavesdroppers.
- High-resolution ranging.
- Interference rejection.

These properties come about as a result of the coded signal format and wide signal bandwidth. A single receiver or a group of receivers may be addressed by assigning a given reference code to them, whereas others are given a different code. Selective addressing can then be as simple as transmitting the proper code sequence as modulation.

Not all of these characteristics are necessarily available from the same system at the same time. It is somewhat anomalous, for instance, to expect at the same time a signal that is easily hidden but can also be received in the face of a large amount of interference. Signal-hiding requirements and interference are often at odds, but the same system might be used for both by using lower-power transmission when low detectability is desired and high power transmissions when maximum interference rejection is needed.

When codes are properly chosen for low cross correlation, minimum interference occurs between users, and receivers set to use different codes are reached only by transmitters sending the correct code. Thus more than one signal can be unambiguously transmitted at the same time and the same frequency. Selective addressing and code-division multiplexing are implemented by the coded modulation format.

Because of the wideband signal spectra generated by code modulation, the power transmitted is low in any narrow region. At any rate, the density of a spread spectrum signal is far less than that of more conventional signals in which all the transmitted power is sent in a band of frequencies commensurate with the baseband information bandwidth.

Again, because of the coded signal employed, an eavesdropper cannot casually listen to messages being sent. Though the may not be “secure”, some conscious effort must be made to decode the message [13].

Resolution in ranging is afforded in accordance with the code rate used, and the sequence length determines maximum unambiguous range. Ranging has been the best known use of spread spectrum system and is discussed in Appendix B of this thesis.

3.3 Properties of Spreading Code

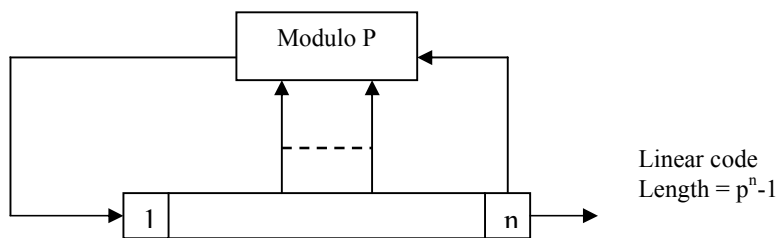
As was mentioned the spreading sequence $c(t)$, is a sequence of binary digits shared by transmitter and receiver. Spreading consists of multiplying (XOR) the input data by the spreading sequence [47]. The spreading codes are chosen so the resulting signal is noise like; therefore, there should be an approximately equal number of ones and zeros in the spreading code and few or no repeated patterns. When spreading codes are used in a CDMA application, then there is the further requirement of lack of correlation. When multiple signals are received, each spread with a different spreading code, the receiver should be able to pick out any individual signal using that signal's spreading code. The spread signal should behave as if they were uncorrelated with each other, so that other signals will appear as noise and not interfere with the despreading of the particular signal. Because of the high degree of redundancy provided by the spreading operation, the

dispersing operation is able to cope with the interference of other signal in the same bandwidth. To summarize, the necessary properties of spreading code are:

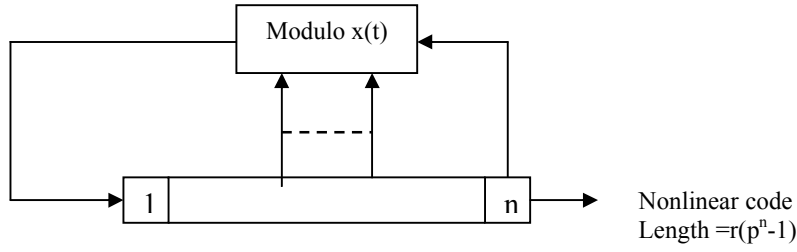
- It must be deterministic.
- It must appear random to a listener.
- The correlation property
 - Cross-Correlation: The correlation of two different codes. This should be as small as possible
 - Auto-Correlation: The correlation of a code with a time-delayed version of itself. In order to reject multi-path interference, this function should equal 0 for any time delay other than zero.
- The code must have a long period

3.3.1 Linear Codes

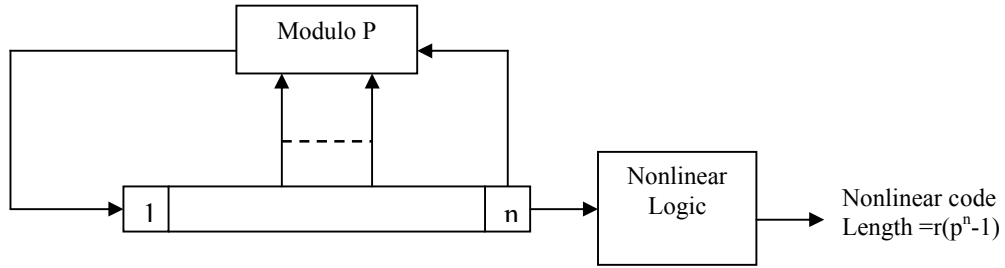
The work here emphasizes more on the linear code as their use is unexcelled for their ability to reject interference. They are widely used for ranging applications. The only disadvantage of linear code is that they are not secure. They are easily decipherable once a short sequential set of chips ($2n+1$) from the sequence is known. This is shown in [48]. However, if the band-spreading code is not a secure code, the overall system could still be secure if the information itself were encoded by a cryptographically secure technique. The point here is that encoding in some form is necessarily sufficient for security purposes. Figure 3.2 is a schematic of linear and non-linear code generator where there are n stages of the shift register and each stage has p possible states.



(a) Linear code generator for p -ary shift register (each stage has p possible states)



(b) Nonlinear code generator using p-ary shift register (there are $p^n - 1$ possible states for each feedback condition)



(c) Nonlinear code generator based on linear generator

Figure 3.2: Linear and nonlinear generator configurations: **(a)** linear code generator for p-ary shift register (each stage has p possible states); **(b)** nonlinear code generator using p-ary shift register (there are $p^n - 1$ possible states for each feedback condition); **(c)** nonlinear code generator based on linear generator.

3.4 Maximal Sequence

Maximal codes are by definition, the longest codes that can be generated by a given shift register or a delay element of a given length. In binary shift register sequence generators, which are the only type considered in this thesis, the maximum length sequence is $2^n - 1$ chips, where n is the number of stages in the shift register. A shift register sequence generator consists of a shift register working in conjunction with appropriate logic, which feeds back a logical combination of the state of two or more of its stages to input. The output of a sequence generator, and the contents of its n stages at any sample (clock) time, is a function of the outputs of the stages fed back at the preceding sample time. Feedback connections have been tabulated for maximal code generators for 3 to 100 stages, so that some sequences of any length from 7 through $2^{36} - 1$ chips are readily available. A number of feedback connections are listed in Table 3.1 [13].

Number Of Stages	Code Length	Maximal Taps
2	3	[2,1]
3	7	[3,1]
4	15	[4,1]
5	31	[5,2][5,4,3,2][5,4,2,1]
6	63	[6,1][6,5,2,1][6,5,3,2]
7	127	[7,1][7,3][7,3,2,1][7,4,3,2] [7,6,4,2][7,6,3,1][7,6,5,2][7,6,5,4,2,1][7,5,4,3,2,1]
8	255	[8,4,3,2][8,6,5,3][8,6,5,2] [8,5,3,1][8,6,5,2][8,7,6,1] [8,7,6,5,2,1][8,6,4,3,2,1]
9	511	[9,4][9,6,4,3][9,8,5,4][9,8,4,1] [9,5,3,2][9,8,6,5][9,8,7,2] [9,6,5,4,2,1][9,7,6,4,3,1] [9,8,7,6,5,3]
10	1023	[10,3][10,8,3,2][10,4,3,1][10,8,5,1] [10,8,5,4][10,9,4,1][10,8,4,3] [10,5,3,2][10,5,2,1][10,9,4,2]
11	2047	[11,1][11,8,5,2][11,7,3,2][11,5,3,5] [11,10,3,2][11,6,5,1][11,5,3,1] [11,9,4,1][11,8,6,2][11,9,8,3]
12	4095	[12,6,4,1][12,9,3,2][12,11,10,5,2,1] [12,11,6,4,2,1][12,11,9,7,6,5] [12,11,9,5,3,1][12,11,9,8,7,4] [12,11,9,7,6,][12,9,8,3,2,1] [12,10,9,8,6,2]
13	8191	[13,4,3,1][13,10,9,7,5,4] [13,11,8,7,4,1][13,12,8,7,6,5] [13,9,8,7,5,1][13,12,6,5,4,3] [13,12,11,9,5,3][13,12,11,5,2,1] [13,12,9,8,4,2][13,8,7,4,3,2]
14	16,383	[14,12,2,1][14,13,4,2][14,13,11,9] [14,10,6,1][14,11,6,1][14,12,11,1] [14,6,4,2][14,11,9,6,5,2] [14,13,6,5,3,1][14,13,12,8,4,1] [14,8,7,6,4,2][14,10,6,5,4,1] [14,13,12,7,6,3][14,13,11,10,8,3]
15	32,767	[15,13,10,9][15,13,10,1][15,14,9,2] [15,1][15,9,4,1][15,12,3,1][15,10,5,4] [15,10,5,4,3,2][15,11,7,6,2,1] [15,7,6,3,2,1][15,10,9,8,5,3] [15,12,5,4,3,2][15,10,8,7,5,3] [15,13,12,10][15,13,10,2][15,12,9,1] [15,14,12,2][15,13,9,6][15,7,4,1]

		[15,4][15,13,7,4]
--	--	-------------------

Table 3.1: Feedback connections for linear m-sequences

3.4.1 Properties

M-sequence is also called PN code or maximal code [13]. Two important properties for PN codes are randomness and unpredictability [36]. Traditionally, the concern in the generation of a sequence of allegedly random numbers has been that the sequence of numbers be random in some well-defined statistical sense. The following two criteria are used to validate that a sequence of numbers is random.

- **Uniform Distribution:** The distribution of numbers in the sequence should be uniform; that is, the frequency of occurrence of each of the numbers should be approximately the same. For a stream of binary digits, we need to expand on this definition because we are dealing with only 2 numbers (0 and 1). Generally, we desire the following two properties:
 - **Balance Property:** In a long sequence, the fraction of binary ones should approach $1/2$ [13].
 - **Run Property:** A run is defined as a sequence of all 1s or a sequence of all 0s. The appearance of the alternate digit signals the beginning of a new run. About one-half of the runs of each type should be of length 1, one fourth of length 3, and so on [13].
- **Independence:** No one value in the sequence can be inferred from the others.

Although there are well-defined tests for determining that a sequence of numbers matches a particular distribution, such as the uniform distribution, there is no such test to prove independence. Rather a number of tests can be applied to demonstrate that a sequence does not exhibit independence. The general strategy is to apply a number of such tests until the confidence that independence exists is sufficiently strong.

- **Correlation Property:** If a period of the sequence is compared term by term with the cycle shift of itself, the number of terms that are the same differs from those that are different by at most 1. Table 3.2 shows that the net correlation is $A - D$ is -1 for all except zero-shift or synchronous conditions, and $2^n - 1 = 7$ for the zero shift condition. This is typical of all m-sequences.

Autocorrelation is defined as the integral

$$\psi(\tau) = \int_{-\infty}^{\infty} f(t)f(t-r)dt, \quad (3.1)$$

Which is a measure of the similarity between a signal and a phase-shifted replica of itself. An autocorrelation function is a plot of autocorrelation over all phase shifts (t-r) of the signal, where Δt is one chip interval. Autocorrelation is of most interest in choosing code sequences that give the least probability of a false synchronization.

Cross-correlation is the measure of similarity between two different code sequences. The only difference between autocorrelation and cross-correlation is that in the general convolution integral for autocorrelation, a different term is substituted:

$$\psi_{\text{(cross)}} = \int_{-\infty}^{\infty} f(t)g(t-r)dt \quad (3.2)$$

Cross-correlation is of interest in several fields such as (a) code division multiple access system (or any code addressed system) in which receiver response to any signal other than the proper addressing sequence and (b) anti-jamming systems that must employ codes with extremely low cross-correlation as well as unambiguous autocorrelation.

Shift	Sequence	Agreements(A)	Disagreements(D)	A-D
1	0111001	3	4	-1
2	1011100	3	4	-1
3	0101110	3	4	-1
4	0010111	3	4	-1
5	1001011	3	4	-1
6	1100101	3	4	-1
7	1110010	7	0	7

Table 3.2: Reference sequence: 1110010

- **Linear Addition Properties:** Another valuable property of m-sequences is the way in which two (or more) sequences add. When two m-sequences each of different lengths, say 2^n-1 and 2^p-1 are linearly (modulo-2) added, the result is a composite sequence with a length $(2^n-1)(2^p-1)$. This composite is not maximal but may be a segment of a longer maximal sequence. The primary applications of these composite sequences have been in the JPL [13] ranging technique and GPS systems.

Possibly the most valuable linear addition property is that the addition of two m-sequences each of length r produces a composite sequence of length r , but not maximal. The composite sequence itself is different for each combination of delay between the two sequences. That is, a pair of sequence generator of length r can generate r nonmaximal linear codes, each of r chips long. More important, if the component m-sequences are properly chosen, the set of r composite sequences will have low and bounded cross-correlation. For example, a pair of ten-stage shift registers generators (see Figure 3.3) would be capable of generating 1023 different 1023-chip nonmaximal linear codes in addition to the two basic linear maximal codes. For each change in the feedback logic to either of the two shift registers a new set of 1023 codes would be produced.

A disadvantage of the shift and add property is that the linear maximal codes are also predictable by anyone who knows the current code state, so that future operation can be anticipated.

- **State Exhaustion:** The number of states possible for a set of n elements, each capable of r discernible states are r^n . A binary shift register generator with maximally connected feedback goes through 2^n-1 states in generating a (2^n-1) -chip m-sequence. These states are n -tuples that may be employed to control a processor such as a frequency synthesizer or a Monte Carlo test generator.

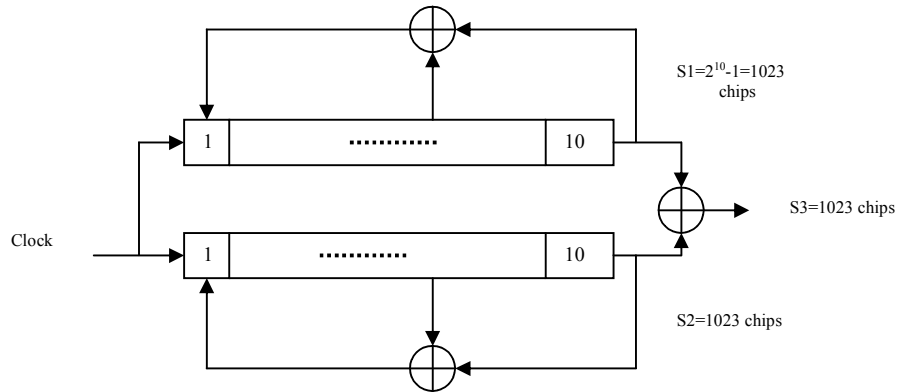


Figure 3.3: Shift Register Generator for 1023-chip Nonmaximal Codes.

3.4.2 Implementation

Linear feedback shift registers (LFSR) can be implemented in two ways. The Fibonacci implementation consists of a simple shift register in which a binary-weighted modulo-2 sum of the taps is fed back to the input. (The modulo-2 sum of two 1-bit binary numbers yields 0 if the two numbers are identical and 1 if they differ: $0+0=0$, $0+1=1$, $1+1=0$.)

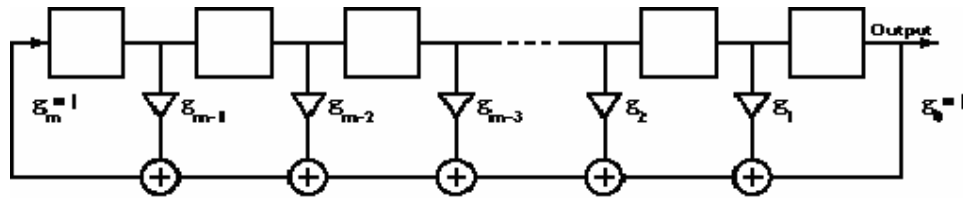


Figure 3.4: Fibonacci implementation of LFSR.

For any given tap, weight g_i is either 0, meaning "no connection," or 1, meaning it is fed back. Two exceptions are g_0 and g_m , which are always 1 and thus always connected. Note that g_m is not really a feedback connection, but rather is the input of the shift register. It is assigned a feedback weight for mathematical purposes. The Galois implementation consists of a shift register, the contents of which are modified at every step by a binary-weighted value of the output stage.

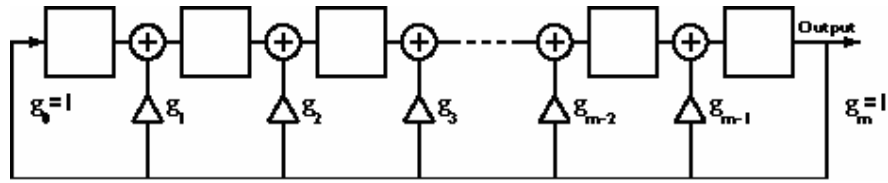


Figure 3.5: Galois implementation of LFSR

Careful inspection reveals that the order of the Galois weights is opposite that of the Fibonacci weights.

Given identical feedback weights, the two LFSR implementations will produce the same sequence. However, the initial states of the two implementations must necessarily be different for the two sequences to have identical phase. The initial state of the Fibonacci form is called the *initial fill* or *initial vector*, and this initial fill comprises the first m bits output from the generator. The initial state of the Galois generator must be adjusted appropriately to attain the equivalent initial fill.

When implemented in hardware, modulo-2 addition is performed with exclusive-OR (XOR) gates. The Galois form is generally faster than the Fibonacci in hardware due to the reduced number of gates in the feedback loop, thus making it the favored form.

It should be noted that, in some industries, the Fibonacci form LFSR is referred to as a *simple shift register generator* (SSRG), and the Galois form is referred to as a *multiple-return shift register generator* (MRSRG) or *modular shift register generator* (MSRG).

3.4.2.1 Convention for Feedback Specification

A given set of feedback connections can be expressed in a convenient and easy-to-use shorthand form, with the connection numbers being listed within a pair of brackets. In doing so, connection g_0 is implied, and not listed, since it is always connected. Although g_m is also always connected, it is listed in order to convey the shift register size (number of registers).

A set of feedback taps for a Galois generator is denoted as

$$[f_1, f_2, f_3, \dots, f_J]_g$$

where subscript J is the total number of feedback taps (not including g_0), $f_1 = m$ is the highest-order feedback tap (and the size of the LFSR), and f_j are the remaining feedback taps. The g subscript signifies the Galois LFSR form.

The set of feedback taps for the equivalent Fibonacci generator is denoted as

$$[f_1, m-f_2, m-f_3, \dots, m-f_J]_f$$

where the f subscript signifies the Fibonacci LFSR form. Note that subtracting the feedback tap numbers from m is equivalent to reversing the order of the feedback taps (as they are defined in Figures 3.4 and 3.5).

As an example, consider an LFSR of size $m = 8$ with feedback connections at g_8, g_6, g_5, g_4 , and implied g_0 . The feedback taps are specified as $[8, 6, 5, 4]_g$ for the Galois form, and $[8, 8-6, 8-5, 8-4]_f = [8, 2, 3, 4]_f = [8, 4, 3, 2]_f$ for the Fibonacci form. Note that the taps are customarily arranged in a descending order.

A set of feedback taps specified in this format is called a *feedback tap set*, *feedback set*, or *feedback pattern*.

It is important to recognize that feedback taps given in this shorthand form don't conform to the order of the weights given in Figure 1 for the Fibonacci generator. As such, it is best not to use Figures 3.4 and 3.5 in connection with this feedback convention. Rather, one should simply consider the first tap listed as being the output of the generator, the second tap being that just to the left of it, and so on, regardless of whether the generator is a Fibonacci or a Galois form. Any LFSR can be represented as a polynomial of variable X, referred to as the generator polynomial:

$$G(X) = g_m X^m + g_{m-1} X^{m-1} + g_{m-2} X^{m-2} + \dots + g_2 X^2 + g_1 X + g_0 \quad (3.3)$$

In tables of m-sequence feedback sets, neither the Fibonacci nor the Galois form is specified. This is because any given set will work with either implementation. If a given

feedback set is used on both the Fibonacci and Galois forms, the sequence produced by one form will be the mirror image of the sequence produced by the other.

One other related convention should be mentioned: An LFSR with m shift register stages is said to be an R_m LFSR. For example, an R_8 generator is one with eight stages. An alternative to this convention is PN_m , or PN_8 in this example. (PN is an acronym for pseudonoise, which is a term used for maximal length pseudorandom sequences).

3.5 Gold Sequence

For CDMA applications, m-sequences are not optimal. For CDMA, we need to construct a family of spreading sequences, one for each which, in which the codes have well-defined cross-correlation properties. In general, m-sequences do not satisfy the criterion. One popular set of sequences that does are the Gold sequences. Gold sequences are attractive because only simple circuitry is needed to generate a large number of unique codes.

A Gold sequence is constructed by the XOR of two m-sequences with the same clocking. Figure 3.6 shows the schematic for Gold code generation.

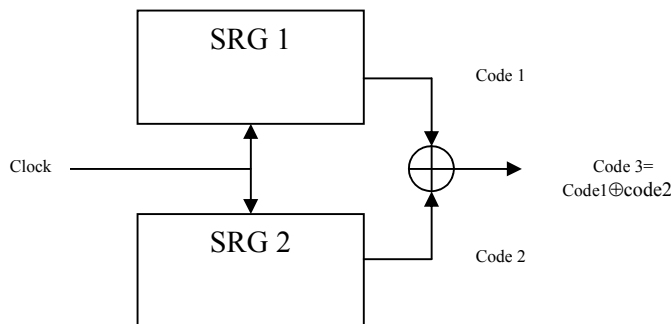


Figure 3.6: Gold code sequence generator configuration

Figure 3.7 is an example of a 31-bit Gold code generator. In this example the two shift registers generate the two m-sequences and are then bitwise XORed. In general, the length of the resulting sequence is not maximal. Further, the desired Gold sequences can only be generated by preferred pairs of m-sequences. These preferred pairs can be

selected from tables of pairs or generated by an algorithm. [13] lists sets of preferred pairs and describes the algorithm.

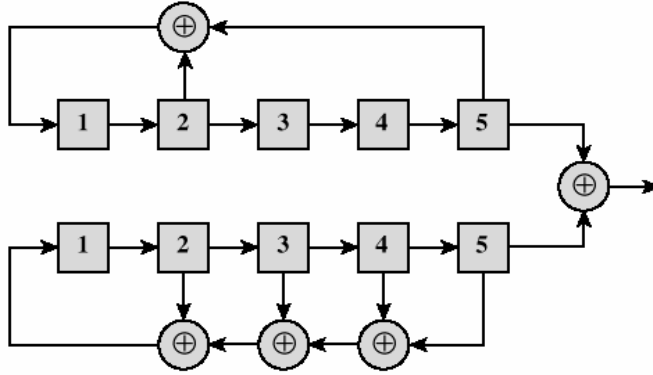


Figure 3.7: Generation of 31 bit Gold code.

Next, the mathematical condition that led to a Gold code is discussed [36].

Let, a is a binary vector of period N . a' is decimated value of a and is $a[q]$

If and only if $\gcd(n, q) = 1$, a' is a m-sequence (period $= N$),

Two m-sequences are said to be preferred if,

- 1- $n/4 \neq 0$; that is all n except 0, 4, 8, 12...
- 2- q is odd and $q = (2k + 1)$ or $q = (22k - 2k + 1)$ for some k ,
- 3- $\gcd(n, k) = 1$ (for n odd)
 $= 2$ (for $n \equiv 2 \pmod{4}$)

Gold codes have three-valued autocorrelation and cross-correlation

function: $\{-1, -t(m), t(m) - 2\}$, where

$$t(m) = \begin{cases} 2^{(m+2)/2} + 1 & \text{For even } m \\ 2^{(m+1)/2} + 1 & \text{For odd } m \end{cases}$$

The sequence generated is $[a, a', a \oplus a', a \oplus Da', a \oplus D^2a', \dots, a \oplus D^{N-1}a']$ where, D = delay element \approx one bit shift of a' relative to a . Period of Gold sequence is $N = 2^n - 1$ [where, n = number of bits in shift registers]. Family length of Gold code is $N+2$ i.e. $2^n + 1$.

3.6 Kasami Sequence

Kasami codes have popular use in 3G wireless schemes. They can be classified as (1) large Kasami set or (2) small Kasami set. Small kasami set has family size $(M) = 2^{n/2}$ and period $= N = 2^n - 1$. Their maximum cross-correlation is $2^{n/2} - 1$. Large kasami set contains both gold sequence and small set of kasami sequences as subset. Its period is $N = 2^n - 1$. Maximum cross-correlation is $2^{(n+2)/2}$.

For generation of small kasami code, n is chosen even. A sequence a is defined with period $N = 2^n - 1$. This sequence is decimated by $q = 2^{n/2} + 1$. The resulting sequence a' has period $2^{n/2} - 1$. Final sequence is generated by XORing the bits from a & a' .

For generation of large kasami code, one set is defined by starting with an m-sequence, a with a period N . That sequence is decimated by $q = 2^{n/2} + 1$ to form a' . That Sequence a' is further decimated by $q = 2^{(n+2)/2} + 1$ to form a'' . Final set is formed by taking XOR of a, a', a'' [36].

3.7 Orthogonal Codes

Unlike PN sequences, an orthogonal code is a set of sequences in which all pair wise cross correlations are zero. An orthogonal set of sequences is characterized by the following quantity [49][50].

$$\sum_{k=0}^{M-1} \phi_i(k\tau) \phi_j(k\tau) = 0 \quad i \neq j \quad (3.4)$$

Where M is the length of each of the sequences in the set, ϕ_i and ϕ_j are the i th and j th members of the set, and t is the bit duration.

Both fixed and variable length orthogonal codes have been used in CDMA systems. For the CDMA applications, each mobile user uses one of the sequences in the set as a spreading code, providing zero cross correlation among all users.

3.7.1 Walsh Codes

Walsh codes are the most common orthogonal codes used in CDMA applications. A set of Walsh codes of length n consists of n rows of an $n \times n$ Walsh matrix. The matrix is defined recursively as follows:

$$W_1 = (0) \quad W_2 = \begin{pmatrix} 00 \\ 01 \end{pmatrix} \quad W_4 = \begin{pmatrix} 0000 \\ 0101 \\ 0011 \\ 0110 \end{pmatrix} \quad W_8 = \begin{pmatrix} 00000000 \\ 01010101 \\ 00110011 \\ 01100110 \\ 00001111 \\ 01010101 \\ 00111100 \\ 01101001 \end{pmatrix} \quad W_{2n} = \begin{pmatrix} W_n & W_n \\ W_n & \overline{W_n} \end{pmatrix}$$

Where n is the dimension of the matrix and the over score denotes the logical NOT of the bits of the matrix. The Walsh matrix has the property that every row is orthogonal to every other row and to the logical NOT of every other row.

Orthogonal spreading codes such as the Walsh sequences can only be used if all the users in the same CDMA channel are synchronized to the accuracy of a small fraction of one chip. Because the cross correlation between different shifts of Walsh sequences is not zero, if tight synchronization is not provided, PN sequences are needed.

3.7.2 Variable-Length Orthogonal Codes

Third-generation mobile CDMA systems are designed to support users at a number of different data rates. Thus, effective support can be provided by using spreading codes at different rates while maintaining orthogonality. Suppose that the minimum data rate to be supported is R_{\min} and that all other data rates are related by powers of 2. If a spreading sequence of length N is used for the R_{\min} data rate, such that each bit of data is spread by $N = 2^n$ bits of the spreading sequence (transmit the sequence for data bit 0; transmit the

complement of the sequence for data bit 1), then the transmitted data rate is NR_{\min} . For a data rate of $2 \times R_{\min}$, a spreading sequence of length $N/2 = 2^{n-1}$ will produce the same output rate of $N \times R_{\min}$. In general, a code length of 2^{n-k} is needed for a bit rate of $2^k R_{\min}$.

A set of variable-length orthogonal sequence is readily generated from Walsh matrices of different dimensions. For example, see [47]

3.8 Multiple Spreading

When sufficient bandwidth is available, a multiple spreading technique can prove highly effective. A typical approach is to spread the data rate by an orthogonal code to provide mutual orthogonality among all users in the same cell and to further spread the result by a PN sequence to provide mutual randomness (low cross correlation) between users in different cells. In such a two-stage spreading, the orthogonal codes are referred to as channelization codes, and the PN codes are referred to as scrambling codes. Figure 3.8 illustrates the technique of multiple spreading.

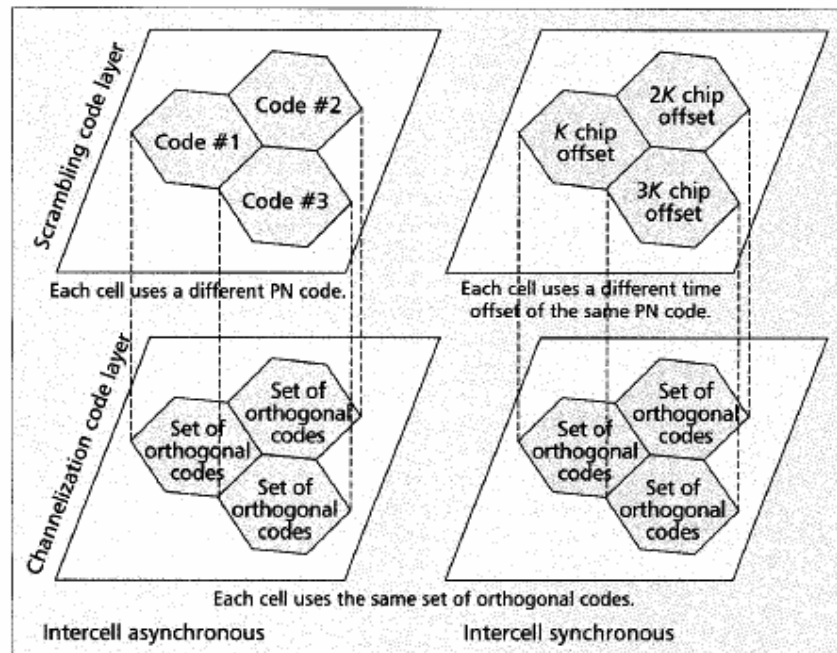


Figure 3.8: Multiple Spreading

The work presented in this thesis considers combination of spreading and coding in CDMA system. Since CDMA is a form of direct sequence spread spectrum, spreading sequences are used for spreading the signal (increase the bandwidth). Coding considered here is convolutional coding. This is a type of FEC coding. In the following section, convolutional code is described briefly.

3.9 Forward Error Correction

Forward error correction (FEC) [51] is frequently employed in communication systems where it is important that a message be received with as few errors as possible. Examples include space communications [52] and audio disc players [53]. FEC coding sacrifices resources, in terms of the data rate, to provide some extra information about a particular data bit. This information is then used to estimate the original data bit, with greater integrity than if the original data rate had been used.

FEC codes fall into two main categories; linear block codes, which append one or more code digits to the original data bit, and non-linear convolutional codes, which use a number of input digits to calculate the code word, as shown schematically in figure 3.9.

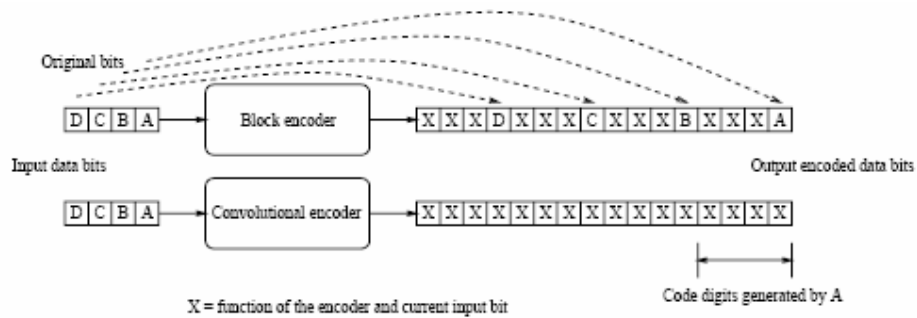


Figure 3.9: Forward error correction using block and convolutional encoders.

3.9.1 Convolutional Codes

Convolutional codes are fundamentally different from block codes in that information sequences are not grouped into distinct blocks and encoded [54]. Instead a continuous sequence of information bit is mapped into a continuous sequence of encoder output bits.

The mapping is highly structured, enabling a decoding method considerably different from that of block codes to be employed. It can be argued that the convolutional coding can achieve a larger coding gain than can be achieved using block coding with the same complexity. Figure 3.10 shows a general block diagram of a convolutional encoder.

A convolutional code is generated by passing the information sequence through a finite state shift register. In general, the shift register contains N k -bit stages and n linear algebraic function generators based on the generators polynomials as shown in figure 3.10.

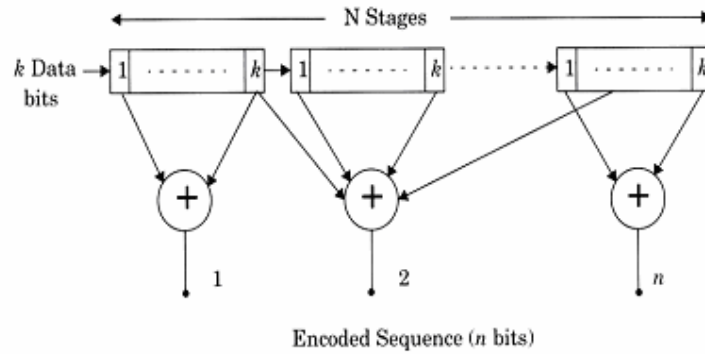


Figure 3.10: General block diagram of convolutional encoder

The input data is shifted into and along the shift register, k bits at a time. The number of output bits for each k bit user input data sequence is n bits. The code rate $R_c = k/n$. The parameter N is called the *constraint length* and indicates the number of input data bits the current output is dependent upon. The constraint length determines how powerful and complex the code is. Following is an outline of the various ways of representing convolutional codes.

Generator Matrix: The generator matrix for a convolutional code can define the code and is semi-infinite since the input is semi-infinite in length. Hence, this is not a convenient way of representing a convolutional code.

Generator Polynomials: For convolutional codes, we specify a set of n vectors, one for each of the n modulo-2 adder. A 1 in the i th position of the vector indicates that the corresponding shift register stage is connected and 0 indicate no connection.

Logic Table: A logic table or lookup table can be built showing the outputs of the convolutional encoder and the state of the encoder for all the specific input sequences present in the shift register.

State Diagram: Since the output of the encoder is determined by the input and the current state of the encoder, a state diagram can be used to represent the encoding process. The state diagram is simply a graph of the possible states of the encoder and the possible transitions from one state to another.

Tree Diagram: The tree diagram shows the structure of the encoder in the form of a tree with the branches representing the various states and the outputs of the coder.

Trellis Diagram: Close observation of the tree reveals that the structure repeats itself once the number of stages is greater than the constraint length. It is observed that all branches emanating from two nodes having the same state are identical in the sense that they generate identical output sequences. This means that the two nodes having the same label can be merged. By doing this throughout the tree diagram, we can obtain another diagram called a *trellis diagram* which is a more compact representation.

3.9.1.1 Example of Convolutional Encoder

To illustrate the principles, figure 3.11 shows a constraint length 3, rate $\frac{1}{2}$ encode defined by $(7,5)_8$. The time delay Z^{-1}_{bit} in the shift register arrangement represents a delay of one data bit, in contrast to Z^{-1} used previously, which represents a delay of one chip. Knowledge of the encoder permits the construction of a transition table, as shown in table 3.1 in which there are four distinct states, corresponding to the values of the previous two bits.

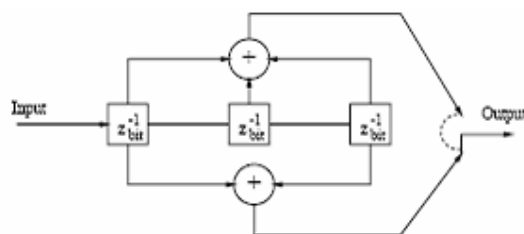


Figure 3.11: Rate $\frac{1}{2}$, constraint length 3 $(7,5)_8$ convolutional encoder.

An alternative representation of the transition table is the state diagram, shown in figure 3.12, in which the nodes are labeled as in the transition table and the output code sequences are shown circled for the appropriate combination of current state and input data bit.

Previous two data bits	Current state	Input data bit	Output code word	New state
00	a	0	00	a
	a	1	11	b
01	b	0	10	c
	b	1	01	d
10	c	0	11	a
	c	1	00	b
11	d	0	01	c
	d	1	10	d

Table 3.3: Transition table showing output code words for each input data bit at each state for the $(7,5)_8$ convolutional encoder.

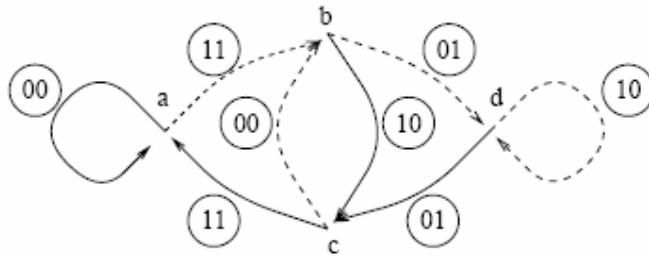


Figure 3.12: The state diagram for the $(7,5)_8$ convolutional encoder.

In the figure, the transitions produced by an input of 0 are shown as solid lines, while those corresponding to 1 are shown as dashed lines. Thus, the state diagram may be used to calculate the output of the coder for a given stream of input data bits. It may also be employed to derive the theoretical performance as described below.

3.9.1.2 Theoretical Analysis of Convolutional codes

The error correcting power of a particular code configuration depends on the ability to identify and correct individual bit errors. To analyze the theoretical performance of a convolutional coding structure, the distance (in terms of the Hamming metric) between code words will be considered. In this analysis, attention will be fixed on all-zeros codeword (00 in this case where the rate $R = 1/2$).

From the state diagram in figure 3.12, it is possible to calculate the transfer function $T(d)$, which provides the distance (or weight) spectrum of the code, denoted $\{a_k\}_{k=d_{free}}^{\infty}$, where d_{free} is the free distance of the code [53], which represents the minimum possible run of ones before the all-zeros codeword may again be output for an input of zero. Splitting node a into two and denoting the new node (representing the output) as e , the transfer function is given by

$$T(d) = \frac{X_e}{X_a} \quad (3.5)$$

Where X_i represents the distance measure in arriving at node i .

In this case, the transfer function is given by

$$T(d) = d^2 \left(\frac{d}{1-d} \right) \left(\frac{d^2(1-d)}{1-2d} \right) = \frac{d^5}{1-2d} = \sum_{k=5}^{\infty} a_k d^k \quad (3.6)$$

So that $d_{free} = 5$ and the elements of the weight spectrum are given by $a_k = 2^{k-5}$.

This then provides a mechanism for calculating an upper bound on the error performance of the convolutional code, since if the probability of error in choosing between any two particular code-words is given by

$$P_2 = Q \left(\sqrt{2 \frac{E_b}{N_o} R \cdot d} \right) \quad (3.7)$$

Where R is the rate of the code and d is the distance, then the total error probability is bounded by

$$\begin{aligned} P_e &\leq \sum_{d=d_{free}}^{\infty} a_d P_2(d) \\ &= \sum_{d=d_{free}}^{\infty} a_d Q \left(\sqrt{2 \frac{E_b}{N_o} R \cdot d} \right) \\ &\cong \sum_{d=d_{free}}^{d_{upper}} a_d Q \left(\sqrt{2 \frac{E_b}{N_o} R \cdot d} \right) \end{aligned} \quad (3.8)$$

Where d_{upper} is chosen so that sufficiently accurate results may be obtained. Optimum connections for various rate and constraint length convolutional codes may be found *e.g.* [55]. Catastrophic codes, for which there exists at least one path of zero Hamming

distance from a non-zero state to itself, are rarely used due to instability problems, and will not be considered here.

3.10 Conclusion

The properties of spreading codes in general are discussed. Some important codes like Gold, Kasami (small and large) and maximal length sequence are considered and their family size, correlation values etc are summarized. The mathematical backgrounds of generation of these codes are also explored.

Chapter 4

Phase Optimization

4.1 Introduction

The direct-sequence (DS) code-division multiple access has received considerable attention during the past years. Standardization and research & development (R&D) projects in design stage need the proper selection of spreading sequence and optimization of them. Candidate pseudonoise sequence (PN) sets from the selected families are then used as examples in theoretical analysis and in Monte Carlo simulations of various alternative candidate systems and sub-systems at the specification phase.

This chapter contains sections describing the need for phase optimization of spreading codes, various types of phase optimization techniques, definitions, quality ordering of optimization rules from the viewpoint of reduced multiple-access interference (MAI). The results are useful for CDMA system designers in order to obtain an idea of the significance of PN code phase optimization and agreed spreading code sets.

4.2 Correlation Parameters and Performance Measures

One common method for selecting CDMA codes is to search for a family of codes in which the maximum absolute values (θ_A, θ_C) of the even (periodic) auto-correlation function (ACF) and the cross-correlation function (CCF) are small (*e.g.* Gold codes), with the hope of finding a subset in which the maximum values of the function $(\hat{\theta}_A, \hat{\theta}_C)$ are also small. The ultimate goal is to minimize the parameter $\hat{\theta}_A$ and $\hat{\theta}_C$ by finding the optimum phase-shift combination for each of the K codes in a set [58]-[61]. It is believed that the optimum phase shifts will maximize the SNR and minimize the bit error probability, i.e. minimize the amount of MAI.

The average signal-to-noise ratio at the output from a BPSK type asynchronous DS-CDMA receiver of the j^{th} user can be expressed in terms of the sum of the AIP values ($r_{i,j}$) of K users and the SNR of the AWGN channel (E_b / N_o) as follows [59] [60].

$$\text{SNR}_j = \left\{ \frac{N_0}{2E_b} + Q_a \right\}^{-1} \quad (4.1)$$

$$Q_a = \frac{1}{6p^3} \sum_{i=1, i \neq j}^K r_{i,j} \quad (4.2)$$

$$r_{i,j} = 2\mu_{i,j}(0) + \mu_{i,j}(1) \quad (4.3)$$

$$\mu_{i,j}(n) = \sum_{k=1-p}^{p-1} C_i(k)C_j(k+n) \quad (4.4)$$

Where $C_i(k)$ and $C_j(k)$ are aperiodic auto-correlation functions (ACFs)[58][59] of codes i and j respectively and p is the code length (period). The parameter $\mu_{i,j}(n)$ can also be expressed with the aid of the aperiodic cross correlation functions (CCFs), $C_{i,j}(k)$ between codes i and j [60][61]

$$\mu_{i,j}(n) = \sum_{k=1-p}^{p-1} C_{i,j}(k)C_{i,j}(k+n) \quad (4.5)$$

Using the following relationship between the even($\theta_{i,j}(k)$), odd ($\hat{\theta}_{i,j}(k)$) and aperiodic CCF:

$$\sum_{k=0}^{p-1} |\theta_{i,j}(k)|^2 + \sum_{k=0}^{p-1} |\hat{\theta}_{i,j}(k)|^2 = 2 \sum_{k=1-p}^{p-1} |C_{i,j}(k)|^2 \quad (4.6)$$

AIP can be re-written as follows [62][63]:

$$r_{i,j} = \sum_{k=0}^{p-1} \theta_{i,j}^2(k) + \sum_{k=0}^{p-1} \hat{\theta}_{i,j}^2(k) + \sum_{k=1-p}^{p-1} C_{i,j}(k)C_{i,j}(k+1) \quad (4.7)$$

It is demonstrated in [64]-[66] that $r_{i,j}$ can be approximated by the sum of square-sums of the even and odd CCF on the right hand side of Eq.(4.7). This also means that $r_{i,j} \approx 2\mu_{i,j}(0)$ in Eq.(4.3). The two square-sums in Eq.(4.7) represent the unnormalized mean-square cross-correlation values of the even and odd CCF. The crucial parameter $\mu_{i,j}(0)$ can be bounded by using the Cauchy inequality as follows [67]:

$$p^2 - 2\sqrt{S_i S_j} \leq \mu_{i,j}(0) \leq p^2 + 2\sqrt{S_i S_j} \quad (4.8)$$

$$\text{Where } S_i = \sum_{k=1}^{p-1} C_i^2(k) \text{ and, } S_j = \sum_{k=1}^{p-1} C_j^2(k) \quad (4.9)$$

Are the side-lobe energies of the aperiodic ACFs of codes i and j respectively. The following formula, analogous to Eq. (4.6), links the side-lobe energies of the aperiodic ($C_i(k)$), even ($\theta_i(k)$) and odd ($\hat{\theta}_i(k)$) ACFs.

$$\sum_{k=1}^{p-1} |\theta_i(k)|^2 + \sum_{k=1}^{p-1} |\hat{\theta}_i(k)|^2 = 4 \sum_{k=1}^{p-1} |C_i(k)|^2 \quad (4.10)$$

Using (4.8), the upper bound of the AIP is defined

$$r_{i,j} \leq 4p^2 + 6\sqrt{S_i S_j} \quad (4.11)$$

Eqs (4.1)-(4.11) are the necessary basic tools needed to define various phase optimization criteria that are next discussed.

4.2.1 Definition of AO / LSE, LSE / AO and MSE / AO Phase Optimization Criteria

One common method for selecting spreading codes is to search a set or a family of sequences in which the maximum absolute values of the even (periodic) ACF and CCF (θ_a, θ_c) are relatively small (e.g. Gold codes) with the hope of finding a subset in which the maximum values of odd functions ($\hat{\theta}_a, \hat{\theta}_c$) are also small. The ultimate goal is to minimize the parameters ($\hat{\theta}_a, \hat{\theta}_c$) by finding the best phase-shift combination for each of the K sequences in a set (θ_a and θ_c do not depend on phase-shift). In [58]-[60], criteria were proposed to optimize the odd ACF. Based on (4.8)-(4.11), it is commonly believed that by minimizing the maximum sidelobe value of the odd ACF and the aperiodic sidelobe energy of each sequence for a set of K sequences, the amount of MAI is reduced and thus the SNR of (4.1) is improved. The AO/LSE criterion is defined first.

The maximum sidelobe of the odd ACF of sequence x is defined $\hat{M}(x) = \max \{ |\hat{\theta}(l)| : 1 \leq l < p \}$. (4.12)

It is desirable to make the sidelobe of as small as possible (this combats multipath signals and aids code synchronisation) [4]. Let $\hat{\theta}_{AO}(x)$ denote the maximum value of $\hat{M}(T^n x)$, where the minimum is over all the phases $n, 0 \leq n < p$, of sequence x (T^n is the discrete phase-shift operator). Typically, there exists more than one phase-shift which achieves the minimum. Therefore, it is useful to consider the number of times $\hat{\theta}(T^n x)(l)$ achieves the maximum value. For a sequence u let $\hat{L}(u)$ be the number of values $l, 1 \leq l < p$, for which $\hat{\theta}(u)(l) = \hat{M}(u)$. A phase n of a sequence x is an auto-optimal (AO) phase, if $\hat{M}(T^n x) = \hat{\theta}_{AO}(x)$ and if $\hat{L}(T^n x) \leq \hat{L}(T^k x)$ for all phases k for which $\hat{M}(T^k x) = \hat{\theta}_{AO}(x)$. In order to determine $\hat{\theta}_{AO}(x)$ for a given sequence x , the odd ACF for $T^n x, 0 \leq n < p$, must be computed for each n . Since, in general, the AO phase is not unique, auto-optimality can be further refined by considering the AO phases the odd ACF which correspond with the least sidelobe energy (LSE) of the aperiodic. The phase n of a sequence x is auto-optimal with least sidelobe energy (AO/LSE) if it is auto-optimal, and if the sidelobe energy $S_x(T^n x) \leq S_x(T^m x)$ for all auto-optimal phase m . In contrast to the non-uniqueness of AO phases, the AO/LSE phase is in most cases unique.

It can be seen that the upper bound of the AIP is minimized if the sidelobe energies of the sequences i and j are minimized. That is why it is reasonable to emphasize the sidelobe energy parameter instead of the peak sidelobe. Hence it is of interest to determine at first, the least aperiodic sidelobe energy phases of a sequence x . As before, there will be ties for some sequences (i.e. phases n and m for which $S_x(T^n x) \leq S_x(T^m x)$ for all k). Thus those LSE phases which have the minimum $\hat{M}(x)$ are considered and these are referred to as being auto-optimal among the set of least sidelobe energy phases. This amounts to a reversal of the order in which the AO and the LSE criteria are applied to obtain the AO/LSE phases. Hence, the notation LSE/AO is used. In [61][65], numerical results concerning AO/LSE and LSE/AO optimized AIP values and the corresponding sequences are presented.

More than ten years after the definition of AO / LSE and LSE / AO criteria, a third optimization criterion was proposed in [68] called the maximum sidelobe energy auto-optimal (MSE/AO) criterion. It is based on the observation that the lower bound in (4.8) is instead maximized. The exact definition of the MSE/AO criterion is analogous to the definition of the LSE/AO criterion except that the minimization criterion is replaced by maximization. The MSE/AO rule, though, auto-optimal, produces an odd ACF with large sidelobes. This is not an issue for gold-start synchronization schemes where no data modulation is present (only the periodic ACF appears)[68].

4.2.2 Definition of CO/MSQCC and MSQCC/CO phase optimization criteria.

The basic problem in the use of inequalities (4.8) and (4.11) is that it can not be guaranteed that the LSE/AO and MSE/AO criteria really result in minimized AIP values and thus a reduced MAI. It is known that the ACF and CCF are not independent [4]. Better ACF properties can be gained at the expense of worse CCF properties and vice-versa. From the academic point of view, it is interesting to know how much advantage in the SNR could be obtained, compared with the criteria prescribed in the preceding section, if the mean-square cross-correlation (MSQCC) values between the reference code and the remaining codes in a set are minimized in addition to the maximum magnitudes of the odd CCF. Eq.(4.7) suggests that it might be advantageous. Since well known PN sequence families possess an approximately equal even (periodic) MSQCC value (equivalently the square-sum of the values of the even CCF). Since the periodic MSQCC value is also independent of the sequence phase, the only possibility to try to reduce the amount of MAI is to minimize the MSQCC values of the odd functions. Further, (4.6) means that the value of the odd square sum is minimum when the value of the aperiodic square sum reaches its minimum. There are two options for optimization namely the CO/MSQCC and MSQCC/CO criteria. The CO/MSQCC criterion is defined first. The maximum correlation magnitude of the odd CCF between sequences x and y is defined as follows:

$$\hat{M}(x, y) = \max \{ |\hat{\theta}_{x,y}(l)| : 0 \leq l < p \} \quad (4.13)$$

It is desirable to make the odd cross-correlation value as small as possible for the purpose of CDMA. Let $\hat{\theta}_{co}(x, y)$ denote the minimum value of $\hat{M}(x, T^n y)$, where the minimum is over all relative phase-shifts $n, 0 \leq n < p$, between sequences x and y . (The phase of sequence x is kept fixed and the phase of sequences y is shifted relative to x). As in the case of ACF, there exists more than one phase-shift which achieves the minimum. Therefore, it is useful to consider the number of times $\hat{\theta}(x, T^n y)(l)$ achieves its maximum value. For sequences u and v , let $\hat{L}(u, v)$ be the number of values $l, 0 \leq l < p$, for which $\hat{\theta}(u, v)(l) = \hat{M}(u, v)$. A shift n between sequences x and y is a cross-optimal (CO) phase, if $\hat{M}(x, T^n y) = \hat{\theta}_{co}(x, y)$ and if $\hat{L}(x, T^n y) \leq \hat{L}(x, T^k y)$ for all phases k for which $\hat{M}(x, T^k y) = \hat{\theta}_{co}(x, y)$. In order to determine $\hat{\theta}_{co}(x, y)$ between sequence x and $T^n y$, the odd CCF must be computed for each $n, 0 \leq n < p$. Since the CO phase is not unique, cross optimality is refined by considering those CO phases of the odd CCF which correspond the minimum square-sum cross-correlation (MSQCC) value of the aperiodic CCF. The following abbreviations are defined as:

$$S_{ap}(x, y) = \sum_{k=1-p}^{p-1} C_{x,y}^2(k), \quad (4.14)$$

$$S_{od}(x, y) = \sum_{k=0}^{p-1} \hat{\theta}_{x,y}^2(k) \quad (4.15)$$

The phase n between sequences x and y is cross optimal with a minimum square-sum (or mean-square) cross-correlation value (CO/MSQCC) if it is CO, and if the $S_{ap}(x, T^n y) \leq S_{ap}(x, T^m y)$ for all CO phases m . In contrast to non-uniqueness of CO phases, the CO/MSQCC phase is in most cases unique.

The CO/MSQCC criterion emphasizes more on the mean-square correlation value than on peak correlation value. It can be concluded from (5) and (6) that the emphasis of the mean-square cross-correlation parameter instead of the peak correlation might be beneficial in order to reduce the MAI. Hence, at first, it is of interest to determine the phases corresponding the minimum square-sum cross-correlation value between sequences x and y . As before, there may appear ties for some sequence pairs (i.e., phases n and m for which $S_{ap}(x, T^n y) = S_{ap}(x, T^m y) \leq S_{ap}(x, T^k y)$ for all k .) Therefore, those

MSQCC phases which have the minimum $\hat{M}(x, y)$ are considered and these are referred to as being CO among the minimum square-sum cross-correlation phases. This amounts to a reversal of the order in which the CO and the MSQCC criteria are applied to obtain the CO / MSQCC phases. Hence the notation MSQCC / CO is used.

4.2.3 Significance of PN Sequence Initial Phases

There is a need for fixed PN code sets for test purposes from the standpoint of numerical analysis and simulation. An agreement on test sequence sets and their initial phases for fixing the probability distribution function (PDF) of the multiple-access interference (MAI) random variable is necessary in order to make the numerical examples of different research groups and authors commensurable in large system design projects and in the CDMA literature. Situations where a need for fixed PN code sets exists include BER performance analysis, computer simulation of various CDMA system configurations, code acquisition and tracking performance analysis, analysis of multi-user and interference cancellation receivers and comparison of modulation methods.

4.3 Optimization Results

Figure 4.1 – 4.13 are curves obtained from simulation. The spreading codes used are of length 31, 63, 127, 255 and 511 when codes are Gold, Kasami and m-sequence. Signal-to-noise ratio (SNR) at the output of a DS-CDMA receiver is the performance measure. The results thus obtained are discussed in the following section and conclusions are drawn.

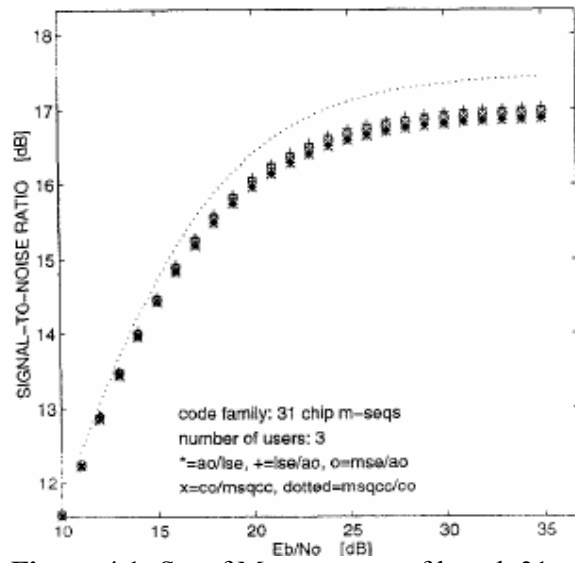


Figure 4.1: Set of M-sequences of length 31

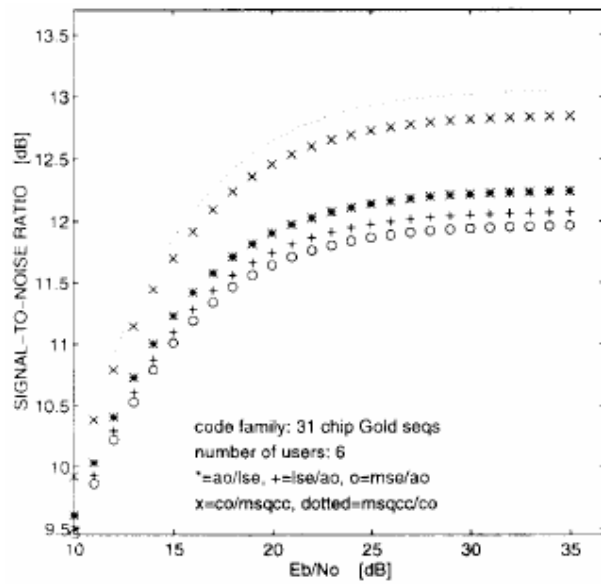


Figure 4.2: Set of Gold sequences of length 31

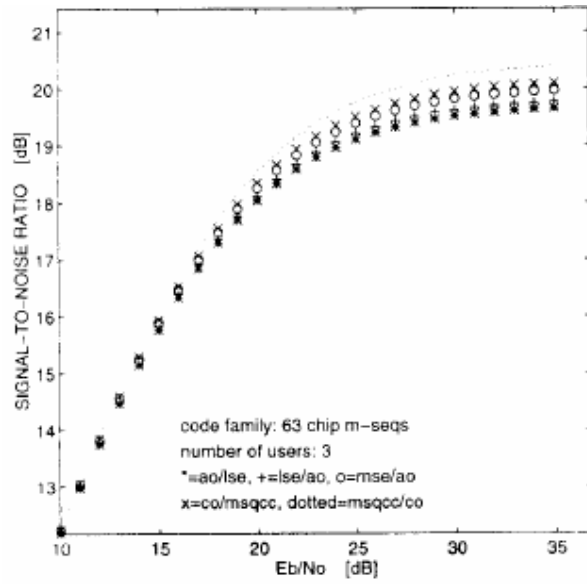


Figure 4.3: Set of M-sequences of length 63.

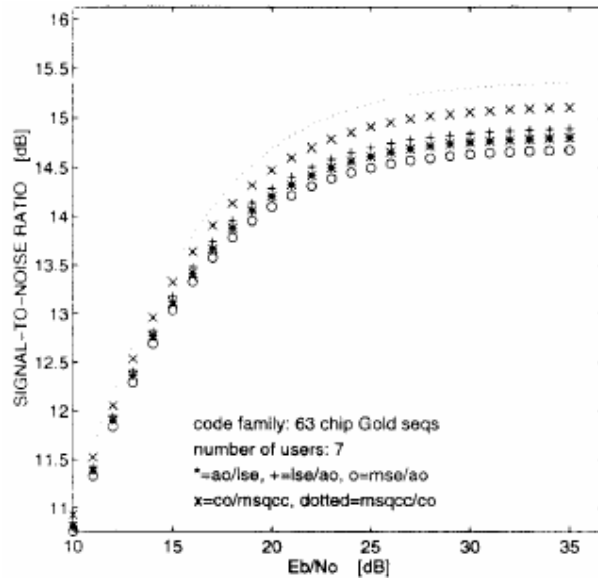


Figure 4.4: Set of Gold sequences of length 63.

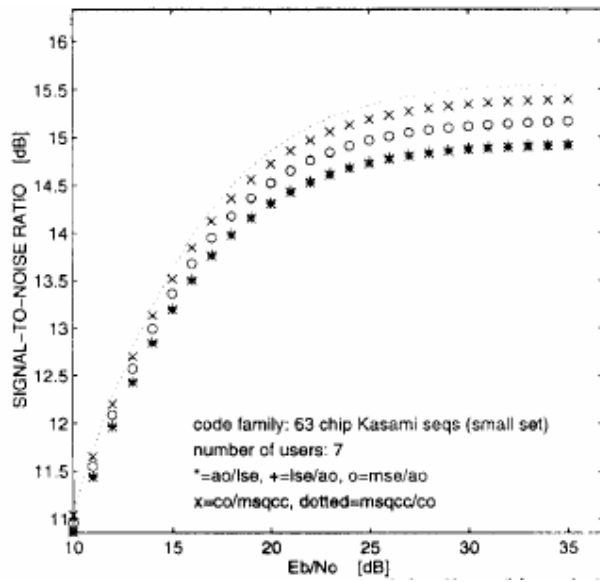


Figure 4.5: Set of Kasami sequences (small family) of length 63.

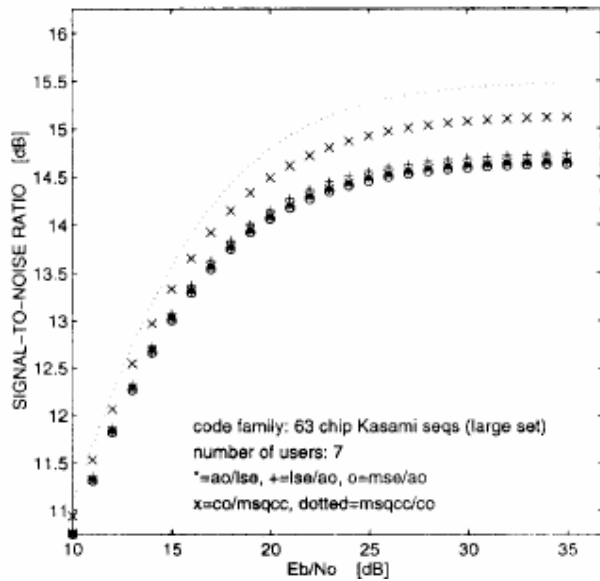


Figure 4.6: Set of Kasami sequences (large family) of length 63.

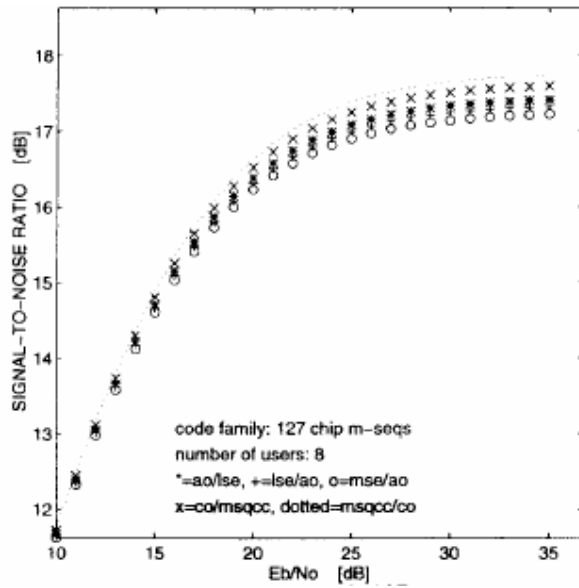


Figure 4.7: Set of M- sequences of length 127.

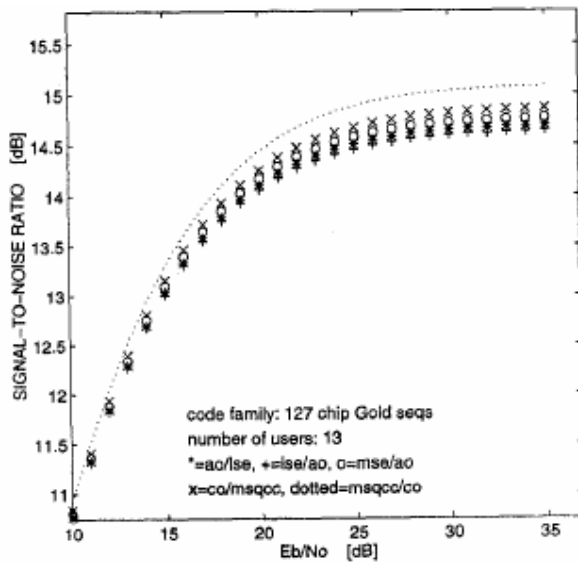


Figure 4.8: Set of Gold sequences of length 127.

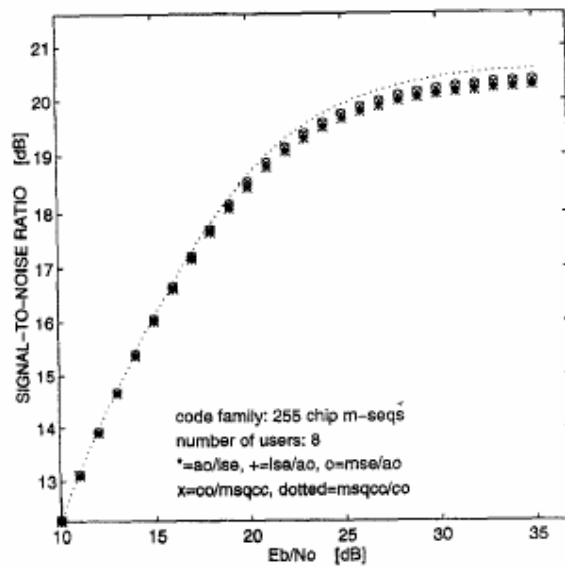


Figure 4.9: Set of M-sequences of length 255.

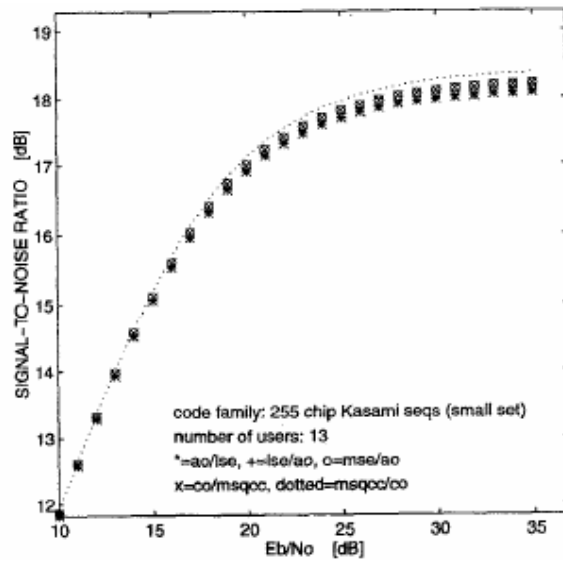


Figure 4.10: Set of Kasami-sequences (small family) of length 255.

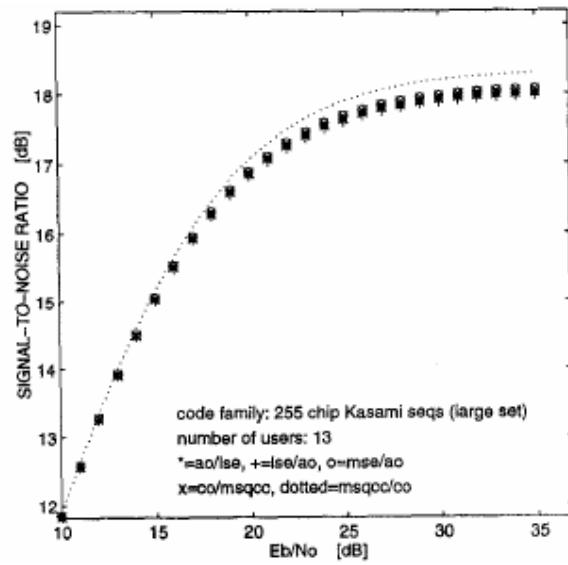


Figure 4.11: Set of Kasami -sequences (large family) of length 255.

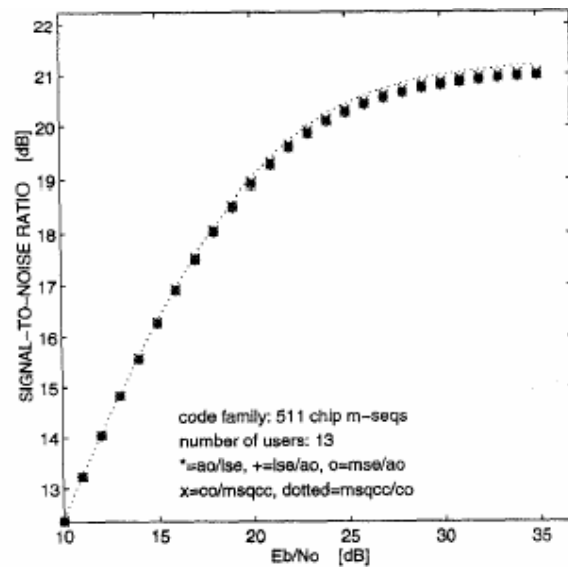


Figure 4.12: Set of M -sequences of length 511.

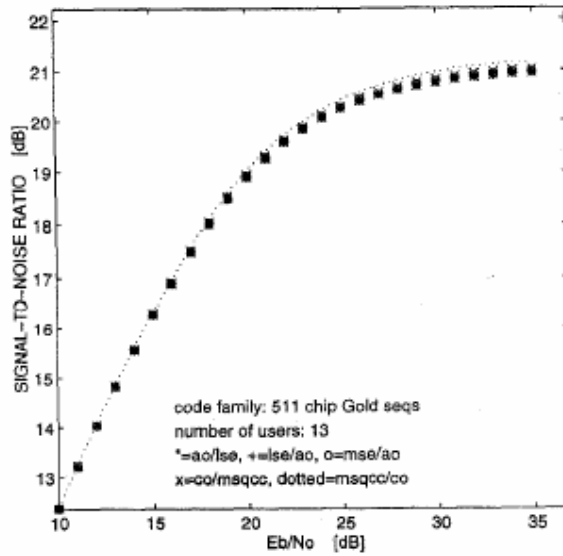


Figure 4.13: Set of Gold sequences of length 511.

4.3.1 Discussion

The five phase optimization criteria were applied to 13 sets of binary PN code sequences of length 31-511 derived from the well-known families of Gold, Kasami (the large and the small family) and maximum-length sequences.

At first, some general observations are summarized. It is concluded that a phase optimization criterion of any kind does not yield considerable advantage, unless the system parameter E_b/N_0 is considerably greater than 10dB. Below that value, the AWGN dominates. The phenomena described is analogous to the case where the relative performance between various PN code families is compared over that range, either with the SNR or with the bit error probability (i.e., below some E_b/N_0 value there is no noticeable difference between code families.) The gain-threshold, i.e., the value of E_b/N_0 beyond which there is an expected benefit from the optimization, depends on the sequence length. Roughly speaking, the gain threshold is typically within the range of 10-15dB for sequences of period 31-63, and within the range of 15-25 dB for sequences of period 127-511. In order to improve the resolution between curves, the E_b/N_0 axis was chosen to begin from the value of 10 dB. (Note also from equations 4.1 and 4.2) that

$\text{SNR}_j = 2E_b/N_0$ when there is no MAI, i.e., there exists a 3 dB difference between these two SNRs).

It can also be concluded from figures 4.1-4.13 that phase optimization begins to lose its importance when the sequence length increases (one criterion still remains the best). The phase optimization problem seems then to become more academic than practical. The attainable gain is probably not worth obtaining since the computational load increases. If the code length is 255 or longer, there is no large difference between AO / LSE, LSE/AO, MSE / AO and CO / MSQCC criteria. It can be expected that the differences in the SNR performance between various criteria are larger when the code length is short.

In most cases, the SNR curves of the AO / LSE, LSE / AO and MSE / AO optimized sets formed a cluster that typically located below the curves of the CO/MSQCC and MSQCC/CO optimized curves. An important conclusion that can be drawn from figures 4.1-4.13 is that, unfortunately, the AO / LSE, LSE / AO and MSE / AO criteria can not be put into the order of quality, i.e. none of these criteria are superior or inferior with respect to CDMA capability. The order of the quality among these three criteria varies from family to family. This conclusion was supported by extensive simulations. Basically, the phenomenon results from the fact that optimization of ACFs does not guarantee minimum AIP values and thus a reduced amount of MAI, although the AIP value depends on the ACFs according to (4.4). It can also be predicted from inequality (4.8).

When the discussion is extended to the CO / MSQCC and MSQCC / CO criteria, it can be concluded that the MSQCC / CO criterion results in a smaller MAI compared with the CO / MSQCC criterion. In addition, the MSQCC / CO criterion is clearly the best among the studied criteria. The dark side of the use of the MSQCC / CO and CO / MSQCC is that they require more computation in order to optimize a whole set of codes. The standpoint in this paper is purely academic.

It can be concluded that the emphasis on the mean-square cross-correlation value as an optimization selection or design criterion of a code family really seems to be more realistic than the emphasis on the maximum cross-correlation value. Unfortunately, the periodic MSQCC value is approximately equal for most PN code families. So, the benefit results from the optimization of the odd function. To see large differences between various code families, the MSQCC is probably not the best correlation parameter. However, it should be noted that the MSQCC is directly related to the system performance, the optimization of which is the ultimate goal of a CDMA designer.

Finally, it is also recommended to use the MSQCC / CO criterion as a sieve to choose sequences for the purpose of numerical analysis of BEP in order to gain the best results and to avoid uncertainty. The AO / LSE optimized sequence sets have often been used as example of BEP analysis in the past.

4.4 Conclusion

In this chapter various code phase optimization criteria are compared with each other. 13 sets of code lengths 31, 63, 127 and 511 are used as examples. It is concluded that a criterion of any kind does not give any advantage unless E_b/N_o is better than 10dB. The optimization also loses its importance when the code length is ≥ 255 . The MSQCC/CO criterion results in the best SNR performance. The CO/MSQCC criterion is the second best. It is also recommended to use MSQCC/CO criterion instead of, e.g., the AO/LSE criterion to choose PN sequences for the purpose of numerical analysis of bit error probability of an asynchronous CDMA system to obtain the best results and to avoid uncertainty.

Chapter 5

Nonlinear Receiver

5.1 Introduction

The task of the receiver is to recover the intended data $x(n)$ by collapsing the spectrum of the received signal vector $\underline{y}(n)$. This is performed by integrating the product of the received signal with a locally held replica of the required user's spreading sequence. Practically, this is achieved by the correlator receiver, shown in Figure 5.1. The received signal, consisting of N_r chips is passed to the block of delay elements, where Z^{-1} represents a delay of one chip, until the complete N_r -chip signal has been read in. These values are then passed in parallel to the multiplier block, which forms the scalar product of $\underline{y}(n)$ and the tap weight vector $\underline{w} \in C^{N_r}$ where N_r is the number of tap weights, which is set to 8 in the figure.

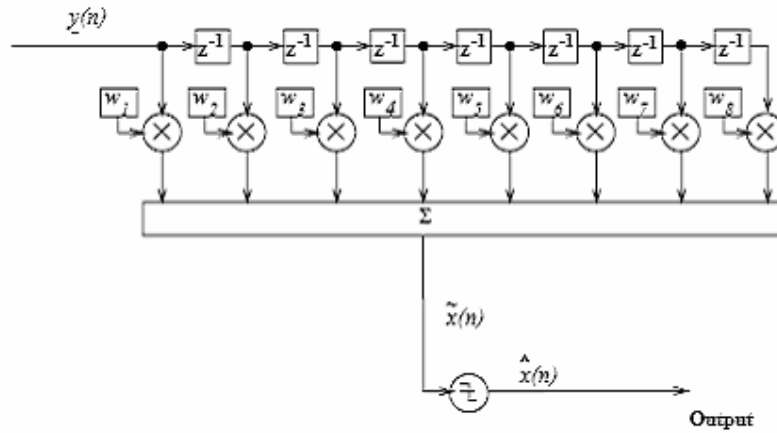


Figure 5.1: DS-CDMA correlator receiver with 8 tap delay.

This filter block produces a soft output, $\tilde{x}(n)$ which is then passed to the sign-decision block to give a hard estimate, $\hat{x}(n)$ of the original data bit, $x(n)$ for the user of interest. The conceptually simplest receiver, the matched filter (MF) receiver, is simply the correlator receiver with M tap weights, $\{w_j : 1 \leq j \leq M\}$, matched to the complex conjugate time-

reverse of the original spreading sequence of the required user which, without loss of generality, we may take to be user 1. In practice, the acquisition and synchronization of the chip-level signal is a highly non-trivial task [10]. Techniques to achieve synchronization involve the use of a pilot signal, which may be modeled by one additional user, whose data is constant. Perfect timing will be assumed in the following, except where stated.

This chapter begins with the description of receivers in general. Later sections are devoted for description of popular receiver structures. After indicating previous works in the field of CDMA receiver design, a new nonlinear receiver based on RBF architecture has been proposed. The proposed receiver also exploits the preprocess based design. Following that section, the method of centre calculation for the RBF receiver has been shown. A method of reducing the computational complexity by reducing the number of centres has also been shown. Both Mahalanobis and Euclidean distance measures are exploited for centre calculation. The chapter ends with results obtained from simulation and conclusion.

5.2 Multiuser receiver

A CDMA receiver can either process the received signal at the chip rate or symbol rate (user bit rate), (see Figure 5.2 and Figure 5.3 for two different MUD receiver structures). Figure 5.2 shows chip rate receivers, which consists of a bank of *matched filters* (MFs) or RAKEs. A bank of MFs is for the non-dispersive AWGN channel, whereas RAKEs are considered for multipath channels. Current mobiles have a simple RAKE because of its simplicity, whereas base stations can have a bank of MFs (or RAKEs) as depicted in figures 5.2 and 5.3. However, structure Figure 5.2 suffers from MAI and therefore has limited performance. Performance improvement can be gained, when carrier to interference ratio (CIR) information from the interferers is taken into account to combat MAI, as structure in Figure 5.3 suggests. This structure is known as the *multiuser detector* (MUD) and is usually suggested for the asynchronous uplink receiver [71]. It could also be used in a modified version as a single user detector in mobiles and might be implemented in the next generation of mobile systems.

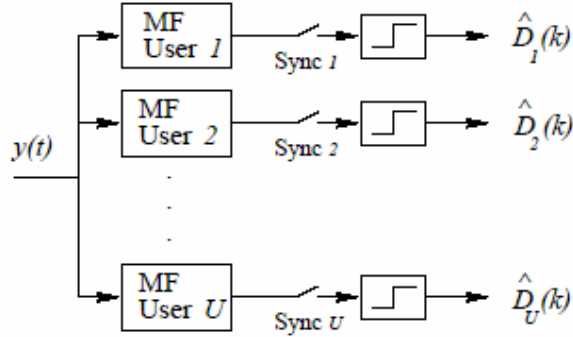


Figure 5.2: Conventional bank of single user receivers with MFs or RAKEs.

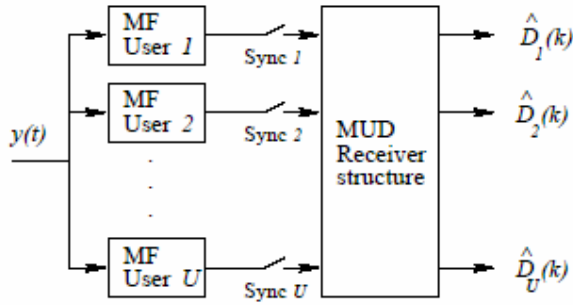


Figure 5.3: Verdu's proposed multiuser detector scheme with MFs for the AWGN channel.

A receiver structure which processes the received signal at the chip rate is known as a *chip level based* (CLB) receiver. Receivers, shown in Figure 5.3, which process at the symbol rate and consist of a front end bank of filters, will be called *preprocessing based* (PPB) receivers.

Verdu [72] showed, based on Forney's paper [73], that the U user maximum likelihood detector for CDMA in AWGN consists of a bank of U single user matched filters followed by a Viterbi algorithm with a time complexity of $O(2^U)$ per bit (binary signalling). This receiver structure shall be called Verdu's receiver (for DS-CDMA). The complexity of the Verdu receiver makes it unsuitable for practical applications. Verdu's receiver structure is often considered in the literature as the optimum receiver for CDMA, in terms of minimizing the number of incorrectly detected symbols. However, there is also evidence that a MAP based receiver outperforms Verdu's receiver, as has been proven for equalizers. Moreover, Jung and Alexander [74] investigated MUD receivers

and also state that the optimum CDMA receiver, defined as the receiver with the least detection errors, is a MAP detector such as that in [75]. Thus, the optimum detector is a *maximum likelihood symbol detector* (MLSD) since it minimizes the symbol error probability and not the sequence error probability as Verdu's receiver does. The optimum receiver is also too complex to implement since it compares the received signal against all possible signal states.

Because all optimum receivers are too complex for practical applications, the search for simpler and near optimum receivers became vital and goes on. Most proposals are based on the multiuser concept, which is preprocessing based (PPB) for several reasons. First, they relate to Verdu's MUD receiver, since they consider it optimum. Second, when long spreading sequences are used, as suggested for *wideband* CDMA (WCDMA) [76], then matrix and vector manipulations become very expensive, whereas preprocessing reduces the signal dimensionality to a reasonable size, from N to U , since generally the number of users is smaller than the number of chips. Third, preprocessing filters (RAKEs) are fast, easy to build and embed into hardware as a simple block, while the output signal has sufficient statistics.

5.3 Linear receiver

The general form of a linear receiver is given by $\hat{D} = \text{sgn}(\mathbf{w}^T \mathbf{y})$ where the $\text{sgn}(\cdot)$ function returns the sign of the operand and where the filter weight vector \mathbf{w} is chosen to minimize a cost function, while \hat{D} is the estimated transmitted bit of the desired user d and \mathbf{y} is the received signal, see Figure 5.4 and 5.5.

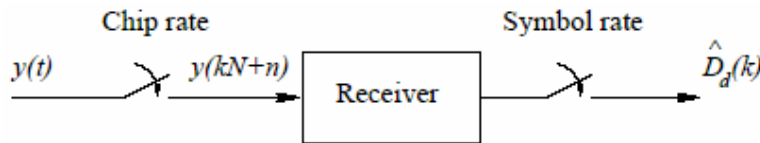


Figure 5.4: Chip rate based receiver.

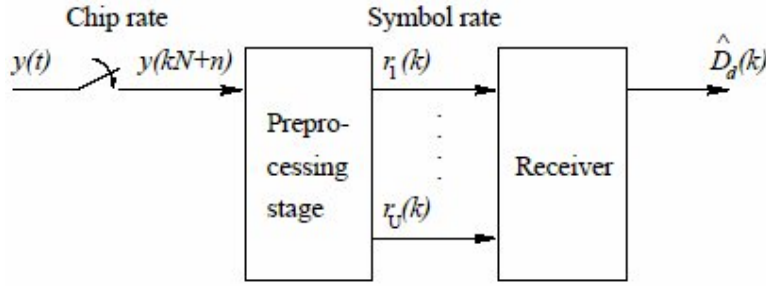


Figure 5.5: Symbol rate based receiver.

5.3.1 Matched Filter Receiver

A very simple and well known detector for SS signals is the matched filter detector, as shown in Figure 5.5. The matched filter detector [77] basically consists of a tapped-delay-line (TDL) filter of which the number of taps equals the spreading sequence length N . The output vector (K) of the tapped delay line $\underline{y}(k) = [y(k), y(k-1), \dots, y(k-N+1)]^T$ is multiplied with a vector of constant weight \underline{w} . $\underline{w} = [w_0, w_1, \dots, w_{N-1}]^T$. The resulting scalar product is applied to a decision function e.g. a *sign* function. For the matched filter case, the weights w_k are matched to the user specific sequence code. $w_l = p n_u(N-1-l)$, for $0 \leq l < N$. So that the matched filter output can be summarized as follows:

$$\tilde{D}(k) = \underline{w}^T \cdot \underline{y}(k) = \sum_{l=0}^{N-1} w_l \cdot y(k-l) \text{ Provided that the receiver is perfectly synchronized to}$$

the transmitter, the TDL extracts a set of chips that represents a particular sequence and the multiplication with the weights is equivalent to despreading operation. A following decision device such as *sign* function leads to the final estimate $\hat{D}(k)$ of the transmitted data bit $D(k)$, hence $\hat{D}(k) = \text{sgn}(\tilde{D}(k))$. The theoretical performance P_e of a MF receiver for a single cell system with U users, long random codes, where N is the number of chips (processing gain) in AWGN is:

$$P_e^{MF} = Q\left(\sqrt{\frac{N}{\sigma^2 + (U-1)}}\right),$$

$$\text{where } Q(x) = 0.5 \text{erfc}\left(\frac{x}{\sqrt{2}}\right)$$

and σ^2 denotes the noise power, derived from:

$$E_b/N_0 = N/2\sigma^2,$$

Where $\sigma^2 = N_0/2$ is the two sided noise power spectral density and E_b is the bit energy.

In a single user system, the matched filter is the optimum receiver for signals corrupted by only AWGN. In a multi user environment, however, the performance degrades rapidly with increasing number of users- the matched filter is multiple-access limited-and strong interferers with high power compared to the desired user cause severe problem. This latter effect is called the near-far problem. Due to these problems, other solution has been searched for. The optimal linear receiver for multi-user detection is Wiener filter and is described in the next section.

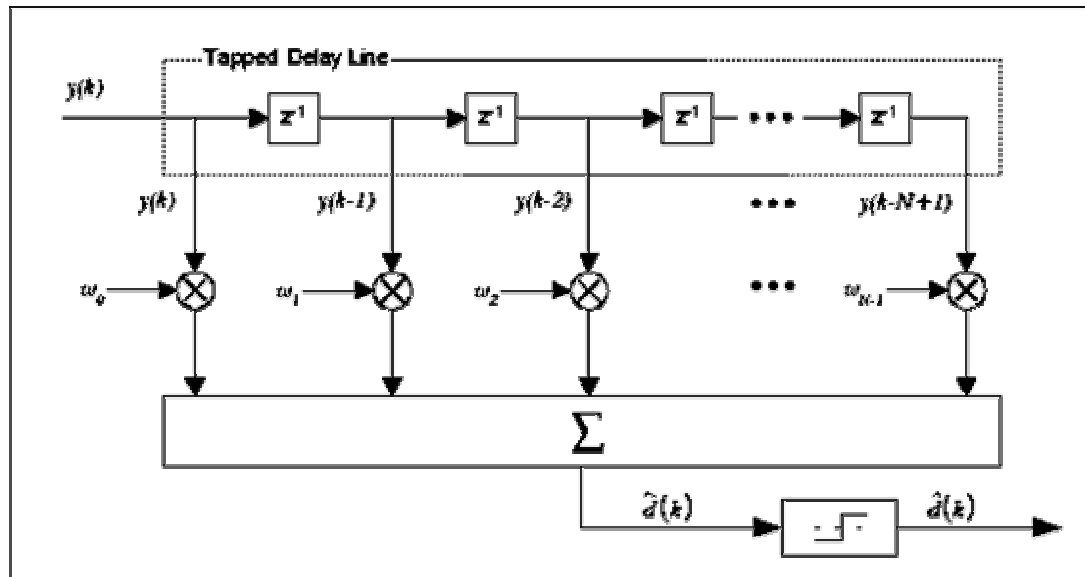


Figure 5.6: Matched filter

5.3.2 Wiener Filter

A typical performance criterion for different receivers is the bit error rate (BER). The optimal receiver for time invariant channel is, with respect to BER, the Wiener filter [77], also known as optimal MMSE detector.

The Wiener filter has same structure as a matched filter as depicted in figure 5.6. In contrast to the matched filter with weights equal to the spreading code, the Wiener filter determines the optimum setting of weights with the goal to minimize error signal given by:

$e(k) = d(k) - \hat{d}(k)$. In a mean-square sense, where $d(k)$ is the desired response and $\hat{d}(k)$ is the output signal of the receiver.

Let J denote the mean-squared error as $J = E[e^2(k)]$, where E is the statistical expectation operator. Considering the linear character of the expectation operator, one readily obtains

$$J = \Phi_d - 2 \sum_{n=0}^{N-1} w_n \Phi_{dy}(n) + \sum_{n=0}^{N-1} \sum_{m=0}^{N-1} w_n w_m \Phi_{yy}(n, m) \text{ or to use a more compact style,}$$

$J = \Phi_d - 2 \underline{w}^T \underline{\Phi}_{dy} + \underline{w}^T \underline{\Phi}_{yy} \underline{w}$, where Φ_d is the mean-squared value of the desired response $d(k)$, $\Phi_d = E(d^2(k))$. $\underline{\Phi}_{dy}$ is the cross-correlation vector between the desired response $d(k)$ and the TDL output vector $\underline{y}(k)$ $\underline{\Phi}_{dy} = E[d(k) \underline{y}(k)]$ and $\underline{\Phi}_{yy}$ denotes the autocorrelation matrix between the TDL output signals: $\underline{\Phi}_{yy} = E(\underline{y}(k) \underline{y}^T(k))$

To minimize the mean-squared error, one simply calculates the gradient of J with respect to the different weights w_n , i.e. $\nabla_{w_n} = \frac{\partial J}{\partial w_n}$, and sets the resulting equations to zero. This

leads to a set of equations $\underline{\Phi}_{yy} \underline{w}_{opt} = \underline{\Phi}_{dy}$, where the \underline{w}_{opt} denotes the optimal weight in the mean-square sense. These weights are then obtained by a simple matrix inversion of $\underline{\Phi}_{yy}$, hence $\underline{w}_{opt} = \underline{\Phi}_{yy}^{-1} \underline{\Phi}_{dy}$. In the considered CDMA system, the autocorrelation matrix $\underline{\Phi}_{yy}$ can be summarized as $\underline{\Phi}_{yy} = \underline{PN}^T \cdot \underline{P} \cdot \underline{PN} + \sigma_n^2 \underline{I}$ where \underline{PN} is $N \times U$ matrix with the spreading codes of the different users as columns, i.e.

$$\underline{PN} = \begin{bmatrix} pn_{1,1} & pn_{2,1} & \dots & pn_{U,1} \\ pn_{1,2} & pn_{2,2} & \dots & pn_{U,2} \\ \dots & \dots & \dots & \dots \\ pn_{1,N} & pn_{2,N} & \dots & pn_{U,N} \end{bmatrix},$$

\underline{P} is $U \times U$ matrix with the users powers $p_u = A_u^2$ as its main diagonal and zeros elsewhere, σ^2 is the noise variance and \underline{I} is a U -dimensional unit matrix. Assuming that the signals of the desired user-interfering user and the desired user-additive noise are uncorrelated,

leads to the crosscorrelation vector that equals the spreading code vector of the desired user.

$$\underline{\Phi}_{dy} = p_1 \begin{bmatrix} pn_{1,1} \\ pn_{1,2} \\ \vdots \\ pn_{1,N} \end{bmatrix}$$

where p_1 denotes the power of user 1. The minimum mean-squared error (MMSE) of the Wiener filter or MMSE detector output can thus be summarised as:

$$e_{\min} = E[d^2(k)] - w_{opt}^T \underline{\Phi}_{dy}$$

The theoretical performance of the MMSE receiver is:

$$P_e^{MMSE} = Q\left(\sqrt{\frac{T}{1 - \frac{T}{T_{xy}}}}\right)$$

To obtain the average BER performance, above equation must be averaged over all users in the system to give $\overline{P_e^{MMSE}}$. Figure 5.7 shows synchronized two user system, from which the MMSE description is derived.

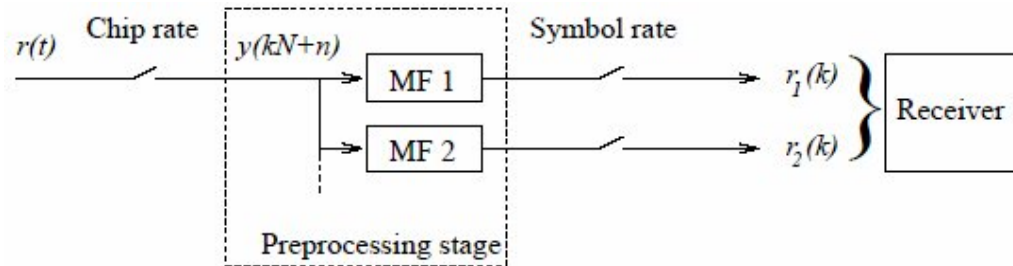


Figure 5.7: A bank of matched filters, the preprocessing stage, as for the optimum multiuser receiver.

Received signal (see appendix A) for bit k , here denoted as $y(kN+n)$, is preprocessed and fed as signal $\mathbf{r}(k) = [\mathbf{r}_1(k), \mathbf{r}_2(k)]^T$ into the receiver. Simulation results for linear CDMA receivers are presented in Figures 5.8 and 5.9. The simulation scenarios were set

with short randomly generated spreading sequences ($N = 7$) and noise power $E_b/N_0 = 7$ dB. The simulation results show how the MF suffers from MAI and is outperformed by the decorrelating (DECO) and the MMSE receiver.

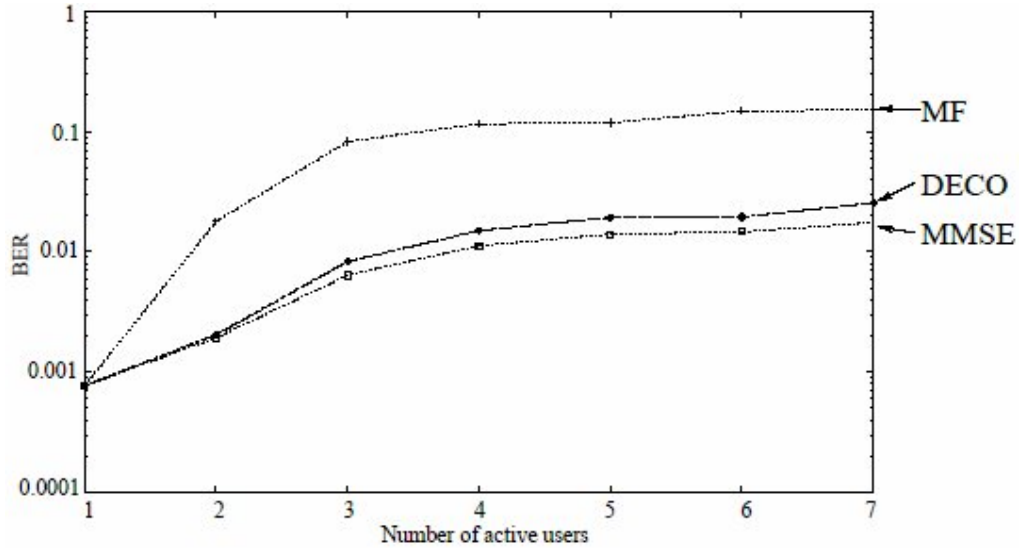


Figure 5.8: BER against the number of users in AWGN at $E_b/N_0 = 7$ dB and with randomly generated spreading codes with 7 chips.

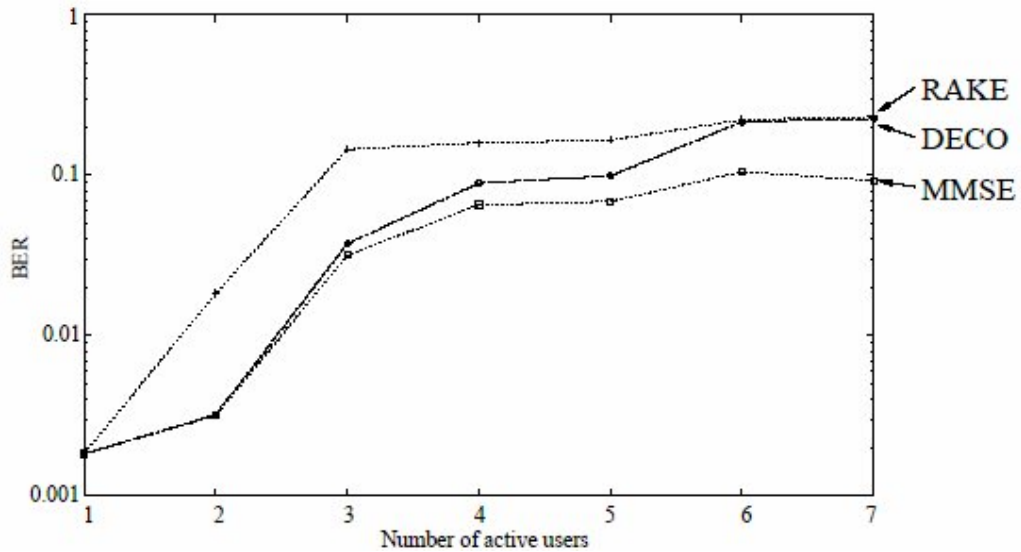


Figure 5.9: BER against the number of users in a stationary multipath, at $E_b/N_0 = 7$ dB and with randomly generated spreading codes with 7 chips.

5.4 Nonlinear receiver

A straightforward way to improve the performance of CDMA receivers is to cancel MAI. This class of receivers, known as *interference cancellers*, has drawn much attention. Most designs use combinations of linear receiver for pre and post filtering since it keeps the complexity low [78]-[82]. However, in order to cancel MAI well, a good estimate of each users signal power is essential; otherwise interference is added and not subtracted.

The *multistage detector* (MSD) proposed by Varanasi and Aazhang [83] improves each stage's estimate by subtracting an MAI estimate obtained from the previous stage, a linear processing followed by an iterative nonlinear processing step. Kechriotis and Manolakos [84] showed that the MSD is a special case of a discrete time approximation of their proposed *Hopfield Neural Network* (HNN) [85]. Moreover, the HNN can correspond to an infinite number of stages of MSD sharing similar characteristics.

Aazhang *et al.* [86] investigated the MLP for high bandwidth efficiency. The open question of determining the number of neurons was solved by assigning a sufficient number of neurons by analyzing the decision boundary first. Once again, the MLP NN showed excellent performance at the expense of long training time, computational complexity and network size uncertainty.

5.5 RBF for DS-CDMA

The MMSE filter has its limitations when we introduce multi-user interference. MF generally fails to construct a simple plane or hyper-plane in non-linear situations. Any signal, in particular digital signals, can be viewed as pattern. The following figure (Figure 5.10) shows that DS-CDMA can also be viewed as a pattern recognition problem [87].

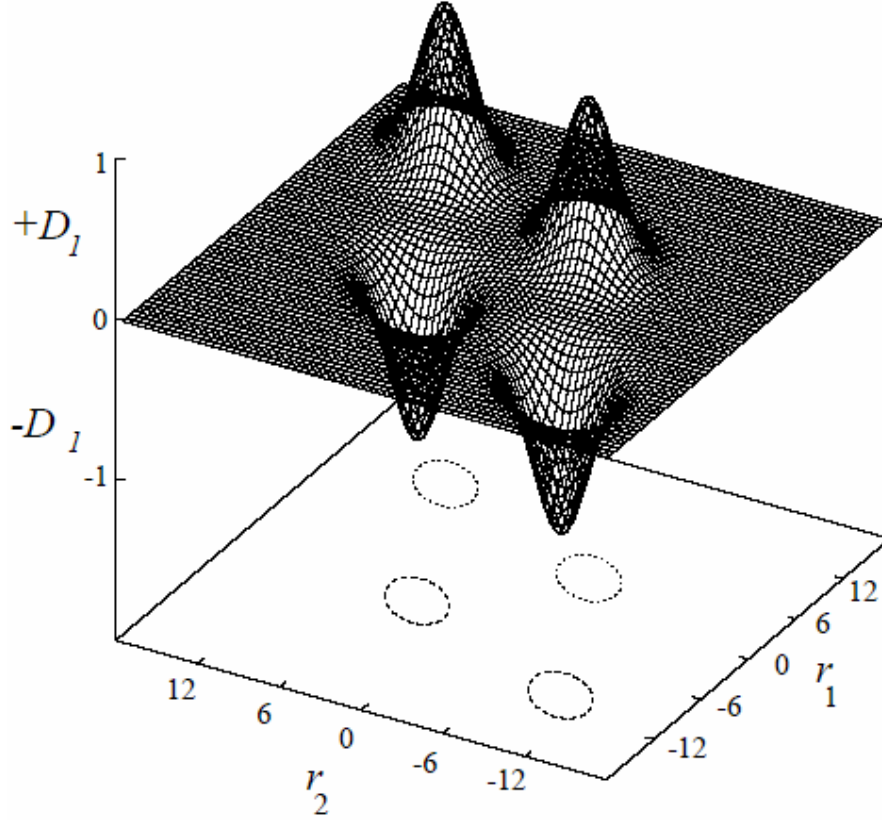


Figure 5.10: The decision surface (shape) of the Bayesian receiver structure for a two user CDMA scenario in AWGN and $E_b/N_0 = 7$ dB. The axis r_1 and r_2 are the outputs of the preprocessor. Each hub represents the noise distribution around one of the four possible noise free signal states.

A network which performs well as a pattern recognizer, must be able to construct decision boundaries, or must have a memory. These are typical features of neural networks. Thus, common network solutions are *associative memory networks*, e.g. HNNs, MLPs, RNNs and RBFNs [88].

Mitra and Poor [89] applied the RBF network for CDMA as an adaptive RBF. The received signal is $\mathbf{r} = \mathbf{s}_d + \mathbf{g}$ where \mathbf{s}_d is the desired signal vector and \mathbf{g} is the noise component inclusive of MAI. The observation density conditioned on a hypothesis H_i , for $i=0$ or 1 is:

$$p(\mathbf{r}/i) = \frac{1}{2^{U-1}} \sum_{m=1}^{2^{U-1}} \frac{1}{\sqrt{(2\pi)^N} \sigma^N} \exp\left(-\frac{\|\mathbf{r} - \mathbf{s}_d(i) - \mu_m\|^2}{2\sigma^2}\right), \quad (5.1)$$

Where U is the number of users, σ^2 is the Gaussian noise variance, $\mathbf{s}_d(i)$ is the desired signal vector given H_i and μ_m is the m th permutation of the interferer's signal's. The likelihood ratio becomes then:

$$LR = \frac{\sum_{m=1}^{2^{U-1}} \exp\left(-\frac{\|\mathbf{r} - \mathbf{s}_d(1) - \mu_m\|^2}{2\sigma^2}\right)}{\sum_{m=1}^{2^{U-1}} \exp\left(-\frac{\|\mathbf{r} - \mathbf{s}_d(0) - \mu_m\|^2}{2\sigma^2}\right)} \quad (5.2)$$

The Bayesian decision rule [90] is:

$$\delta = \text{sgn}\left\{\sum_{m=1}^{2^{U-1}} \exp\left(-\frac{\|\mathbf{r} - \mathbf{s}_d(1) - \mu_m\|^2}{2\sigma^2}\right) - \sum_{m=1}^{2^{U-1}} \exp\left(-\frac{\|\mathbf{r} - \mathbf{s}_d(0) - \mu_m\|^2}{2\sigma^2}\right)\right\} \quad (5.3)$$

5.6 CLB RBF

A class of network models, which possess universal approximation capabilities, is the radial basis function network [91][92]. The RBFN is also referred to as neural network in [89], where its adaptive characteristics have been investigated. RBF methods perform an approximation of mappings from a set of data points in a multi dimensional space [93]. The approximation problem requires a mapping for every input vector onto a target vector. In CDMA the mapping is performed from the N - dimensional input space (processing gain) of $\mathbf{y}(k)$ for transmitted symbol k , to a 1-dimensional target (output) space, which is the bit of the desired user, D_d . The data set consists of all M , M may be 2^u , possible received signals $\mathbf{y}(m)$ for $m = 1, 2, 3, \dots, M$, together with the corresponding targets $D_d(m)$, the desired user bit, which can be obtained from a generating matrix. For clarity, $\mathbf{y}(m)$ shall be denoted as \mathbf{y}_m and corresponds to the m th row of a generating matrix, e.g. \mathbf{P} (see appendix A). Ideally, there exists a function $f(\mathbf{y})$ such that: $f(\mathbf{y}_m) = D_d(m)$, for $m = 1, 2, 3, \dots, M$. The RBF approach [90][93] introduces a set of M basis functions, one for each data point. They take the form $\phi(\|\mathbf{y}(k) - \mathbf{y}_m\|)$ where $\phi(\cdot)$ may be nonlinear function. Thus each function depends on the Euclidean distance $(\|\mathbf{y}(k) - \mathbf{y}_m\|)$ between the received signal $\mathbf{y}(k)$ and the legitimate data point \mathbf{y}_m . Many functions for

$\phi(\cdot)$ have been proposed. However the Gaussian is the most common. The network output is a linear combination of M weighted basis functions:

$$f(\mathbf{y}(k)) = \sum_{m=1}^M w_m \phi(\|\mathbf{y}(k) - \mathbf{y}_m\|) \quad (5.4)$$

The received signal $\mathbf{y}(k)$ consists of the signal component and Gaussian noise. Since the noise component $g(n)$ added onto each vector element $\{y_n(k)\}$ is neither correlated with noise or other components, $y(k)$ has a univariate normal density, defined as:

$$p(x) = \frac{1}{\sqrt{2\pi}\sigma} \exp\left(-\frac{(x-\mu)^2}{2\sigma^2}\right), \quad (5.5)$$

for which $\mu = E(x)$ and $\sigma^2 = E[(x-\mu)^2]$. The univariate normal density is fully described by its mean μ and its variance σ^2 . These normally distributed samples tend to cluster about the mean with a spread proportional to the standard deviation σ [94]. This fact results in circular distributed signal $\mathbf{y}(k)$ about its mean. Figure 5.11 illustrates the fact for a two user PPB CDMA system. There the preprocessed signal \mathbf{r} forms circular clusters about the four possible means (centres), where the diameter of each circle is proportional to σ^2 , the noise power. The circles were derived from contour lines of the Bayesian decision surface, the circles represent a slice of Gaussian shaped bell, which represents the noise spread, see also Figure 5.9. Therefore, the CLB RBF for CDMA has a Gaussian basis function and is defined by:

$$f(\mathbf{y}(k)) = \sum_{m=1}^M w_m \exp\left(-\frac{\|\mathbf{y}(k) - \mathbf{y}_m\|^2}{2\sigma^2}\right) \quad (5.6)$$

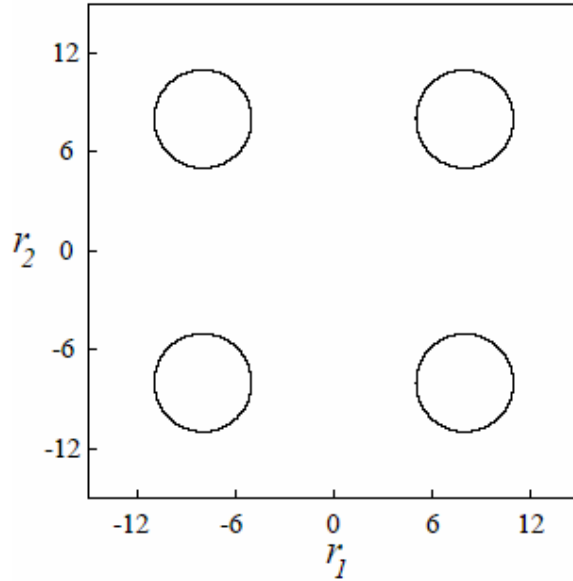


Figure 5.11: Circular clusters of two user CDMA system. (Noise is uncorrelated)

The parameter σ^2 controls the smoothness or spread about a mean \mathbf{y}_m of the approximating function and represents the noise power. The parameter \mathbf{y}_m is known in the literature as the RBF centre and shall be denoted from now onwards as \mathbf{c}_m . If the data set of all possible received signals is known, \mathbf{c}_m is known and the network is determined. Otherwise, \mathbf{c}_m must be constructed according to an established clustering algorithm [89][90]. Of course, the network is only fully determined, if w_m and σ^2 are also known. Assuming that the noise power is known, e.g. from measurements, then w_m and \mathbf{c}_m are the remaining two unknowns. In CDMA both can be pre-calculated. Figure 5.12 shows a CLB RBFN.

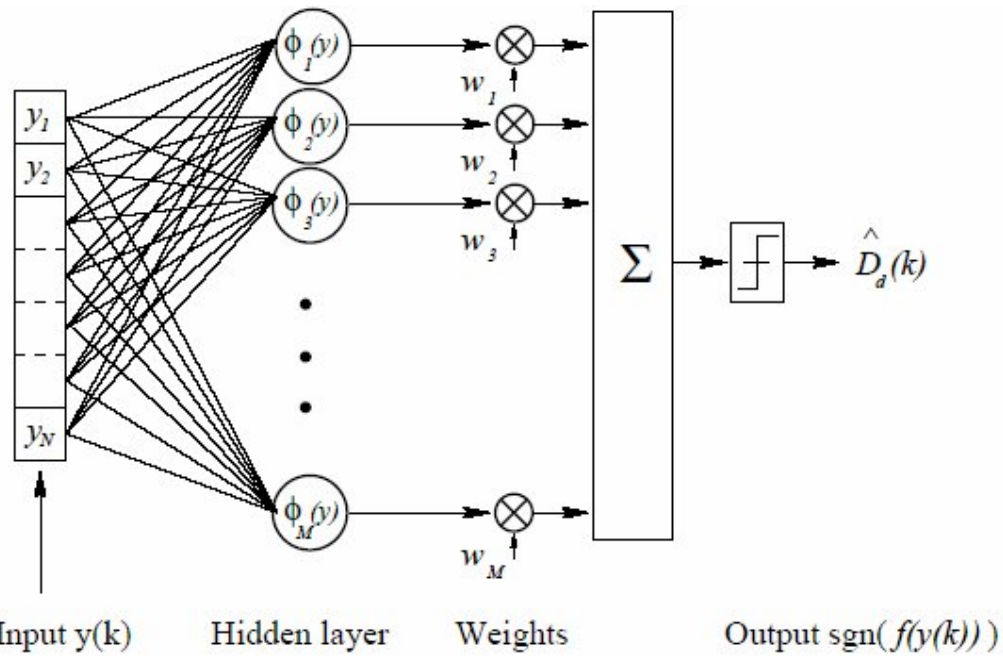


Figure 5.12: The structure of the CLB RBF network.

The network consists of four parts. First, the input layer, which is at the left hand side, where the synchronized N chips of $\mathbf{y}(k)$ are fed into the network. The next layer is the hidden layer, which consists of M centers (also called neurons, units or nodes), and represent the points around which received signals lie or cluster. Each center is connected to all chips of the input layer. The hidden layer performs a mapping from the input space \mathfrak{R}^N to the hidden space \mathfrak{R}^M . The output of the m^{th} centre is determined by $\phi_m(\mathbf{y}(k)) = \phi(\|\mathbf{y}(k) - \mathbf{c}_m\|)$. Next, the output of each center $\phi_m(\mathbf{y})$ is weighted by w_m and summed over all M values. This is a mapping from \mathfrak{R}^M to \mathfrak{R} . Finally, the sum is sliced (for antipodal signaling by a step function with outputs $\{+1, -1\}$) and the estimate of the desired user bit is produced, hence: $\hat{D}_d(k) = \text{sgn}(f(\mathbf{y}(k)))$.

5.6.1 CLB Based RBF Receiver

Consider the construction of all possible received signals in CDMA for U users in a memoryless (AWGN) channel with their unique spreading sequences. These signals form a set with $M = 2^U$ points in \mathfrak{R}^N and are stored in a $(M \times N)$ matrix \mathbf{P}^{AWGN} , where each row represents a point, hence $[\mathbf{p}_1, \mathbf{p}_2, \dots, \mathbf{p}_M]^T$. The spreading codes are stored in a $(U \times 1)$ partitioned matrix

\mathbf{C} with vector elements $[\mathbf{c}_1 \mathbf{c}_2 \dots \mathbf{c}_U]^T$. The notation $\{\mathbf{c}_u\}$ indicates the u^{th} spreading sequence, whereas $\{\mathbf{c}_m\}$ shall refer to the m^{th} RBF center. Instead of using the term signal, the term point shall be used, since each signal vector can be seen as a point in the vector space. All possible points are derived from:

$$\mathbf{P}^{AWGN} = \mathbf{BC} = \begin{bmatrix} 11\dots 11 \\ 11\dots 1-1 \\ 11\dots -11 \\ \dots \\ -1-1\dots 1-1 \\ -1-1\dots -11 \\ -1-1-1-1 \end{bmatrix} \begin{bmatrix} \mathbf{c}_1^T \\ \mathbf{c}_2^T \\ \mathbf{c}_3^T \\ \dots \\ \mathbf{c}_{U-2}^T \\ \mathbf{c}_{U-1}^T \\ \mathbf{c}_U^T \end{bmatrix} = \begin{bmatrix} \mathbf{c}_1^T + \mathbf{c}_2^T + \dots + \mathbf{c}_{U-1}^T + \mathbf{c}_U^T \\ \mathbf{c}_1^T + \mathbf{c}_2^T + \dots + \mathbf{c}_{U-1}^T - \mathbf{c}_U^T \\ \mathbf{c}_1^T + \mathbf{c}_2^T + \dots - \mathbf{c}_{U-1}^T + \mathbf{c}_U^T \\ \dots \\ -\mathbf{c}_1^T - \mathbf{c}_2^T - \dots + \mathbf{c}_{U-1}^T - \mathbf{c}_U^T \\ -\mathbf{c}_1^T - \mathbf{c}_2^T - \dots - \mathbf{c}_{U-1}^T + \mathbf{c}_U^T \\ -\mathbf{c}_1^T - \mathbf{c}_2^T - \dots - \mathbf{c}_{U-1}^T - \mathbf{c}_U^T \end{bmatrix} \quad (5.7)$$

where \mathbf{B} is a $(M \times U)$ combination matrix with all possible binary signal combinations as its rows, and code vector \mathbf{c} having all user spreading sequences \mathbf{c}_u as its elements. Column u of \mathbf{B} becomes the RBF weight vector \mathbf{w} if the RBF is thought as a single user detector for the u^{th} user [87]. Elements $[\mathbf{p}_1 \mathbf{p}_2 \dots \mathbf{p}_M]^T$ consist of the sum of spreading codes in equation (5.7) and become the M CLB RBF centers $[\mathbf{c}_1 \mathbf{c}_2 \dots \mathbf{c}_M]^T$. The $(M \times I)$ vector \mathbf{p}^{AWGN} with its vector elements can also be denoted as $(M \times N)$ matrix \mathbf{P}^{AWGN} , since the spreading codes \mathbf{c}_u are of length N . Now the RBF is constructed for the memoryless (Gaussian) scenario with 2^U centres, where each centre has vector length N . Note the notation used for spreading codes \mathbf{c}_u , centers \mathbf{c}_m and points \mathbf{p}_m^{AWGN} .

The RBF centre construction for channels with memory is computationally much more demanding, and can be carried out in different ways. Two different approaches shall be discussed. Further, it is assumed that a perfect estimate of the L - tap channel impulse response H_{ch} (chip spaced) is available at the receiver.

Full Multipath: Centres \mathbf{P}^{FM} are derived from the previous, current and next symbol sequence; hence 2^{3U} centres with length $(N+L-1)$.

Extended Gaussian: Centres \mathbf{P}^{EG} are derived by convolving each memoryless (gaussian) centres with H_{ch} ; hence the number of centres is 2^U and the vector length of each centre is $(N+L-1)$.

The different aspects of constructing RBF centre vectors shall be discussed in conjunction with Figure 5.13. Here a fully synchronised receiver is assumed. IS-95 has a three finger RAKE receiver implemented at the mobile, which combines the three strongest multipath components [95]. This structure can be seen as an FIR filter, whose filter weights are equal to the convolution of the spreading sequence of the desired user with H_{ch} . Thus there are $(N+L-1)$ chips of $\mathbf{y}(k)$ taken into account to estimate the transmitted bit \hat{D}_d . Symbol $\mathbf{y}(k)$ consists of two ISI affected chip sequences named head and tail, as shown in Figure 5.12. The $(L-1)$ head chips are affected by the previous transmitted symbol sequence, whereas the tail chips are the head chips of the next symbol, into which the current symbol spreads. In order to take all the energy of the current symbol into account, the chip or vector span at the receiver must be $(N+L-1)$. Due to the fact that a RAKE receiver can implement a *maximum ratio combining* (MRC) or an *equal gain combining* (EGC) receiver, the term RAKE shall be replaced by MRC or EGC in order to specify the structure used [1][53]. Another approach is to take a MF receiver instead of a RAKE. This results in a much simpler receiver structure. Of course, this is at the cost of severe performance degradation since ISI and *inter chip interference* (ICI) is not appropriately taken into account.

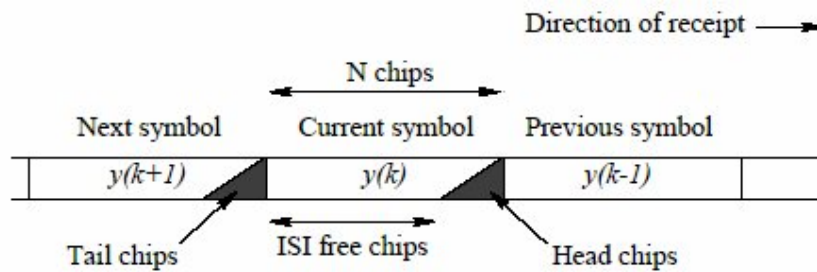


Figure 5.13: Center construction (From a chip level perspective)

Figure 5.13 depicts the statements made so far. A pure MF receiver would suffer from the ISI affected head chips and the neglected ICI. Hence, a simple MF as the receiver in a

multipath environment is usually not implemented. The first step to improve system performance is by taking H_{ch} into account and combating ICI. The extended Gaussian RBF centres fulfill this requirement. It provides the RBFN with a reasonable number of centres, where the matrix containing all RBF centres has a size of $(2^U \times (N+L-1))$.

Finally, the structure which corresponds best to the maximum likelihood symbol by symbol detection scheme is named the full multipath implementation, since all possible received symbols become centres. Of course, its complexity is prohibitively high for practical implementations since the matrix \mathbf{P}^{FM} containing all centres has size $(M \times (N+L-1))$ with $M=2^{3U}$. The centres of the full multipath implementation are given by the product between an extended code matrix \mathbf{C}^{ECM} and a matrix \mathbf{H} describing the channel characteristics. The extended code matrix shall be of size $(M \times 3N)$, where the first N columns represent the previous, the next N columns the current and the last N columns the next symbol. Again, the starting point is a combination matrix \mathbf{B} , but this time of size $(M \times 3U)$, thus:

$$\mathbf{B}^{ECM} = \begin{bmatrix} 1 & \dots & 1 & 1 & \dots & 1 & 1 & \dots & 1 \\ 1 & \dots & 1 & 1 & \dots & 1 & 1 & \dots & -1 \\ 1 & \dots & 1 & 1 & \dots & -1 & 1 & \dots & 1 \\ \dots & \dots & \dots & \dots & \dots & \dots & \dots & \dots & \dots \\ -1 & \dots & -1 & -1 & \dots & -1 & -1 & \dots & -1 \\ -1 & \dots & -1 & -1 & \dots & -1 & -1 & \dots & 1 \\ -1 & \dots & -1 & -1 & \dots & -1 & -1 & \dots & -1 \end{bmatrix} \quad (5.8)$$

In order to simplify the notation, \mathbf{B}^{ECM} is partitioned into three sub-matrices, thus:

$$\mathbf{B}^{ECM} = [\mathbf{B1} \mid \mathbf{B2} \mid \mathbf{B3}] \quad (5.9)$$

Where each sub-matrix has size $(M \times U)$. The next step is to compute the $(M \times 3N)$ matrix \mathbf{C}^{ECM} with the Hadamard product. Therefore, each sub-matrix is multiplied by the spreading codes. This results in three $(M \times N)$ sub-matrices, but since they are adjacent

$$\text{the rows are of length } 3N: \mathbf{C}^{ECM} = \left[\mathbf{B1} \begin{bmatrix} \mathbf{c}_1^T \\ \vdots \\ \mathbf{c}_U^T \end{bmatrix} \mid \mathbf{B2} \begin{bmatrix} \mathbf{c}_1^T \\ \vdots \\ \mathbf{c}_U^T \end{bmatrix} \mid \mathbf{B3} \begin{bmatrix} \mathbf{c}_1^T \\ \vdots \\ \mathbf{c}_U^T \end{bmatrix} \right] \quad (5.10)$$

Finally, the $(M \times (N+L-1))$ matrix \mathbf{P}^{FM} containing all possible sequences for three adjacent symbols is constructed. In order to find \mathbf{P}^{FM} the matrix \mathbf{H} has to be derived. The channel impulse response H_{ch} with coefficients $\{h_1, h_2, \dots, h_L\}$ is stored in a $((N+L-1) \times 3N)$ matrix \mathbf{H} . \mathbf{H} does not have to be $(3N \times 3N)$ since only the current symbol together with its ISI affected head and tail chips is of interest. Thus, a $((N+L-1) \times 3N)$ matrix is sufficient where the first $(N+L-1)$ columns in \mathbf{H} . So for instance for $L=3$ and $N=5$, it becomes:

$$\mathbf{H} = \begin{bmatrix} 000h_3h_2h_1 & 000000000 \\ 0000h_3h_2h_1 & 000000000 \\ 00000h_3h_2h_1 & 000000000 \\ 000000h_3h_2h_1 & 000000000 \\ 0000000h_3h_2h_1 & 000000000 \\ 00000000h_3h_2h_1 & 000000000 \\ 000000000h_3h_2h_1 & 000000000 \end{bmatrix} \quad (5.11)$$

Then, all possible centres are found from the product between:

$$\mathbf{P}^{FM} = \mathbf{C}^{ECM} \mathbf{H}^T. \quad (5.12)$$

Matrix \mathbf{H} for the extended Gaussian approach is given in (6.11). It is a truncated version of (6.9) with size $((N+L-1) \times N)$ since no ISI has to be taken into account, hence:

$$\mathbf{H} = \begin{bmatrix} h_1 & 00 \dots 000 \\ h_2h_1 & 0 \dots 000 \\ \dots & \dots \\ 000 \dots 0h_Lh_{L-1} \\ 000 \dots 00h_L \end{bmatrix} \quad (5.13)$$

The centres \mathbf{P}^{EG} of the extended Gaussian RBF are given by the product between \mathbf{P}^{AWGN} and \mathbf{H} . Thus the M centers with length $(N+L-1)$ are derived from the $((N+L-1) \times N)$ channel matrix \mathbf{H} and the M memoryless RBF centres in \mathbf{P}^{AWGN} :

$$\mathbf{P}^{EG} = \mathbf{P}^{AWGN} \mathbf{H}^T = [\mathbf{p}_1 \mathbf{p}_2 \dots \mathbf{p}_M]^T \mathbf{H}^T \quad (5.14)$$

$$= \begin{bmatrix} \mathbf{p}_1 \\ \mathbf{p}_2 \\ \dots \\ \mathbf{p}_{M-1} \\ \mathbf{p}_M \end{bmatrix} \begin{bmatrix} h_1 & 00 \dots 000 \\ h_2h_1 & 0 \dots 000 \\ \dots & \dots \\ 000 \dots 0h_Lh_{L-1} \\ 000 \dots 00h_L \end{bmatrix}^T$$

5.7 Preprocessed based RBF receiver

It has been seen in Figure 5.7 that multiuser receivers exploit preprocessed signals. Preprocessing can be done with different pre-filter structures. For the memoryless channel, matched filtering is optimum [53]. In multipath, the simple MF is no longer optimum since it does not take ISI effects into account, but receiver structures based on Price's RAKE [96] do. The preprocessing approach taken in this work rests upon the MRC, where the MRC is derived from the RAKE [1]. Since real data has been used, the MRC weights the output of each RAKE finger with its corresponding l th channel coefficient, while $(L-1)$ fingers process a delayed version of $\mathbf{y}(k)$. If the weights are unity, the RAKE structure corresponds to the EGC [1]. This process takes advantage of the fact that matched filters enhance the SNR, while in addition the signal dimensionality is reduced. Thus, more sophisticated receiver algorithms can be exploited in order to enhance the performance by combating MAI and ISI more effectively. However, the general approach is to assume uncorrelated noise at the receiver input. This is achieved by embedding a noise whitening filter between the preprocessor and the actual receiver. Generally, no attempts are made to take correlated noise into account due to the assumption made that the noise is uncorrelated, which simplifies the analysis. A noise whitening filter as such shall not be considered in this work.

The correlated nature of the noise is easily pointed out. All MFs match the same sampled sequence $\mathbf{y}(k)$ against their (user) specific sequence \mathbf{c}_u . Thus the noise becomes correlated, since the orthogonality among the spreading codes can be destroyed by multipath or when nonorthogonal spreading codes are employed in the first place. Therefore, all possible received PPB signals in a memoryless channel are given by:

$$\mathbf{R}^{AWGN} = \mathbf{P}\mathbf{C}^T = \mathbf{B}\mathbf{C}\mathbf{C}^T = \begin{bmatrix} 11\dots 11 \\ 11\dots 1-1 \\ 11\dots -11 \\ \dots\dots\dots \\ -1-1\dots 1-1 \\ -1-1\dots -11 \\ -1-1-1-1 \end{bmatrix} \begin{bmatrix} \mathbf{c}_1^T \\ \mathbf{c}_2^T \\ \mathbf{c}_3^T \\ \dots \\ \mathbf{c}_{U-2}^T \\ \mathbf{c}_{U-1}^T \\ \mathbf{c}_U^T \end{bmatrix} \begin{bmatrix} \mathbf{c}_1^T \\ \mathbf{c}_2^T \\ \mathbf{c}_3^T \\ \dots \\ \mathbf{c}_{U-2}^T \\ \mathbf{c}_{U-1}^T \\ \mathbf{c}_U^T \end{bmatrix}^T \quad (5.15)$$

Resulting in

$$\mathbf{R}^{AWGN} = \mathbf{B}\mathbf{S}$$

$$= \begin{bmatrix} 11\dots 11 \\ 11\dots 1-1 \\ 11\dots -11 \\ \dots\dots\dots \\ -1-1\dots 1-1 \\ -1-1\dots -11 \\ -1-1-1-1 \end{bmatrix} \begin{bmatrix} \mathbf{c}_1^T \mathbf{c}_1 \mathbf{c}_1^T \mathbf{c}_2 \dots \mathbf{c}_1^T \mathbf{c}_{U-1} \mathbf{c}_1^T \mathbf{c}_U \\ \mathbf{c}_2^T \mathbf{c}_1 \mathbf{c}_2^T \mathbf{c}_2 \dots \mathbf{c}_2^T \mathbf{c}_{U-1} \mathbf{c}_2^T \mathbf{c}_U \\ \dots\dots\dots \\ \mathbf{c}_{U-1}^T \mathbf{c}_1 \mathbf{c}_{U-1}^T \mathbf{c}_2 \dots \mathbf{c}_{U-1}^T \mathbf{c}_{U-1} \mathbf{c}_{U-1}^T \mathbf{c}_U \\ \mathbf{c}_U^T \mathbf{c}_1 \mathbf{c}_U^T \mathbf{c}_2 \dots \mathbf{c}_U^T \mathbf{c}_{U-1} \mathbf{c}_U^T \mathbf{c}_U \end{bmatrix} \quad (5.16)$$

Which results in the product between the combination matrix \mathbf{B} and the crosscorrelation matrix \mathbf{S} of the user codes. In the case of a memoryless channel and orthogonal spreading codes being used, \mathbf{S} contains zeros on its off diagonals. The received signal \mathbf{r} has vector elements $[\mathbf{r}_1 \mathbf{r}_2 \dots \mathbf{r}_M]^T$ (the output of each MF), where each \mathbf{r}_m is equivalent to the m^{th} row in \mathbf{B} . Hence, the properties of signal \mathbf{r}_m^T depend on \mathbf{B} . In the case of orthogonal spreading, the received signals (seen as points) will form a hypercube in \Re^U centered at the origin, because \mathbf{B} contains all possible binary combinations, which are the 2^U vertices for the U -dimensional space. If nonorthogonal codes are employed, the hypercube becomes skewed due to \mathbf{S} . The matrix \mathbf{S} affects the noise statistics at the preprocessor output. The noise is no longer univariate normal but multivariate normal distributed:

$$p(\mathbf{r}) = \frac{1}{\sqrt{(2\pi)^U} \sqrt{|\mathbf{S}|}} \exp\left(-\frac{(\mathbf{r} - \mu)^T \mathbf{S}^{-1} (\mathbf{r} - \mu)}{2}\right) \quad (5.17)$$

where \mathbf{r} is U dimensional mean vector, \mathbf{S} is the $(U \times U)$ covariance matrix. $\mu = E[\mathbf{r}]$ is the mean and $\mathbf{S} = E[(\mathbf{r} - \mu)(\mathbf{r} - \mu)^T]$ is the expected value of the matrix, found by taking the expected values of its components [94]. Thus, the covariance matrix is equivalent to the crosscorrelation matrix of the users' spreading codes and noise, since the signal's mean is zero. The effect of correlated noise is shown in Figure 5.14 for a two user PPB CDMA system with nonorthogonal spreading codes. Compared with Figure 5.11, it shows an elliptical distributed signal, whereas orthogonal codes result in a circular distribution about each mean. The exponential term (within the brackets) in (5.17) is known in pattern

recognition literature as the *Mahalanobis* distance measure [94][90][97]. Figure 5.15 illustrates the impact of the two distance measures presented. It shows the decision boundaries for a two user DS-CDMA scenario in AWGN with $E_b / N_o = 7\text{dB}$ and 7 chip Gold codes.

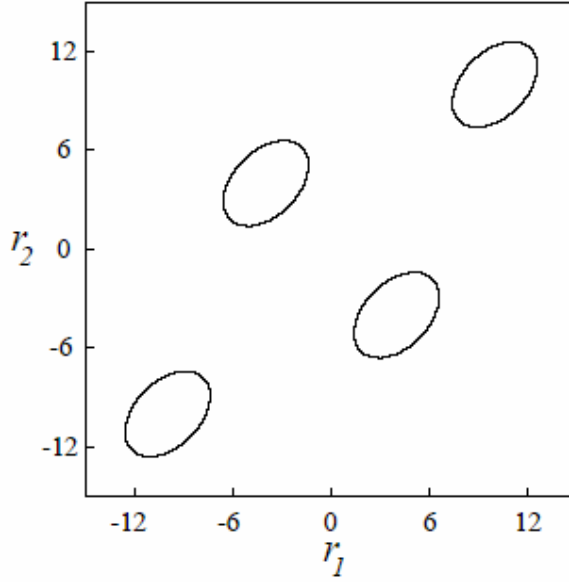


Figure 5.14: Elliptical clusters of two user CDMA system. (Noise is correlated)

The next step is to replace the Euclidean distance measure used in (5.6) by the Mahalanobis distance measure in (5.17). Therefore, the new radial basis function has the form:

$$f(\mathbf{r}(k)) = \sum_{m=1}^M w_m \exp\left(-\frac{(\mathbf{r}(k) - \mathbf{c}_m)^T \mathbf{S}^{-1} (\mathbf{r}(k) - \mathbf{c}_m)}{2}\right) \quad (5.18)$$

where the centres \mathbf{c}_m are the preprocessed CLB RBF centres, which can also be constructed according to equation (5.17). Vector $\mathbf{r}(k)$ is the signal fed into the PPB RBFN, which has a correlated noise component. Since this RBF receiver structure takes the correlated noise into account, it must perform as well as the CLB RBF, which implements the Bayesian function and hence is optimum for the non-dispersive AWGN scenario.

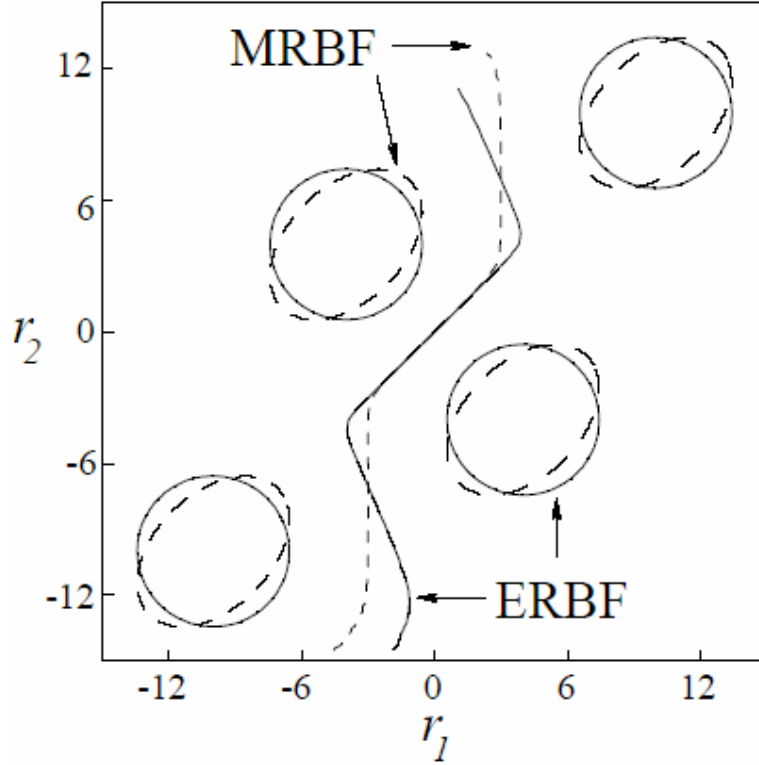


Figure 5.15: Two decision boundaries for two different PPB RBF structures for a two user CDMA system with 7 chip Gold codes and $E_b / N_0 = 7\text{dB}$. Shown are the decision boundaries obtained with Euclidean distance measure (ERBF) and Mahalanobis distance measure (MRBF).

5.8 Reduced PPB RBF receiver

The Mahalanobis based RBF also has 2^{3U} centres in a multipath scenario though with shorter centre vectors, which are of length U . However, this implies 2^{15} centres when five users are active. Clearly, this is a prohibitively large network for mobile telephony applications. In order to reduce the RBF complexity, the properties of the processed signals should be analysed. Then, it may be possible to find a technique to reduce the network size.

It was found that there exists 2^U clusters, where 2^{2U} points form a cluster. It can be explained with figure 5.16.

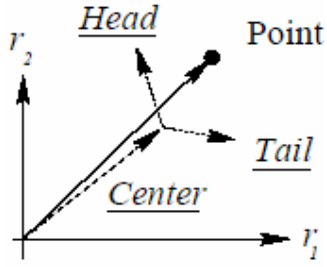


Figure 5.16: The effect of ISI on the chips (vector perspective)

The effect of ISI on the chips within a symbol causes interference. The head and tail chips are understood as rotating vectors, which depend on the transmitted user bits in the previous and next symbol, and cause the preprocessed signal (point) to lie differently (spread). In figure 5.16 a vector representation is given for a single point based on the illustration presented in Figure 5.13. A vector *Centre* is given by the chips unaffected by ISI. On top of this vector, the ISI affected vectors *Head* and *Tail* are added. Since vectors *Head* and *Tail* are dependent on the previous, current and next symbol, they are not fixed and can “rotate”. Hence they can point in different directions. The shape of these clusters is dependent on the correlation among the spreading codes and the channel impulse response. Generally, if the codes are orthogonal the clusters tend to look circular, whereas highly correlated codes form very elliptical clusters.

5.8.1 Center construction

In order to exploit the finding that 2^{2U} centres form one cluster and can be replaced by a single centre, its construction must be derived. For convenience, the centres of the reduced PPB RBF are named *super centres* while centres for the normal PPB RBF are simply named centres. The super centres represent μ in equation 5.17. Thus the 2^U super centres can be derived from the 2^{3U} centres given in (5.14). Again, Figure 5.12 will help to explain the procedure. The 2^{3U} centres are constructed from the 2^U previous, 2^U current and 2^U next symbol combinations. In order to find one super centre, all points must be averaged, which can be constructed from the different head and tail combinations (ISI causing sequences). In other words, take one Centre (see figure 5.15) and find all associated *Head* and *Tail* sequences, add them up and divide the sum by the number of them. This is still a time consuming task, since it is based on the 2^{3U} centres. A much simpler derivation was found. The previously stated procedure does the following. It

averages the ISI component induced by the previous symbol and current symbol, respectively. Since this takes all possible combinations of them into account, while the current symbol is left unchanged, the ISI component will cancel itself. In other words, since the signal (spreading code) is assumed to be antipodal and the number of symbol combinations is even, the average of the signal (in “head” and “tail”) is zero. Hence, what is left is the current symbol convolved with H_{ch} . Hence, the super centres can be found by preprocessing the CLB centres \mathbf{p}^{AWGN} constructed according to the extended Gaussian method. The covariance matrix \mathbf{S} is left unchanged, since the super centres do not change correlation properties between the spreading codes.

5.9 Simulation result

This section presents simulation results obtained from Monte-Carlo simulations. Different RBF structures are compared in terms of their BER performance against established receivers. Results for the memoryless channel demonstrate the claim that the PPB RBF with Mahalanobis distance measure performs as well as the CLB RBF receiver. Then, simulation results conducted in a stationary multipath environment are presented. Due to the large complexity of some receiver structures only stationary channels are considered.

5.9.1 AWGN channel

A DS-CDMA system with U users and seven chip spreading codes is considered. The SNR was chosen to be $E_b / N_0 = 7\text{dB}$. Three RBF structures are compared against the known PPB MMSE receiver [98]. A CLB RBF receiver (CRBF) acts as the optimum performance bound since it is equivalent to a Bayesian structure. Two PPB RBF receivers are investigated. The PPB RBF with Euclidean distance measure (ERBF) and the PPB RBF with Mahalanobis distance measure (MRBF).

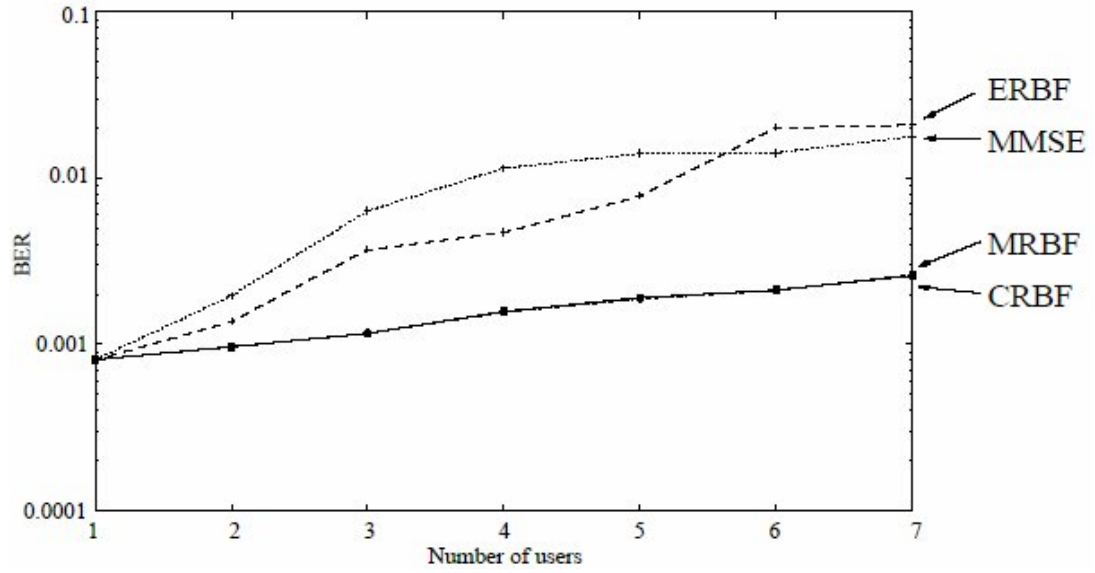


Figure 5.17: BER against the number of users for a CDMA scenario in AWGN with randomly generated 7 chip spreading codes and $E_b / N_0 = 7\text{dB}$ in an AWGN channel.

Figure 5.17 shows results obtained from a set of randomly generated spreading sequences. It can be seen from Figure 5.17 that the MMSE is a long way from achieving optimum performance. Moreover, the ERBF structure suffers severely from not constructing the optimum decision boundary and performs even worse than the MMSE when the MAI is high. Further, the results show that the MRBF performs as well as the CRBF. Therefore, the Mahalanobis distance measure is the optimum distance measure for a PPB RBF receiver structure.

Figure 5.18 shows results obtained from a set of seven chip Gold spreading sequences. Again, the results lead to the same conclusion. MMSE and ERBF perform poorly, while MRBF and CRBF perform optimally.

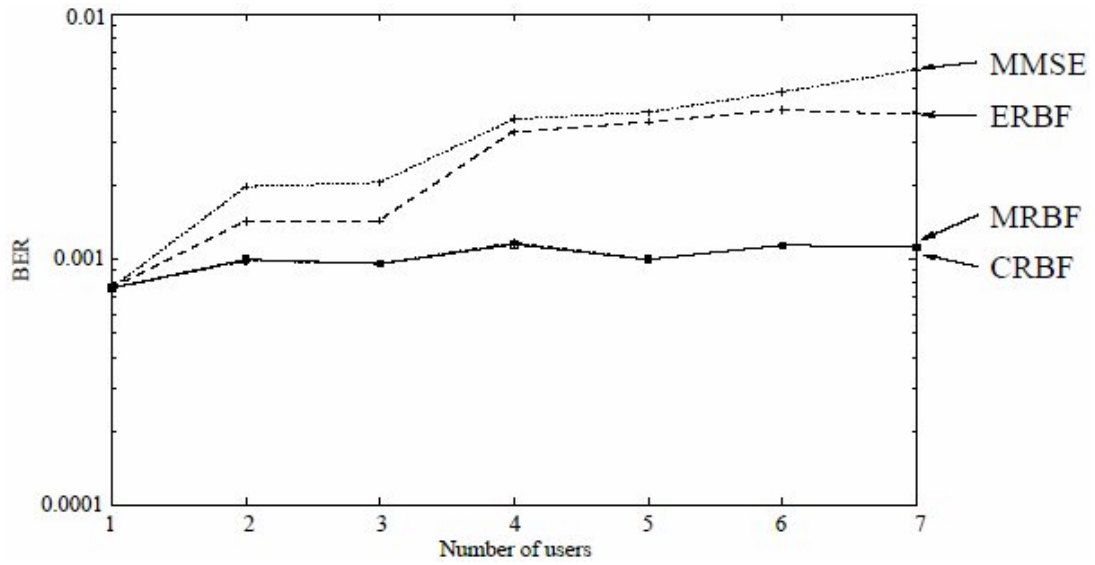


Figure 5.18: BER against the number of users for a CDMA scenario in AWGN with 7 chip Gold spreading codes and $E_b / N_0 = 7\text{dB}$ in an AWGN channel.

5.9.2 Multipath channel

A PPB DS-CDMA system with U users and short spreading codes is considered with preprocessing by a bank of MRC filters. Further, perfect knowledge of the channel impulse response is assumed. The number of active users is kept small since some receivers become too complex to simulate e.g. if $U > 6$. Different RBF structures are compared against the known PPB MMSE receiver. The CLB RBF receiver (CRBF) with 2^{3U} centres of length $(N+L-1)$ and the PPB RBF with Mahalanobis distance measure (MRBF) and 2^{3U} centres of length U are compared against the RBF with 2^U super centres (SRBF) and the RBF with Euclidean distance measure (ERBF) with 2^{3U} centres of length U .

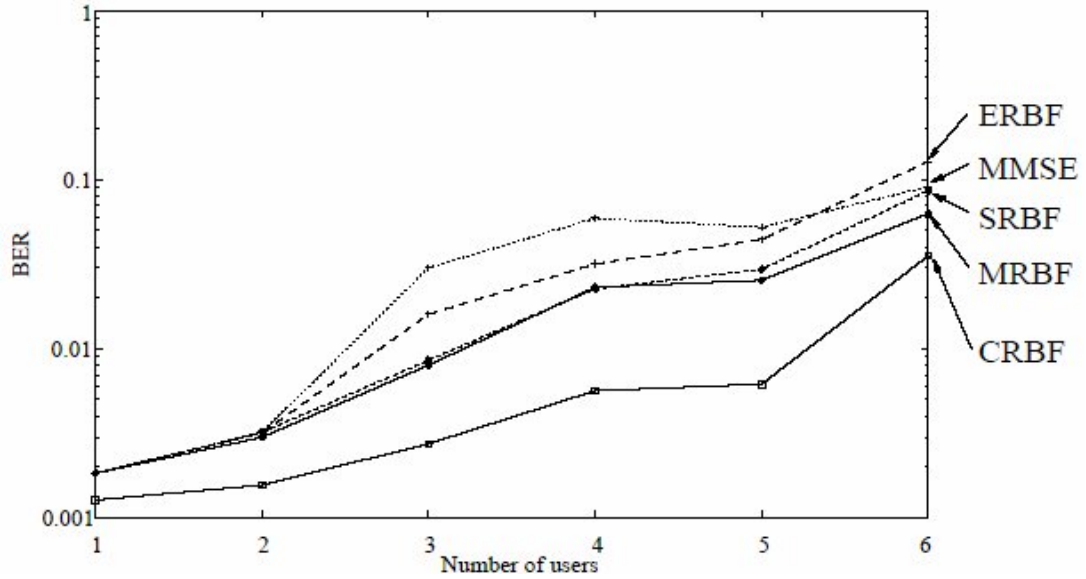


Figure 5.19: BER against the number of users for a CDMA scenario with randomly generated 7 chip spreading codes and $E_b / N_0 = 7\text{dB}$ in a multipath channel.

Figure 5.19 presents the BER performance from a set of randomly generated spreading codes with seven chips. It shows that CRBF, MRBF and SRBF outperform the linear MMSE structure. Moreover, the MRBF and SRBF perform quite similarly over a large number of users, while the ERBF performs less well and is even outperformed by the MMSE at six users. The performance degradation at five users between the SRBF and the MRBF is due to the simplified decision boundary constructed by the SRBF. This becomes more severe as the dimension (U) is increased. However, it was found that the SRBF still outperforms the MMSE. Of interest is the superior performance of the CRBF receiver, which performs much better than the MRBF. Since the preprocessing is done by a bank of RAKEs (MRCs), the noise of the combined signal is no longer white because the output of each finger is weighted by a channel coefficient. This induced additional noise distortion which is not perfectly described by the multivariate normal distribution (5.17). In order to circumvent this problem, preprocessing could be done by a bank of grouped MFs, where each group has L MFs. However, this increases the signal's dimension used at the receiver structure to $(L \times U)$ and makes it more complicated to separate the received signals since all RAKE finger outputs are equally weighted,

especially the weaker ones. Moreover, super centres must be computed differently, if they exist at all.

In Figure 5.20 results obtained from seven chip Gold codes. Figure 5.20 shows that all RBF structures (ERBF is not included) outperform the MMSE. The SRBF and MRBF receivers diverge at 5 users.

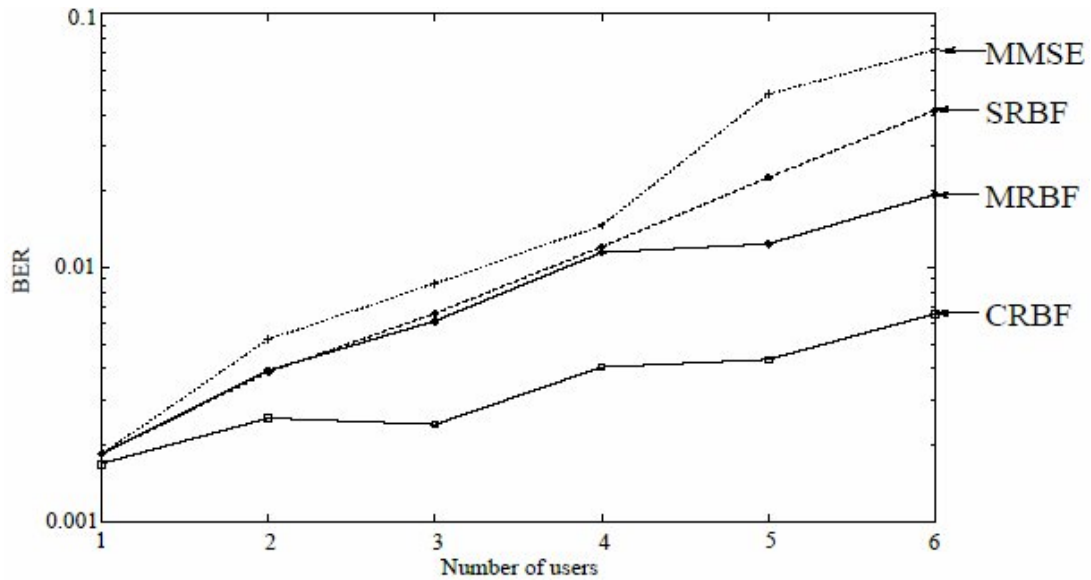


Figure 5.20: BER against the number of users for a CDMA scenario with 7 chip Gold codes and $E_b / N_0 = 7\text{dB}$ in a multipath channel.

Figure 5.21 shows the results obtained for randomly generated spreading codes of length 16 with $E_b / N_0 = 7\text{dB}$. The results are similar to the ones presented in Figure 5.20 in the sense that the MMSE is not greatly outperformed by the RBF based receivers. For comparison the MRC performance is given, which becomes very poor as MAI increases. It is important to note that the SRBF is better than the MMSE with the spreading sequence of length 16.

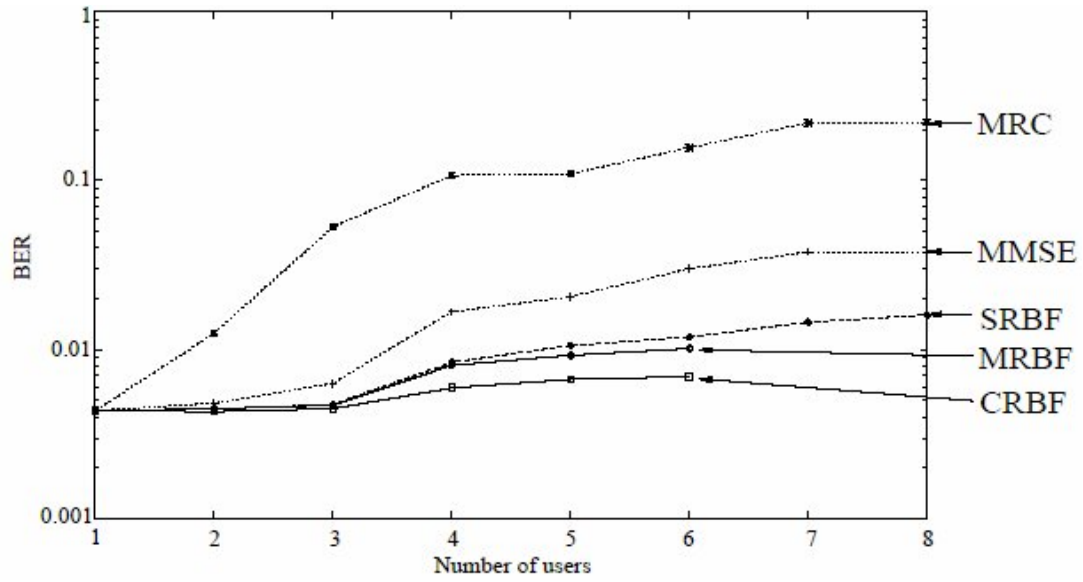
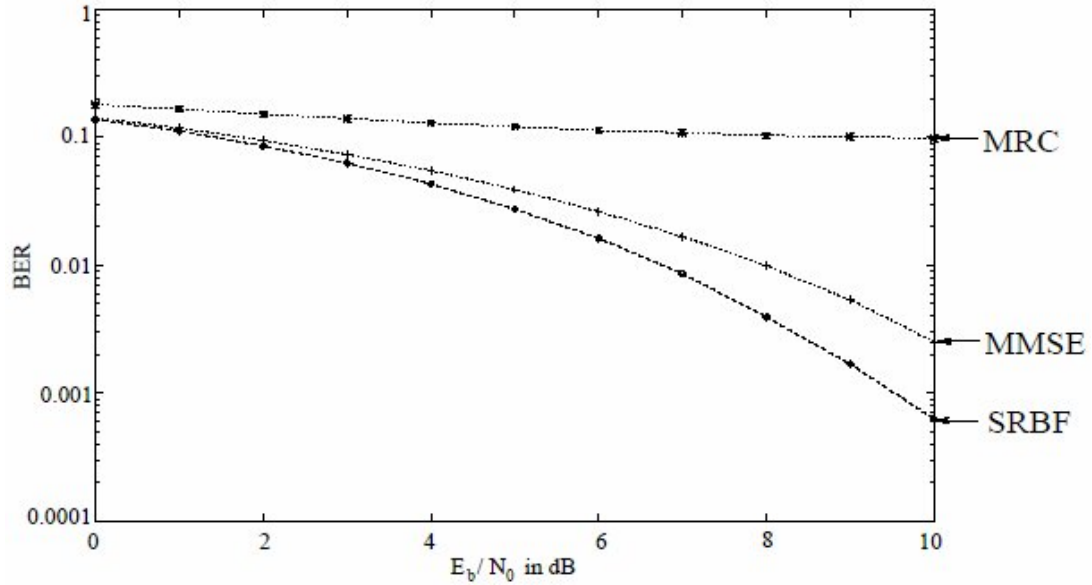
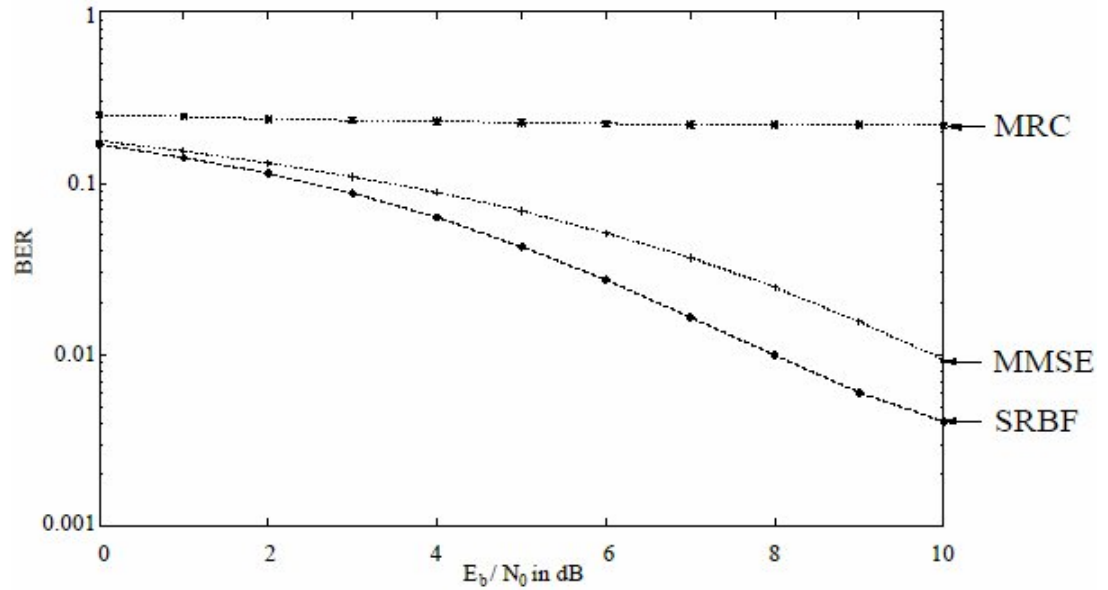


Figure 5.21: BER against the number of users for a CDMA scenario with randomly generated 16 chip spreading codes and $E_b / N_0 = 7\text{dB}$ in a multipath channel.

Results for two different numbers of users over a SNR range between 0dB and 10dB are given in Figure 5.22. The performance for the MRBF is omitted due to its complexity. In both scenarios, figure 5.22(a) and figure 5.22(b), the MRC performs very poorly. Figure 5.22 shows that the performance gap between the SRBF and the MMSE increases, as the number of users increases. In the 4 user scenario, the SRBF has at $E_b / N_0 = 7\text{dB}$ half the error ratio of the MMSE, and has a gain of around 1.5 dB at a BER of 0.01 over the MMSE. For 8 active users, the SRBF has half the error ratio of the MMSE at 7dB and a gain 2dB at a BER of 0.01 over the MMSE.



(a) For 4 users



(b) For 8 users

Figure 5.22: BER against the SNR for a CDMA scenario with randomly generated 16 chip spreading codes and a multipath channel.

5.10 Discussion

This chapter presented the chip rate and symbol rate RBF receiver. The RBF construction for the CLB structure was introduced from which the PPB structure has been derived. Both structures have the same number of centres (2^U) in a memoryless channel which

grows exponentially with the number of users. It has been shown that the Euclidean distance measure used for the CLB RBF is only under certain circumstances optimum for the PPB RBF. This is due to the correlated nature of the noise induced by the preprocessing stage. If nonorthogonal spreading sequences are used, then the Euclidean distance measure must be replaced by the Mahalanobis distance measure. Then, the PPB RBF and the CLB RBF perform the same in AWGN. Applying the PPB RBF for multipath scenarios is of limited use since its computational complexity may exceed the resources available at a mobile. A technique which introduces super centres has been proposed. This technique reduces the number of centres from 2^{3U} to 2^U . Since it rests upon the Mahalanobis distance measure, it also takes the correlation among the spreading codes into account. Although it needs a matrix inversion, its complexity is less since the matrix inversion has to be done only once for a set of spreading codes used. If the set of codes is known a priori then it might be possible to store the matrix inverse in a look up table. Monte-Carlo simulations showed little performance loss over a wide range of users for this RBF structure, if compared with the Mahalanobis based RBF which takes all 2^{3U} into account. However, the proposed technique of computing super centres is restricted to certain CDMA systems in order to be beneficial. These systems must use short spreading sequences, such as 16 chip codes, e.g. UMTS [76]. Because long codes, e.g. as used in IS-95, are less ISI affected (in the Head and Tail chips) hence the ISI free middle part (Centre) provides the receiver with sufficient information in order to detect the transmitted bit.

All multipath simulations exploit a bank of RAKEs based on the MRC, because MRC performs better than EGC. Since each RAKE branch is weighted by a channel coefficient, the noise of the combined signal no longer has a white characteristic. The simulations showed that the CLB RBF performs much better than the PPB RBF. This is because the Mahalanobis distance measure rests upon the assumption that all signals have the same properties described by the multivariate normal distribution. In order to enhance performance, the output of each RAKE finger may be fed into the receiver structure. This increases the dimensionality of the preprocessed signal to (number of RAKE fingers $\times U$) which is still a moderate number since $N \gg U$.

5.11 Conclusion

A new RBF receiver structure for DS-CDMA systems with preprocessing has been presented which does not need whitening filters. The new structure exploits the Mahalanobis distance measure instead of Euclidean distance measure, and takes the correlated nature of the noise component into account, which is induced when a preprocessing stage is used. Results obtained from simulation showed its performance compared against other RBF receivers and the linear MMSE receiver (more results in the thesis.).

It has been shown that in AWGN, this new structure achieves optimum performance while its complexity is reduced, especially for short spreading sequences. For multipath scenarios, we reduced the number of centres from the size of 2^{3U} to 2^U by introducing super centres, with little loss in performance compared with the RBFN which consists of all possible centres.

Chapter 6

Conclusion

6.1 Introduction

This thesis begins with an introduction to mobile communications and DS-CDMA. This thesis can be divided into two parts. First part begins with the review of some popular spreading codes. The spreading codes are optimized by AO/LSE (auto-optimal/least sidelobe energy), LSE/AO (least sidelobe energy/auto-optimal), MSE/AO (maximum sidelobe energy/auto-optimal), CO/MSQCC (cross-optimal/minimum mean-square cross-correlation), and MSQCC/CO (minimum mean-square cross-correlation/cross-optimal) criteria. The performance of these codes at the output of a DS-CDMA system is compared where the signal-to-noise ratio (SNR) at the receiver output is the performance measure. In the second part, a radial basis function (RBF) based receiver is proposed and its performance is evaluated.

6.2 Summary

Chapter 1 is the review of current trends in mobile communications. It also briefly discusses the various existing mobile standards which are adopted across the globe. Properties of spread spectrum communication system which qualify it for military and secure communication applications are also discussed briefly with multiple access techniques.

After reviewing spread spectrum communications and its application to cellular DS-CDMA systems, chapter 2 discusses CDMA principle and IS-95 standard. Structure and important function of various blocks that constitute IS-95 system are also briefly outlined.

Chapter 3 summarizes important properties of some popular spreading codes. Generation logic of these codes is also summarized from a mathematical point of view. Popular

implementation structures are also depicted with schematics. Feedback connections for shift registers for generation of various lengths of maximal length sequences are tabulated comprehensively.

These spreading codes are phase optimized and their performance is compared in chapter 4 when the signal-to-noise ratio (SNR) at the output of a DS-CDMA receiver acts as a performance measure. These codes are optimized by various methods namely, AO/LSE (auto-optimal/least sidelobe energy), LSE/AO (least sidelobe energy/auto-optimal), MSE/AO (maximum sidelobe energy/auto-optimal), CO/MSQCC (cross-optimal/minimum mean-square cross-correlation), and MSQCC/CO (minimum mean-square cross-correlation/cross-optimal) criteria. It is concluded that the MSQCC/CO phase optimization criteria clearly results in the best performance.

In chapter 5, a nonlinear receiver is proposed. This receiver is based on RBF structure and is preprocessing based. This chapter begins with the review of established receivers. DS-CDMA can be viewed as a pattern recognition problem. Hence, it behaves optimally when a nonlinear receiver is used for solving the nonlinear separable condition. Two types of linear receivers namely MMSE and MF are considered and their performances are evaluated. The superiority of the RBF receiver is shown by some simulation results. This RBF receiver takes both the Mahalanobis and the Euclidean distance measure into account for calculating the basis function. Taking computational complexity into account, the number of centers of the receiver is reduced. Performance of this receiver is evaluated by simulations when the spreading sequences considered are seven chip long Gold and random codes.

6.3 Achievement of the thesis

Various types of phase optimization criteria namely AO/LSE (auto-optimal/least sidelobe energy), LSE/AO (least sidelobe energy/auto-optimal), MSE/AO (maximum sidelobe energy/auto-optimal), CO/MSQCC (cross-optimal/minimum mean-square cross-correlation), and MSQCC/CO (minimum mean-square cross-correlation/cross-optimal) are not compared comprehensively previously. This thesis outlines the need for optimization with definitions of above mentioned optimization criteria. The results thus

obtained questions the popular convention of choosing spreading sequences. Generally, the criteria for choosing spreading sequences for DS-CDMA system are based upon the absolute value of crosscorrelations. But, mean square value of crosscorrelation is also important when minimization of multiple access interference (MAI) is the main aim. The results can not only be treated as guidelines for choosing spreading sequences for ranging (see appendix B) and communication purposes, but also can be used for simulation of CDMA system. A receiver is also proposed in this thesis which is nonlinear and hence performs optimally. Keeping in view the need of low complexity of mobile receivers, the number of centres of the proposed RBF receiver is reduced by introducing super centres.

6.4 Limitations of the work

However, the proposed technique of computing super centres is restricted to certain CDMA systems in order to be beneficial. These systems must use short spreading sequences, such as 16 chip codes. Because long codes are less ISI affected (in the Head and Tail chips) hence the ISI free middle part (Centre) provides the receiver with sufficient information in order to detect the transmitted bit.

6.5 Scope for further research

The work presented here considers only stationary channels. There can be further investigation of nonstationary channels. The performance of the proposed receiver can be evaluated in different channel conditions. There also can be further study of the clustering behavior and the results thus obtained can be used for computational complexity reduction. As mentioned earlier, the present system of super centres is calculated only with short spreading sequence. However, the system should be evaluated with long spreading sequence.

Appendix A

System Description

A.1 SS Model

The basic simulation model for spread spectrum system is shown in figure A.1.

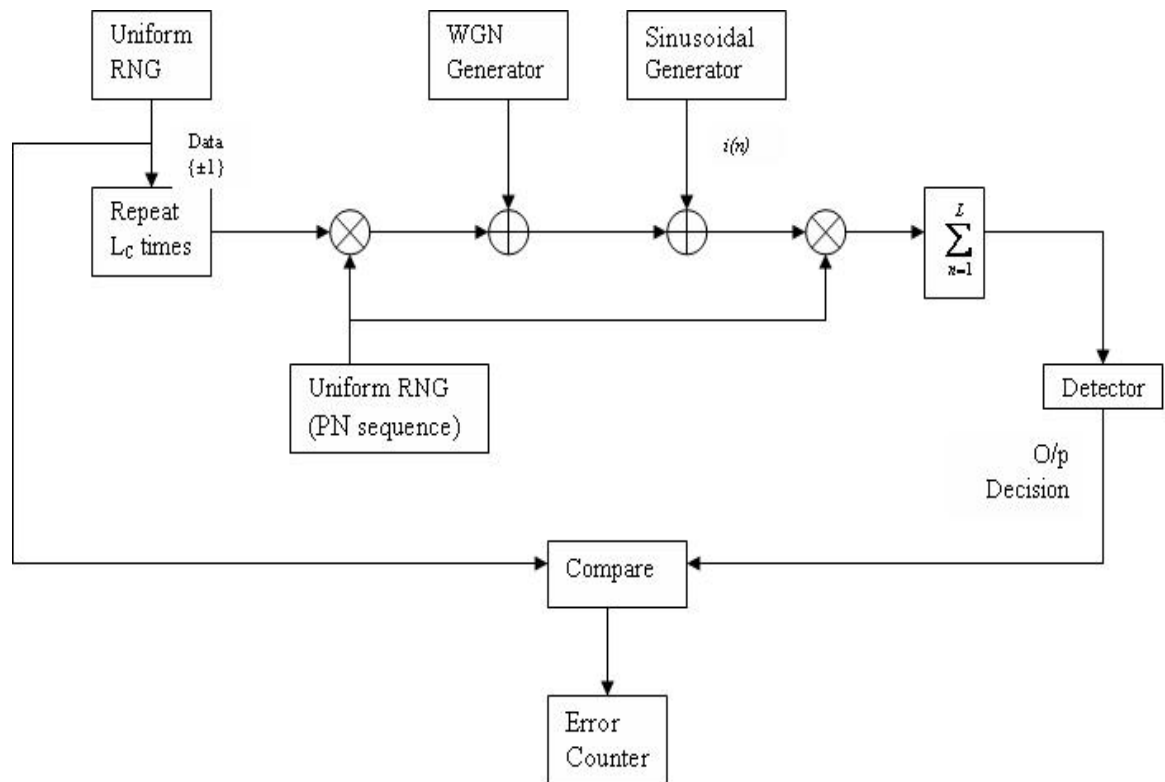


Figure A.1: Spread spectrum model.

The two possible links within a cellular CDMA system are shown next.

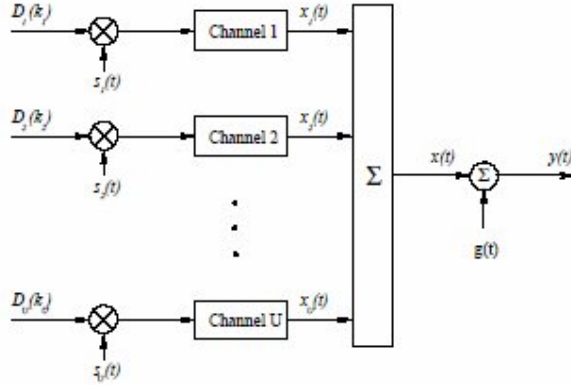


Figure A.2: The uplink scenario (*mobiles to base station*) for U mobiles.

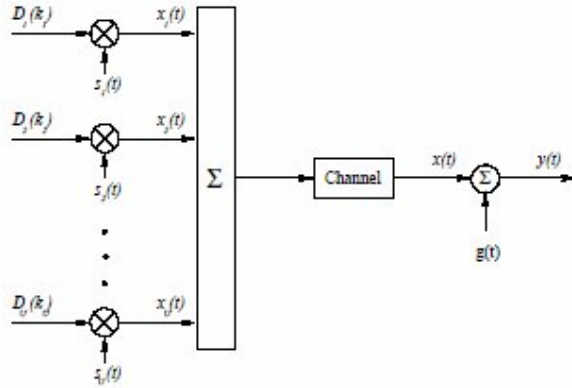


Figure A.3: The downlink scenario (*base station to mobile*).

According to the above figures, the noise corrupted received signal $y(t)$ is defined as:

$$y(t) = x(t) + g(t) = \sum_{u=1}^U x_u(t) + g(t) \quad (\text{A.1})$$

where $g(t)$ denotes the white Gaussian noise with double sided power spectral density $N_o/2$. The u^{th} user's transmitted data bit for bit K is denoted as $D_u(k)$ and is either +1 or -1 with equal probability and all users are transmitting with equal power, normalized to one. Then, the received signal $x(t)$ due to the u^{th} user is given by:

$$x_u(t) = \sqrt{2P_u} \sum_{k=-\infty}^{\infty} D_u(k) s_u(t - kT - \tau_u) \cos(\omega_c t + \phi_u) \quad (\text{A.2})$$

where T is the bit interval, P_u , τ_u and ϕ_u are the power, delay and carrier phase shift of the u^{th} user, and ω_c is the carrier frequency; $s_u(t)$ is the u^{th} spreading sequence (signature) waveform given by:

$$s_u(t) = \sum_{n=0}^{N-1} c_{u,n} \psi(t - nT_c) \quad (\text{A.3})$$

where $c_{u,n} \in \{1, -1\}$ is the n^{th} element of the spreading sequence for user u , $\psi(t)$ is the chip waveform, N the processing gain (number of chips per user bit), and $T_c = T/N$ is the Chip duration. Each user in Figure A.2 has its own delay τ_u which is taken into account in equation (A.2), while the channel delay is incorporated in the channel block. Thus the uplink (mobile to base station) is generally asynchronous. If the delay τ_u is equal for all u , then the communication system is considered synchronous, which is typically the downlink scenario (base station to mobile), see Figure A.3.

In order to simplify the notation, it is assumed that all carrier phases are equal to zero and baseband notation can be used [99]. In the downlink scenario all user signals share the same channel to a specific, whereas in the uplink scenario each user is transmitting through a unique channel with different delays. The channel is modelled by an L -tap filter [53]. The downlink channel impulse response H_{ch} can be estimated from monitoring a pilot tone transmitted by the BS (e.g. IS-95). Since the signal processing task is done on sampled signals, it is more convenient to make use of vector and matrix notation. Therefore equation (A.1) can be rewritten for a fully synchronized downlink antipodal ($\{+1, -1\}$) DS-CDMA system with U independent users and a non-dispersive AWGN channel. It is assumed that the number of active users and their corresponding spreading sequences are known. Each u^{th} user bit $D_u(k)$ is spread by a unique user specific spreading sequence $\mathbf{c}_u = [c_{u,1} c_{u,2} \dots c_{u,N}]$ of length N , with $n = 1, 2, \dots, N$ chips, where the chips are either +1 or -1. Hence, equation (A.1) becomes:

$$y(kN + n) = \sum_{u=1}^U D_u(k) c_{u,n} + g(kN + n) \quad (\text{A.4})$$

The received signal becomes $\mathbf{y}(k)$ in vector notation, where k denotes the k^{th} user bit. Now, the received signal (A.4) shall be described from the view point of set theory. It can be assumed that for a certain period of time the number of users U is constant, hence also the number of possible transmitted noise free signal combinations, which is denoted by M . When U and all U spreading sequences are known, such a set of signals can be

constructed. Therefore, the received signal (A.4) for the k^{th} transmitted symbol may be rewritten as:

$$\mathbf{y}(k) = \mathbf{x}(k)^T + \mathbf{g}(k) \quad (\text{A.5})$$

where $\mathbf{g}(k)$ is a vector containing the random noise and is the only non-deterministic component. Vector $\mathbf{x}(k)$ is drawn from a set X with equal probability, where the M elements \mathbf{x}_m in X are the noise free signal states:

$$X = \{\mathbf{x}_m : 1 \leq m \leq M\}$$

Set X can be given as a matrix, where each row corresponds to an element of this set. The elements of X are the rows of a $(M \times N)$ matrix for a non-dispersive channel, or of a $(M \times (N+L-1))$ matrix for multipath channels, for chip rate receivers. While the elements of X are the rows of a $(M \times U)$ matrix for symbol rate receivers. The matrices shall be referred to as the *generation matrices*.

Appendix B

Ranging application of spread spectrum

B.1 Ranging with SS

The coded modulation characteristic of SS systems uniquely qualifies them for navigation-both range measurement & direct finding. Any RF signal is subject to a fixed rate of propagation (approximately 6 $\mu\text{sec}/\text{mi}$). The signal reaching a receiver at any given instant left the transmitter that sent it sometime before. Because signaling waveforms or modulations are also functions of time. The difference in a signaling waveform as seen at a receiver, from that present at the transmitter can be related directly to distance between them and used to measure the distance. A common type of echo range measurement method is that used in radar system. Many such systems simply transmit a pulse of RF energy and then wait for the return of a portion of the energy due to its being reflected from objects in the signal path. The radar marks the time from the instant of the pulse transmission until its return. The time required for the signal to return is a function of the two way range to the reflecting object, and because the signal propagation rate is known, the range is easily derived.

Any signal used is subject to the same distance / time relations. An unmodulated carrier, for instance, is delayed precisely the same amount as a spread spectrum signal traveling the same distance. The spread spectrum signal has an advantage, however, in that its phase is easily resolvable. The marks on a direct sequence signal are the code sequence modulation, and the basic resolution is one code chip; the higher the chip rate, the better the measurement capability.

B.2 Ranging Techniques

Figure B.1 illustrates a simple direct sequence ranging system.

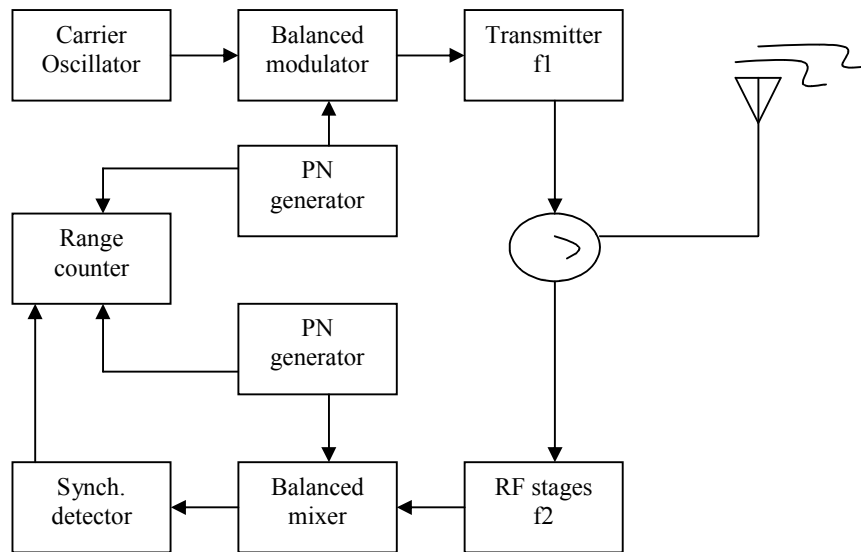


Figure B.1: Direct sequence ranging system (*Transmitter*).

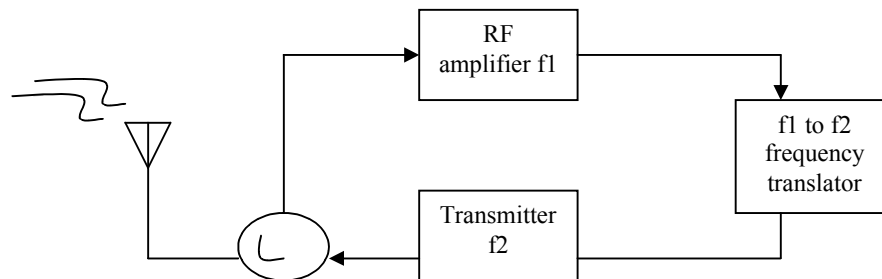


Figure B.2: Direct sequence ranging system (*Receiver*).

The system is duplex as it transmits and receives simultaneously. The transmitter sends a pseudonoise code-modulated signal. The signal at f_1 is simply translated to a different frequency f_2 and is retransmitted. The signal then reaches the first transmitter's site with a time delay corresponding to the two-way signal propagation delay between the two units. A receiver located at the f_1 transmitter location then synchronizes to the return signal. On measuring the number of chips of code delay between the signals being and received, the range to the repeating station can be determined.

Timing is not the only requirement for accurate ranging. Conventional radio communications techniques can only obtain accuracies on the order of meters. Yet

spread-spectrum technology again excels in its ability to allow precision ranging on the order of millimeters. This is accomplished by detecting the phase difference in the PN code sequences of the transmitter and receiver (see Figure B.3). The accuracy of this technique is coupled to the speed of the code sequence: the higher the speed, the finer the resolution.

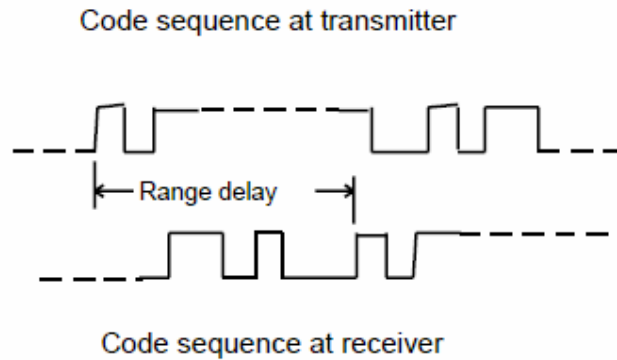


Figure B.3: Code-sequence comparisons at transmitter & receiver.

B.3 Choice of Spreading Sequence

In BPSK transmission, bandwidth is a direct function of the code chip rate. Code repetition rate is simply

$$R_{\text{rep}} = \frac{\text{Clock rate in chips per second}}{\text{Code length in chips}}$$

This repetition rate determines the line spacing in the RF output spectrum. Hence, it is an important consideration in a system design. Another important criterion is that the period of the code must be very large. Table 1 lists various code lengths for a 1-Mcps chip rate. Other consideration should be that the choices of code rate and code length determine the relationship of the repetition rate to the information baseband and use of the system for ranging. The code used in a direct sequence system should be adjusted for repetition rate and length such that noise does not pass into the demodulator especially under jammed conditions. A properly chosen code can not only improve resolution but also can ease range measurement problem. If the chip rate is chosen in such a way that an integral

number of code chip is accumulated for each mile of delay, a simple count of code offset can be used to measure range. Clock rates that are integral multiple of 161,875Hz produce code at rates that are integrally related to the speed of propagation of RF signal.

This relationship may be derived as follows:

Speed of light in vacuum is $c = 2.997926 \times 10^8$ m/s

1 nautical mile = 1.852×10^3 meter

The clock rate (wavelength = 1nmi) = $c/R = 2.997926 \times 10^8 / 1.852 \times 10^3 = 161,875$ Hz

The clock rate for 1 statute mile resolution would be 186,333 Hz. Table B.1, B.2 list the rates and sequence length that should be used for various range resolutions.

Sequence Length	Sequence Period
127	1.27×10^{-4} sec
255	2.55×10^{-4} sec
511	5.11×10^{-4} sec
1023	1.023×10^{-4} sec
2047	2.047×10^{-4} sec
4095	4.095×10^{-4} sec
8191	9.191×10^{-4} sec
131071	1.31×10^{-1} sec
524287	5.24×10^{-1} sec
8388607	8.388 sec
134217727	13.421 sec
2147483647	35.8 min
879609302207	101.7 days
2305843009213693951	7.3×10^4 yr
618970019642690137449562111	1.95×10^9 yr

Table B.1: Code sequence periods for various m-sequence lengths, 1-Mcps rate

Basic accuracy	Nautical mile	Statute mile
0.1 mile	1.61875 Mcps(608ft/chip)	1.86333 Mcps(528ft/chip)
0.05 mile	3.23750 Mcps(304ft/chip)	3.72666 Mcps(264ft/chip)
0.02 mile	8.09375 Mcps(121.6ft/chip)	9.19665 Mcps(105.6ft/chip)

Table B.2: Chip rates for various basic range resolutions

References

- [1] T. S. Rappaport, "The Wireless Revolution" *IEEE Communications Magazine*, pp. 52-71, November 1991.
- [2] A. D. Kucar, "Mobile Radio-An Overview", *IEEE Communications Magazine*, pp. 72-85, November 1991.
- [3] TIA/EIA Interim Standard-95, "Mobile Station - Base Station Compatibility for Dual Mode Wideband Spread Spectrum Cellular System", Telecommunication Industry Association, July 1993
- [4] Gilhousen, et al., "On the Capacity of Cellular CDMA System," *IEEE Transactions on Vehicular Technology*, Vol 40, No 2, pp. 303-311, May 1991.
- [5] T. S. Rappaport, "The Wireless Revolution", *IEEE Commun. Mag.*, vol. 29, no.11, pp. 52-71, Nov. 1991.
- [6] T. S. Rappaport, *Wireless Communications: Principles and Practices*, 2nd Edition, Pearson Education 2004.
- [7] L. Correia, R. Prasad, "An Overview of Wireless Broadband Communications", *IEEE Communications Magazine*, pp. 28-33, January 1997.
- [8] O. Andrisano, V. Tralli, R. Verdone, "Millimeter Waves for Short-Range Multimedia Communication Systems", *Proceedings IEEE*, vol.86, pp. 1383-1401, July 1998.
- [9] H. Xu, R. J. Boyle, T. S. Rappaport, J. H. Schaffner, "Measurements and Models for 38GHz Point-to-Multipoint Radiowave Propagation", *IEEE Journal on Selected Areas in Communications: Wireless Communications Series*, vol. 18, no. 3, pp. 310-321, March 2000.
- [10] R. Pickholtz, D. Schilling, and L. Millstein, "Theory of Spread Spectrum Communiactions: A Tutorial," *IEEE Transactions on Communications*, vol. COM-30, pp. 855-884, May 1982.
- [11] T. Edwards, "Technology trends for personal communications terminals," in *Proceedings Colloquium on Personal Communications in the 21st Century part I and II, ref no.1998/214 and 1998/242*, pp. 5/1-5/8, IEE, February 1998.
- [12] H. Taub and D. L. Schilling, *Principles of Communication Systems*. NY: Tata McGraw-Hill Publishing Company Limited, 2 ed., 1991.

- [13] R. C. Dixon, *Spread Spectrum Systems with Commercial Applications*. JohnWiley and Sons Inc.,1994.
- [14] J. G. Proakis and Masoud Salehi, *Contemporary Communication System Using MATLAB*. Thomson Books/Cole, 1 ed., 1992.
- [15] P. Jung, P. W. Baier, and A. Steil, "Advantages of CDMA and Spread Spectrum Techniques over FDMA and TDMA in Cellular Mobile Radio Applications," *IEEE Transactions on Vehicular Technology*, vol. 42, pp. 357–364, August 1993.
- [16] R. A. Scholtz, "Notes on Spread-Spectrum History," *IEEE Transactions on Communications*, vol. COM-31, pp. 82-84, Jan. 1983.
- [17] E. Biglieri, G. Caire, and G. Taricco, "Coding and Modulation Under Power constraints," *IEEE Personal Communications Magazine*, vol. 5, pp. 32–39, June 1998.
- [18] A. W. Lam and S. Tantaratana, "Theory and Applications of Spread-Spectrum Systems, A Self-Study Course," Naval Postgraduate School, Monterey, CA, May 1994.
- [19] A. B. Glenn, "Low Probabability of Intercept (LPI) Performance in Jamming and Nonjamming Environments for SHF and EHF Satellite Communication Systems", *IEEE Milcom. Conf. Proc.*, October 1981.
- [20] T. Ojanpera, A. Klein, and P. O. Anderson, "FRAMES Multiple Access for UMTS," in *Proceedings Colloquium on CDMA and Applications for third generation mobile systems, ref no.1997/129*, pp. 7/1–7/8, IEEE, May 1997.
- [21] T. Ojanpera and *et al.*, "FRAMES: - Hybrid Multiple Access Technology," in *Proceedings International Symposium on Spread Spectrum Techniques and Applications, Mainz, Germany*, vol. 1, pp. 320–324, IEEE, 1996.
- [22] I. A. Getting, "The Global Positioning System," *IEEE Spectrum*, vol. 30, issue 12, pp. 36-38 and 43-47, Dec. 1993.
- [23] G. J. Morgan-Owen and G. T. Johnston, "Differential GPS positioning," *Electronic & Communications Engineering Journal*, vol. 7, issue 1, pp. 11-21, Feb. 1995.
- [24] R. A. Scholtz, "The Evolution of SS-MA Communications", *Proceedings of the 3rd IEEE International Symposium on Spread Spectrum Techniques and Applications (ISSSTA), Oulu, Finland*, vol. 1, pp. 4-13, July 1994.
- [25] P. G. Fikkema, "Spread Spectrum Techniques for Wireless Communications", *IEEE Signal Processing Magazine*, vol. 14, pp. 26-36, May 1997.

- [26] www.sssmagonline.com "ABCs of Spread Spectrum - A Technology Introduction and Tutorial"
- [27] R. C. Dixon, "A Spread Spectrum Ranging Technique for Aerospace Vehicles" SW IEEE CON, April 1968.
- [28] Baldwin, Jr., E. R. "SICGARS: The Frequency Hopping Jam Resistant Combat Net Radio", *Signal Magazine*, November 1982.
- [29] P. Daly, "Navstar GPS and GLONASS: Global Satellite Navigation Systems," *Electronic & Communication Engineering Journal*, vol. 5, issue 6, pp. 349-357, Feb. 1995.
- [30] F. Adachi, M. Sawahashi, T. Dohi, and K. Ohno, "Coherent DS-CDMA: Promising Multiple Access for Wireless Multimedia Mobile Communications," in *Proceedings International Symposium on Spread Spectrum Techniques and Applications, Mainz, Germany*, vol. 1, pp. 351-358, IEEE, 1996.
- [31] Hak Keong Sim, *Near Maximum Likelihood Multiuser Receivers for Direct Sequence Code Division Multiple Access*. PhD thesis, Department Electrical Engineering, Edinburgh University, UK, November 2000.
- [32] P. Jung, P. W. Baier, and A. Steil, "Advantages of CDMA and Spread Spectrum Techniques over FDMA and TDMA in Cellular Mobile Radio Applications," *IEEE Transactions on Vehicular Technology*, vol. 42, pp. 357-364, August 1993.
- [33] W. C. Y. Lee, "Overview of Cellular CDMA," *IEEE Transactions on Vehicular Technology*, vol. 40, pp. 291-302, May 1991.
- [34] Jos'e Mart'ın Luna Rivera, *Iterative Multiuser Receivers for Coded DS-CDMA Systems*. PhD thesis, Department Electrical Engineering, Edinburgh University, UK, October 2002.
- [35] E. Biglieri, G. Caire, and G. Taricco, "Coding and Modulation Under Power Constraints," *IEEE Personal Communications Magazine*, vol. 5, pp. 32-39, June 1998.
- [36] W. Stallings, *Wireless Communications and Networks*. Pearson Education Inc., 2002.
- [37] ANSI J-STD-008- Personal Station-Base Compatibility Requirements for 1.8-2.0 GHz Code Division Multiple Access (CDMA) Personal Communication Systems, March 1995.

- [38] Electronic Industries Association, "Widband Spread Spectrum Digital Cellular System Dual-Mode Mobile Station - Base Station Compatibility Standard," IS-95, April, 1992.
- [39] Y. Li, "Bit Error Rate Simulation of a CDMA System for Personal Communications," Masters Thesis in Electrical Engineering, Virginia Polytechnic Institute and State University, Blacksburg, VA, August 1993.
- [40] D. P. Whipple, "The CDMA Standard," *Applied Microwave & Wireless*, pp.24-39, winter, 1994.
- [41] E. R. Berlekamp, R. E. Peile, and S. P. Pope, "The Application of Error Control to Communications," *IEEE Communications Magazine*, vol. 25, no.4, pp. 44-57, Apr. 1987.
- [42] S. B. Wicker, *Error Control Systems for Digital Communication and Storage*, Prentice Hall, Inc., New Jersey, 1995.
- [43] F. Ling and D. D. Falconer, "Combined Orthogonal/Convolutional Coding for a Digital Cellular CDMA System," *Proc. 42nd IEEE Veh. Tech. Conf.*, Vol. 1, Denver, CO, pp. 63-66, 1992.
- [44] Robert Ziemer and Robert Peterson, *Introduction to Digital Communications*, Macmillan Publishing Company, New York, 1992.
- [45] Electronic Industries Association, "Cellular System Dual-Mode Mobile Station - Base station Compatibility Standard," IS-54, May 1990.
- [46] M.P. Lotter, L.P. Linde, "A Comparision of Three families of Spreading Sequences for CDMA Applications", *COMSIG '94*.
- [47] E.H. Dinan, B.Jabbari, "Spreading Codes for Direct Sequence CDMA and Wideband CDMA Cellular networks", *IEEE Communications Magazine*, September, 1998.
- [48] B. M. Popovic, "Spreading sequences for multicarrier CDMA systems", *IEEE Transactionson Communications*, vol. 47, NO. 6, pp. 918-926, June 1999.
- [49] Qinghua Shi and Shixin Cheng, "Optimal Spreading Ssequence Design Based on PR-QMF Theory", *ELECTRONICS LETTERS*, Vol.35, No.6, 18th March 1999.
- [50] Ali N.Akansu, M.V.Tazebay and R.A.Haddad, "A New Look at Dgital Orthogonal Transmultiplexers for CDMA Communications",*IEEE trans. On SP-COM* 45, No.1, January 1997.
- [51] P. M. Grant, C.F.N. Cowan, B. Mulgrew and J.H. Dripps, *Analogue and Digital Signal Processing and Coding*. Bromley, UK: Chartwell-Bratt, 1989.

- [52] J. Yuen, M. Simon, W. Miller, F. Pollara, C. Ryan, D. Divsalar and J. Morakis, "Modulation and Coding for Satellite and Space Communications," Proceedings of the IEEE, Vol.63, pp.1692-1716, Dec 1975.
- [53] J. Proakis, *Digital Communications*. New York: McGraw-Hill, 1993.
- [54] Vitrebi, A.J., and Omura, J.K., *Principles of Digital Communication and Coding*, McGraw Hill, New York, 1979.
- [55] K. Larsen, "Short Convolutional Codes with Maximal Free Distance for Rates $1/2$, $1/3$ and $1/4$," IEEE Transactions on Information Theory, vol. IT-18, pp.371-372, 1973.
- [56] H. Donelan, & T. O'Farrell, "Method for generating sets of orthogonal sequences", *Electronics Letters*, vol. 35, No. 18, pp. 1537-1538, September 1999.
- [57] D. Mottier, & D. Castelain, "A spreading sequences allocation procedure for MC-CDMA transmission systems", *Proc. of VTC'00*, Boston, USA, vol. 3, pp. 1270-1275, September 2000.
- [58] D.V. Sarawate, M. B. Purseley., "Cross-correlation Properties of Pseudo-random and Related sequences", Proc of the IEEE Vol. 68, pp. 593-619, May 1980.
- [59] M. B. Purseley, "Performance Evaluation for phase Coded Spread-Spectrum Multiple-Access Communication-Part I: System Analysis", IEEE Trans on Comm. Vol.COM25, pp.795-799, August 1977.
- [60] M. B. Purseley, D.V. Sarawate, "Performance evaluation for Phase-Coded Spread-Spectrum Multiple Access Communication-Part II: Code Sequence Analysis." IEEE Trans on Comm. Vol.COM-25, pp.800-803, August 1977.
- [61] M. B Purseley, H.F.A.Roefes, "Numerical Evaluation of Correlation Parameters for Optimal Phases of Binary Shift Register Sequences", IEEE Trans on Comm. Vol.COM-27, pp.1597-1604, October 1979.
- [62] K.H.A. Kärkkäinen, "Influence of Various PN Sequence Phase Optimization Criteria on the SNR Performance of an Asynchronous DS-CDMA System", in *Proc. 1995 IEEE Military Communications Conference (MILCOM'95)*, San Diego, CA, U.S.A., pp. 641-646, Nov. 1995.
- [63] K.H.A Kärkkäinen, "Meaning of Maximum and Mean-Square Cross-Correlation as a Performance Measure for CDMA Code Families and their Influence on System Capacity", *IEICE Trans. Commun.*, Vol. E76-B, No. 8, pp. 848-854, 1993.

- [64] K.H.A Kärkkäinen, Pentti A. Leppanen, "The Influence of Initial-Phases of a PN Code Set on the Performance of an Asynchronous DS-CDMA System", *Wireless Personal Communications 2000 (WPC00)*, Vol. 13, pp. 279-293, 2000.
- [65] K.H.A Kärkkäinen, Pentti A. Leppanen, "The Importance of Initial Phase Selection agreement of PN Sequences From the Standpoint of Numerical Analysis and Simulation of a DS-CDMA System", *GLOBECOM'98*, pp. 3295-3301, 1998.
- [66] W. H. Mow, "Minimizing the Worst-case Interuser Interference Experienced by any user in CDMA Systems: A Matrix Approach", *Proc. IEEE Fourth International Symposium on Spread Spectrum Techniques and Applications (ISSTA' 96)*, Mainz, Germany, pp. 561-565, September 1996.
- [67] Massey J.L., Mittelholzer T., "Welch bound and Sequence sets for Code Division Multiple Access Systems" in "Methods in communications, security and Computer Science" (Ed.) Berlin: Springer-Verlag, pp. 63-78, 1993.
- [68] T. O'Farrel, "New Signature Code Sequence Design Techniques for CDMA Systems", *Electronics Letters*, vol.27, no. 4, pp. 23-32, 1991.
- [69] F. W. Sun, H. Leib, "Optimal Phases for a Family of Quadriphase Sequences", *IEEE Trans. Inf. Theory*, vol. IT-43, No. 4, pp. 1205-1217, July 1997.
- [70] El-Khamy S.E., Balmesh A.S, "Selection of Gold and Kasami sets for Spread-Spectrum CDMA systems of Limited Number of Users", *Int. Jour. Of Satellite Comm.* Vol. 5, pp. 23-32, 1987.
- [71] S. Verdu, "Demodulation in the Presence of Multiuser Interference: Progress and Misconceptions," in *Intelligent Methods in Signal Processing and Communications*, pp. 15-44, Birkhauser, Boston, USA, 1997.
- [72] S. Verdu, "Minimum Probability of Error for Asynchronous Gaussian Multiple-Access Channels," *IEEE Transactions on Information Theory*, vol. IT-32, pp. 85-96, January 1986.
- [73] G. D. Forney, "Maximum-Likelihood Sequence Estimation of Digital Sequences in the Presence of Intersymbol Interference," *IEEE Transactions on Information Theory*, vol. IT-18, pp. 363-378, May 1972.
- [74] P. Jung and P. D. Alexander, "A Unified Approach to Multiuser Detectors for CDMA and Their Geometrical Interpretations," *IEEE Transactions on Selected Areas in Communications*, vol. 14, pp. 1595-1601, October 1996.
- [75] L. R. Bahl, J. Cocke, F. Jelinek, and J. Raviv, "Optimal Decoding of Linear Codes for Minimizing Symbol Error Rate," *IEEE Transactions on Information Theory*, vol. 20, pp. 284-287, March 1974.

- [76] S. Pike, "The radio interface for UMTS," in *Proceedings Colloquium on Personal Communication in the 21st Century part I and II, ref no.1998/214 and 1998/242*, pp. 7/1–7/11, IEE, February 1998.
- [77] S. Haykin, *Adaptive Filter Theory*. Prentice Hall International, 3rd ed., 1996.
- [78] R. M. Buehrer, N. S. Correal, and B. D. Woerner, "A Comparison of Multiuser Receivers for Cellular CDMA," in *Proceedings International Conference Globecom '96, London, UK*, pp. 1571–1577, IEEE, November 1996.
- [79] D. G. M. Cruickshank, "Optimal and Adaptive FIR Filter Receivers for DS-CDMA," in *Proceedings International Symposium on Personal Indoor and Mobile Communications*, pp. 1339–1343, IEEE, September 1994.
- [80] D. G. M. Cruickshank, "Suppression of multiple access interference in a DS-CDMA system using Wiener filtering and parallel cancellation," *IEE Proceedings - Communication*, vol. 143, pp. 226–230, August 1996.
- [81] J. M. Holtzman, "DS/CDMA Successive Interference Cancellation," in *Proceedings International Symposium on Spread Spectrum Techniques and Applications, Oulu, Finland*, vol. 1, pp. 69–78, IEEE, 1994.
- [82] D. Divsalar, M. Simon, and D. Raphaeli, "A New Approach to Parallel Interference Cancellation for CDMA," in *Proceedings International Conference Globecom '96, London, UK*, vol. 3, pp. 1452–1457, IEEE, November 1996.
- [83] M. K. Varanasi and B. Aazhang, "Multistage Detection in Asynchronous Code-Division Multiple-Access Communications," *IEEE Transactions on Communications*, vol. 38, pp. 509–519, April 1990.
- [84] G. I. Kechriotis and E. S. Manolakos, "Hopfield Neural Network Implementation of the Optimal CDMA Multiuser Detector," *IEEE Transactions on Neural Networks*, vol. 7, pp. 131–141, January 1996.
- [85] J. J. Hopfield and D. W. Tank, "Computing with Neural Circuits: A Model," *Science*, vol. 233, pp. 625–633, August 1986.
- [86] B. Aazhang, B. Paris, and G. Orsak, "Neural Networks for Multiuser Detection in Code-Division Multiple-Access Communications," *IEEE Transactions on Communications*, vol. 40, pp. 1212–1222, July 1992.
- [87] D.G.M. Cruickshank, "Radial basis function receivers for DS-CDMA", *IEE Electronics Letters*, vol. 32, pp. 188-190, February 1996.
- [88] S. Kumar, *Neural Network-A Classroom Approach*, TMH, 2004.

- [89] U. Mitra, H. Vincent Poor, "Neural Network Techniques for Adaptive Multiuser Demodulation", *IEEE Journal on Selected areas in Communications*, vol. 12, no. 9, December 1994.
- [90] C.M. Bishop, *Neural Networks for Pattern Recognition*, Indian edition, Oxford, 1995.
- [91] D. S. Broomhead and D. Lowe, "Multivariable Functional Interpolation and Adaptive Networks," *Complex Systems*, vol. 2, pp. 321–355, 1988.
- [92] S. Haykin, *Neural Networks*. Upper Sadle River, New Jersey, USA.: Prentice Hall International, 1st ed., 1994.
- [93] T. Poggio and F. Girosi, "Networks for Approximation and Learning," *Proceedings of the IEEE*, vol. 78, pp. 1481–1497, September 1990.
- [94] R.O. Duda, P.E. Hart, D.G. Stork, *Pattern Classification*. 2nd edition, John Wiley & Sons Inc. 2000.
- [95] W. Mohr and M.Kottkamp, "Downlink Performance of IS-95 DS-CDMA under Multipath Propagation Conditions," in *Proceedings International Symposium on Spread Spectrum Techniques and Applications, Mainz, Germany*, vol. 3, pp. 1063–1067, IEEE, September 1996.
- [96] R. Price, "A Communication Technique for Multipath Channels," *Proceedings of the IRE*, vol. 48, pp. 555–570, March 1958.
- [97] B. Mulgrew, "Applying Radial Basis Functions," *IEEE Signal Processing Magazine*, vol. 13, pp. 50–65, March 1996.
- [98] H. V. Poor and S. Verdu, "Probability of Error in MMSE Multiuser Detection," *IEEE Transactions on Information Theory*, vol. 43, pp. 858–871, May 1997.
- [99] S. Moshavi, "Multi-User Detection for DS-CDMA Communications," *IEEE Communications Magazine*, vol. 34, pp. 124–136, October 1996.
- [100] R. Michael Buehrer, Neiyer S. Correal-Mendoza, Brian D. Woerner, "A Simulation Comparison of Multiuser Receivers for Cellular CDMA", *IEEE Transactions on Vehicular Technology*, vol. 49, No. 4, July 2000.
- [101] Ashutosh Sabharwal, Urbashi Mitra, Randolph Moses, "MMSE Receivers for Multirate DS-CDMA Systems", *IEEE Transactions on Communications*, vol. 49, No. 12, December 2001.
- [102] Mobile Portable Research Group (MPRG) www.mprg.com "CDMA Receivers for High Spectral Utilization", May 2001.

- [103] S. Q. Ding, C. Xiang, "From Multilayer Perceptrons to Radial Basis Function Networks: A Comparative Study" *Proceedings of the 2004 IEEE Conference on Cybernetics and Intelligent System*, Singapore, 1-3 December, 2004.
- [104] Chen, S., E. Mulgrew, and P. M. Grant, "A clustering technique for digital communications channel equalization using radial basis function networks", *IEEE Transactions on Neural Network*, Vol. 4, no. 4, pp. 570-579, 1993.
- [105] Caruana, R., Lawrence, S., and Giles, C. L., "Overfitting in Neural Networks: Backpropagation, Conjugate Gradient, and Early Stopping", *Neural Information Processing Systems*, Denver, Colorado. Vol. 13, pp. 402-408, 2001.

Biodata

NAME : IPSITA BHANJA

D.O.B. : 23rd March 1979

EDUCATIONAL QUALIFICATION :

Completed Bachelor of Engg. (BE)
in Electronics & Instrumentation Engg.
from REC Rourkela in the year of 2000.

Joined Mtech (Research) in NIT Rourkela
in March 2004.

EXPERIENCE :

Worked as Software Engineer in Zensar
Technologies Ltd., Pune & PSIL (India),
New Delhi.

Served as a Teaching Assistant in the
dept. of Electronics & Communication Engg.

HOME ADDRESS :

C/o T. K. Bhanja
Qr no. C-57, Krishi Vihar,
Unit-8, Bhubaneswar- 751003
Ph- 0674-2561356
Email- ipsitabhanja@yahoo.com